

FILE COPY

AD-A227 661

REPORT DOCUMENTATION PAGE			Form Approved OMB No. 0704-0188	
<p>1. AGENCY USE ONLY (Leave blank)</p> <p>2. REPORT DATE JUNE 1990</p> <p>3. REPORT TYPE AND DATES COVERED Thesis/Dissertation</p>				
4. TITLE AND SUBTITLE A Finite Difference Numerical Analysis of Heat Transfer in Atheromatous Plaque for Percutaneous Transluminal Microwave Angioplasty			5. FUNDING NUMBERS	
6. AUTHOR(S) Lori Ann Yuk Lan Young			8. PERFORMING ORGANIZATION REPORT NUMBER AFIT/CI/CIA - 90-092	
7. PERFORMING ORGANIZATION NAME(S) AND ADDRESS(ES) AFIT Student at: University of Utah			10. SPONSORING/MONITORING AGENCY REPORT NUMBER	
9. SPONSORING/MONITORING AGENCY NAME(S) AND ADDRESS(ES) AFIT/CI Wright-Patterson AFB OH 45433			11. SUPPLEMENTARY NOTES	
12a. DISTRIBUTION / AVAILABILITY STATEMENT Approved for Public Release IAW AFR 190-1 Distribution Unlimited ERNEST A. HAYGOOD, 1st Lt, USAF Executive Officer, Civilian Institution Programs			12b. DISTRIBUTION CODE	
<p>13. ABSTRACT</p> <p>DTIC ELECTE OCT 23 1990 S B D</p>				
14. SUBJECT TERMS			15. NUMBER OF PAGES 117	
17. SECURITY CLASSIFICATION OF REPORT UNCLASSIFIED			18. SECURITY CLASSIFICATION OF THIS CASE	
19. SECURITY CLASSIFICATION OF ABSTRACT			20. LIMITATION OF ABSTRACT	

GENERAL INSTRUCTIONS FOR COMPLETING SF 298

The Report Documentation Page (RDP) is used in announcing and cataloging reports. It is important that this information be consistent with the rest of the report, particularly the cover and title page. Instructions for filling in each block of the form follow. It is important to **stay within the lines to meet optical scanning requirements.**

Block 1. Agency Use Only (Leave Blank)

Block 2. Report Date. Full publication date including day, month, and year, if available (e.g. 1 Jan 88). Must cite at least the year.

Block 3. Type of Report and Dates Covered. State whether report is interim, final, etc. If applicable, enter inclusive report dates (e.g. 10 Jun 87 - 30 Jun 88).

Block 4. Title and Subtitle. A title is taken from the part of the report that provides the most meaningful and complete information. When a report is prepared in more than one volume, repeat the primary title, add volume number, and include subtitle for the specific volume. On classified documents enter the title classification in parentheses.

Block 5. Funding Numbers. To include contract and grant numbers; may include program element number(s), project number(s), task number(s), and work unit number(s). Use the following labels:

C - Contract	PR - Project
G - Grant	TA - Task
PE - Program Element	WU - Work Unit Accession No.

Block 6. Author(s). Name(s) of person(s) responsible for writing the report, performing the research, or credited with the content of the report. If editor or compiler, this should follow the name(s).

Block 7. Performing Organization Name(s) and Address(es). Self-explanatory.

Block 8. Performing Organization Report Number. Enter the unique alphanumeric report number(s) assigned by the organization performing the report.

Block 9. Sponsoring/Monitoring Agency Names(s) and Address(es). Self-explanatory.

Block 10. Sponsoring/Monitoring Agency Report Number. (If known)

Block 11. Supplementary Notes. Enter information not included elsewhere such as: Prepared in cooperation with...; Trans. of ..., To be published in When a report is revised, include a statement whether the new report supersedes or supplements the older report.

Block 12a. Distribution/Availability Statement. Denote public availability or limitation. Cite any availability to the public. Enter additional limitations or special markings in all capitals (e.g. NOFORN, REL, ITAR)

DOD - See DoDD 5230.24, "Distribution Statements on Technical Documents."

DOE - See authorities

NASA - See Handbook NHB 2200.2.

NTIS - Leave blank.

Block 12b. Distribution Code.

DOD - DOD - Leave blank

DOE - DOE - Enter DOE distribution categories from the Standard Distribution for Unclassified Scientific and Technical Reports

NASA - NASA - Leave blank

NTIS - NTIS - Leave blank.

Block 13. Abstract. Include a brief (Maximum 200 words) factual summary of the most significant information contained in the report.

Block 14. Subject Terms. Keywords or phrases identifying major subjects in the report.

Block 15. Number of Pages. Enter the total number of pages.

Block 16. Price Code. Enter appropriate price code (NTIS only).

Blocks 17. - 19. Security Classifications. Self-explanatory. Enter U.S. Security Classification in accordance with U.S. Security Regulations (i.e., UNCLASSIFIED). If form contains classified information, stamp classification on the top and bottom of the page.

Block 20. Limitation of Abstract. This block must be completed to assign a limitation to the abstract. Enter either UL (unlimited) or SAR (same as report). An entry in this block is necessary if the abstract is to be limited. If blank, the abstract is assumed to be unlimited.

**A FINITE DIFFERENCE NUMERICAL ANALYSIS OF HEAT
TRANSFER IN ATHEROMATOUS PLAQUE FOR
PERCUTANEOUS TRANSLUMINAL MICROWAVE
ANGIOPLASTY**

by

Lori Ann Yuk Lan Young

**A thesis submitted to the faculty of
The University of Utah
in partial fulfillment of the requirements for the degree of**

Master of Science

Department of Mechanical Engineering

The University of Utah

June 1990

90 10 22 086

Copyright © Lori Ann Yuk Lan Young 1990

All Rights Reserved

THE UNIVERSITY OF UTAH GRADUATE SCHOOL


SUPERVISORY COMMITTEE APPROVAL

of a thesis submitted by

Lori Ann Yuk Lan Young

This thesis has been read by each member of the following supervisory committee and by majority vote has been found to be satisfactory.

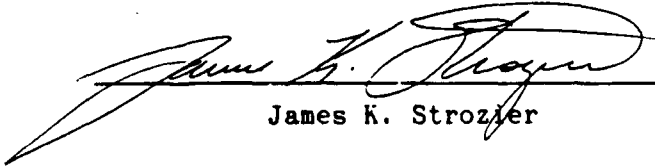
5/3/90


Chairman: Robert F. Boehm

05/03/90


Kuan Chen

3 May 90


James K. Strozler

THE UNIVERSITY OF UTAH GRADUATE SCHOOL

FINAL READING APPROVAL

To the Graduate Council of The University of Utah:

I have read the thesis of Lori Ann Yuk Lan Young in its final form and have found that (1) its format, citations, and bibliographic style are consistent and acceptable; (2) its illustrative materials including figures, tables, and charts are in place; and (3) the final manuscript is satisfactory to the Supervisory Committee and is ready for submission to the Graduate School.

5/8/90
Date



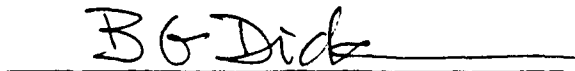
Robert F. Boehm
Member, Supervisory Committee

Approved for the Major Department:



David W. Hoepfner
Chairman, Dean

Approved for the Graduate Council



B. Gale Dick
Dean of The Graduate School

ABSTRACT

Various percutaneous transluminal angioplasty methods have been under development for the treatment of atherosclerosis. The microwave angioplasty method is a new technique that has a tremendous potential for selectively heating atheromatous plaques in arteries with minimal thermal damage. The purpose of this study is to evaluate the heat transfer within the vascular system while being exposed to a high energy electromagnetic field induced by a microwave applicator.

A heat transfer analysis was accomplished using the explicit finite difference method. The angioplasty system was modelled as a two-dimensional cylindrical coordinate thermal system to solve for the conductive heat transfer in the atheromatous plaque, vascular tissue, and muscle. As a first approximation, the convective heat transfer was modelled using a one-dimensional cylindrical coordinate system assuming steady, laminar, fully developed fluid flow and Newtonian fluid properties. Three models with different microwave applicator designs were analyzed in this study. All three models were analyzed for one second of heat generation. Further studies were also conducted to analyze the effect of pulsing the microwave heat source.

Results of this study confirm the theory of selective atheromatous plaque heating. Two of the three models produced temperatures within the 100 to 300°C range to induce plaque ablation. As heat dissipated from the plaque into the blood vessel and muscle tissue, some thermal damage was incurred. Average temperatures in the

blood vessels (60 to 70°C) were sufficiently high to initiate tissue dehydration and shrinkage. Hemolysis due to a significant amount of heating was also observed in the blood. In one of the models, blood temperatures as high as 400°C were computed in the thermal analysis. Pulsing of the microwave heat source did not initially reduce blood vessel wall temperatures. Since the blood temperatures were often higher than that of plaque, heat was always conducted in the outward radial direction. Consequently, the intima layer next to the heated plaque was highly susceptible to thermal injury.

The future of microwave angioplasty is promising. Further development of the applicator design may eliminate some of the hemolysis and tissue damage observed in this preliminary study. The shape of the microwave applicator had a significant effect on the heat generated within the plaque and surrounding tissue. Development of a heat exchanger to limit adverse blood temperature increases during treatment may be of benefit.



Accession For	
NTIS GRA&I	<input checked="checked" type="checkbox"/>
DTIC TAB	<input type="checkbox"/>
Unannounced	<input type="checkbox"/>
Justification _____	
By _____	
Distribution/	
Availability Codes	
Dist	Avail and/or Special
A-1	

TABLE OF CONTENTS

ABSTRACT	iv
LIST OF FIGURES	vii
LIST OF SYMBOLS AND NOMENCLATURE	x
ACKNOWLEDGEMENTS	xii
Chapter	
1. INTRODUCTION	1
Historical and General Background	1
Summary of Current Angioplasty Research	6
2. HEAT TRANSFER THEORY	10
Description of the Angioplasty Model	10
The Bioheat Equation	11
Finite Difference Solution of the Bioheat Equation	15
3. NUMERICAL ANALYSIS AND RESULTS	28
Investigative Procedures and Graphical Results	28
Analysis of Thermal Results	40
Discussion of the Results	53
4. CONCLUSION AND RECOMMENDATIONS	61
Conclusion	61
Recommendation for Further Study	62
Appendices	
A. THE MICROWAVE ANGIOPLASTY METHOD	64
B. THERMAL PROPERTIES OF BIOLOGICAL TISSUES	69
C. FINITE DIFFERENCE ANGIOPLASTY THERMAL ANALYSIS PROGRAM	70
D. THERMAL ANALYSIS FOR ATHEROMATOUS PLAQUE ABLATION	94
E. GLOSSARY OF MEDICAL TERMS	98
REFERENCES	101

LIST OF FIGURES

Figure	Page
1. Typical cross section of a diseased blood vessel	3
2. Restenosis in a blood vessel six months following treatment with transluminal coronary balloon angioplasty . .	5
3. Typical blood vessel cross section following transluminal coronary balloon angioplasty with vessel wall injuries	5
4. Schematic of the microwave angioplasty model	10
5. Axisymmetric percutaneous transluminal microwave angioplasty thermal model with semiinfinite boundary conditions	16
6. Interior node of a single medium (Subroutine INTRIOR)	18
7. Interior node with two media (Subroutine R2MATL)	18
8. Semiinfinite boundary node of a single medium at either of the model in the x direction (Subroutine SIDE1)	19
9. Semiinfinite boundary node with two media at either of the model in the x direction (Subroutine SIDE2)	19
10. Semiinfinite boundary interface node in the muscle tissue (Subroutine INSBND)	20
11. Semiinfinite boundary corner node in the muscle tissue (Subroutine INSCNR)	20
12. Convection at the blood vessel corners (Subroutine CONVCNR)	21
13. Convection at the blood vessel/blood or plaque/blood interfaces (Subroutine CONVBND)	21
14. Subroutine CONV3A or CONV3B	22
15. Subroutine CONV4A or CONV4B	22
16. Subroutine CONV5A or CONV5B	23
17. Subroutine CONV6A or CONV6B	23

18.	One-dimensional finite difference node for modelling convective heat transfer due to vascular blood flow	25
19.	Diagram of Model 1	29
20.	Diagram of Model 2	29
21.	SAR Distribution for Model 1	30
22.	Three-dimensional surface plot of the temperature distribution for Model 1 after one second of heat generation	31
23.	Two-dimensional contour plot of the temperature distribution for Model 1 after one second of heat generation	32
24.	SAR Distribution for Model 2	33
25.	Three-dimensional surface plot of the temperature distribution for Model 2 after one second of heat generation	34
26.	Two-dimensional contour plot of the temperature distribution for Model 2 after one second of heat generation	35
27.	Diagram of Model 3	36
28.	SAR Distribution for Model 3	37
29.	Three-dimensional surface plot of the temperature distribution for Model 3 after one second of heat generation	38
30.	Two-dimensional contour plot of the temperature distribution for Model 3 after one second of heat generation	39
31.	Rate of accumulation of damage in skin tissue as a function of increase in tissue temperature	42
32.	Temperature distribution for various materials in Model 1 at Peak 1	44
33.	Temperature distribution for various materials in Model 1 at Peak 2	45
34.	Temperature distribution for various materials in Model 1 at Peak 3	45

35.	Temperature Distribution for various materials at peak heat generation for Model 2	46
36.	Temperature Distribution for various materials at peak heat generation for Model 3	48
37.	Comparison of the effects of convective heat transfer in blood temperatures using Model 1	48
38.	Comparison of the effects of convective heat transfer in blood temperatures using Model 1 after one second of constant heat generation plus three additional seconds of cooling	49
39.	Heat dissipation after a 0.20 second pulse of microwave heat generation using Model 3	51
40.	Temperature distribution in tissues after a 0.20 second pulse of microwave heat generation using Model 3	51
41.	Temperature distributions for various plaque types	52
42.	Microwave applicator as designed by the University of Utah Department of Electrical Engineering	64
43.	The electrical conductivity in the muscle-fat-air system	65
44.	Boundary condition at the fat and muscle tissues	67
45.	Derivation of the plaque ablation explicit finite difference equation for the convective boundary node	95
46.	Derivation of the explicit finite difference equation for the blood vaporization	97

LIST OF SYMBOLS AND NOMENCLATURE

A	area, m^2
c, c_p	specific heat, $J/(kg \cdot ^\circ C)$
E	magnitude of the electric field, N/C
H	magnitude of the magnetic field, A/m
h	convective heat transfer coefficient, $W/(m^2 \cdot ^\circ C)$
h_{fg}	latent heat of fusion, vaporization, or sublimation, J/kg
h_a	convective heat transfer coefficient at the surface of the microwave applicator, $W/(m^2 \cdot ^\circ C)$
h_p	convective heat transfer coefficient at the surface of the atheromatous plaque or blood vessel, $W/(m^2 \cdot ^\circ C)$
k	thermal conductivity, $W/(m \cdot ^\circ C)$
M	mass, kg
\dot{m}	mass flow rate, $kg/(m^2 s)$
r	radius; refers to the radial direction in the angioplasty model, m
r_0	radius at the bottom of the finite difference node, m
r_1	radius at the top of the finite difference node for one material, or the radius at the interface of two dissimilar materials, m
r_2	radius at the top of the finite difference node for the case where two materials are present, m
r_a	radius at the surface of the microwave applicator, m
r_p	radius at the surface of the plaque or blood vessel, m
q_{acc}	accumulated heat stored during phase change, W/m^3
q_b	heat contribution due to blood flow, W/m^3
q_m	microwave heat generation, W/m^3
T	temperature, $^\circ C$

t time, s
V volume, m^3
x refers to the axial direction of the angioplasty model, m
 α thermal diffusivity, m^2/s
 ϵ complex permittivity
 μ permeability, N/A^2
 ρ density, kg/m^3
 σ electrical conductivity, S/m

ACKNOWLEDGEMENTS

I thank our Heavenly Father for blessing me with the opportunity and talents necessary for completing my master's degree and this project. God blesses us through our associations with others and I express my gratitude to key individuals who have been of tremendous assistance.

First of all, I thank my thesis advisor and mentor Dr. Robert F. Boehm for his outstanding guidance, support, and assistance throughout the course of this project. My appreciation is extended to Dr. Carl H. Durney (Chairman), Dr. Paul McArthur, and Wenquan Sui of the University of Utah Hyperthermia Research Group for providing the heat generation data. A special thanks goes to my friend and colleague Randy Clarksean for providing the computational facilities necessary to complete this project on time. I also thank the members of my thesis advisory committee, Dr. Kuan Chen and Dr. James K. Strozier, for their assistance and review of this project.

I am extremely grateful to the United States Air Force for their financial sponsorship of my graduate degree. In addition, I would like to recognize the staff and my program manager, Capt. Gaylene Ujcik, of the Air Force Institute of Technology for their outstanding support during the course of my studies.

For their long distance moral support, I express my sincere appreciation to my parents Alvin and Esther Young, my sisters Alva Nitta and Sandra Young, and my grandmother Adeline Young.

CHAPTER 1

INTRODUCTION

Historical and General Background

The use of heat for therapeutic applications has been exploited since ancient times. For example, heated metals and lenses were used to control the size of surface lesions and small tumors, and treat other diseases. More sophisticated methods for heating tissues, such as lasers, microwave diathermy and ultrasound, were invented during the 20th century and continue to be further developed.

Hyperthermia treatment is an application of microwave diathermy in which a microwave and radio-frequency heat generator effectively heats tumors, both malignant and nonmalignant, to remove abnormal tissues. Microwave diathermy involves the absorption of high-energy electromagnetic waves by biological tissues. The energy carried by these waves is converted into thermal energy by dielectric and resistive losses (Jain, 1985). By elevating the temperatures of the tumors to 40-42°C, researchers found that local heating of the tissues will result in a total regression of melanomas and sarcomas while increasing the survival rate of patients. The success of this application has been limited by the superior thermoregulation system within the human body, thermal properties of its tissues, and thermal tolerance of the tissues to withstand the higher temperatures without being damaged.

Recent studies have shown that the majority of the heat deposition produced by the electromagnetic field was found in the fat layer of the body (Christensen and Durney, 1981). Although this phenomenon has been detrimental in the application of hyperthermia to shrink tumors, it may be applied to treating patients with atherosclerosis. If the atheromatous plaque layer absorbs most of the heat produced by the microwave applicator, the plaque can be selectively ablated without causing thermal injury to the blood vessel and surrounding muscle tissues.

Atherosclerosis is a condition characterized by the degeneration and hardening of the walls of arteries and valves of the heart. The disease is caused by an accumulation of fatty and other substances in the inner lining of the arteries to form atheromatous plaques as shown in Figure 1. These plaques intrude upon the passageway and gradually obstruct the flow of blood (Miller and Keane, 1987). There are three basic types of atheromatous plaques: (1) calcified plaques that are hard and bony, (2) fibrous plaques that are firm and pliable, and (3) fatty plaques that are loose and buttery (Welch et al., 1985). This condition is a major cause of heart disease such as angina pectoris, coronary occlusion or coronary thrombosis (heart attack), and cerebral vascular accident (stroke).

Atherosclerosis can be treated by in vivo percutaneous transluminal angioplasty. In this procedure, a vascular catheter with an uninflated balloon is inserted into the femoral artery until it reaches the point of blockage. The balloon is then inflated to mechanically crush the plaque and recanalize the blood vessel. The transluminal angioplasty method for treating atherosclerosis is

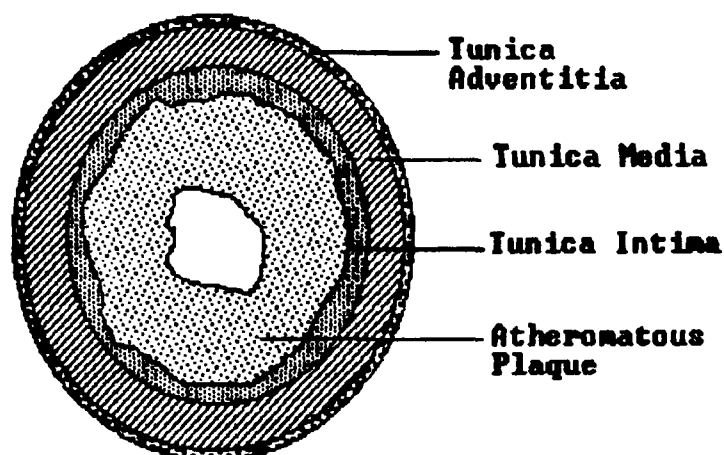


Figure 1. Typical cross section of a diseased blood vessel.

preferred over the coronary bypass in terms of patient recovery and lowered surgical complications as well as reduced medical expenses associated with this procedure.

Modern angioplasty techniques are the by-products of two important technological groundworks: (1) medical imaging based on ionizing energy or X-rays and (2) access into the vascular lumen using a catheter. The X-ray beam was first discovered by Wilhelm Konrad Roentgen in 1895. However, it was not until 1929 that R. Dos Santos et al. demonstrated the use of X-rays to visualize the aorta by using a contrast material injected into the lumbar aorta (Jang, 1986). Robb and Steinberg showed the heart and its central circulatory system could also be visualized by 1938. Several major advances took place in the 1940s with Farinas being the first to develop an aortogram technique using a catheter which was introduced into the femoral artery and threaded through the abdominal aorta (Jang, 1986). By 1948, a radial catheter technique was introduced by Radner. Although his technique lacked the sophistication and quality required to perform transluminal angioplasty, with the advent of TV monitoring systems and video

recorders to provide instant replay capability, the technology developed rapidly in the 1950s to 1970s. In 1953, a method for placing a catheter into the vascular system by surgical exposure of a blood vessel or percutaneous technique was developed by S.I. Seldinger (Jang, 1986). The concept for applying the percutaneous technique to perform transluminal angioplasties was introduced by Dotter in 1964. The first in vivo transluminal coronary angioplasty was performed by Gruentzig in Zurich, Switzerland in 1977. This procedure was introduced to the United States in 1978 by Myler and Stertzer. Since 1977 the technique for performing transluminal angioplasty has advanced significantly in the development of steerable guide-wire system and improved balloon catheters (Jang, 1986).

Thus far, transluminal coronary angioplasty has not shown a significant reduction in mortality or improvement in left ventricular function. In a six year study conducted by Simpfendorfer and associates, approximately 4,000 patients treated by transluminal coronary angioplasty between the years 1981 and 1987 showed an average primary success rate of 90 percent (Simpfendorfer et al., 1988). Despite the relatively high initial success rate, six months following treatment about one third of the patients with single vessel disease had recurring atherosclerotic lesions (restenosis) requiring retreatment or coronary bypass as shown in Figure 2. Moreover, most successful angioplasty procedures resulted in varying degrees of vessel wall injuries that occurred at the site of arterial wall dilation. These injuries included intimal splitting, subintimal dissection, medial tears, and submedial dissection as shown in Figure 3 (Duber et al., 1986).

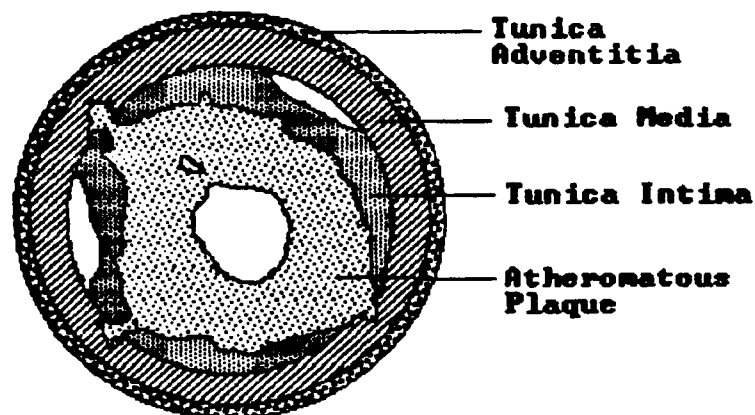


Figure 2. Restenosis in a blood vessel six months following treatment with transluminal coronary balloon angioplasty.

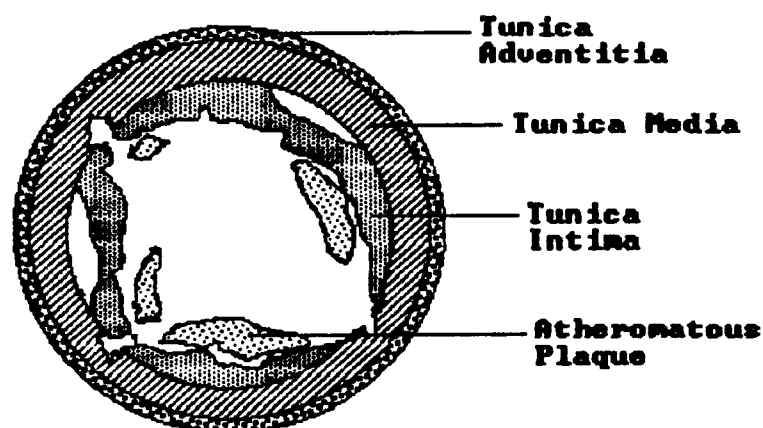


Figure 3. Typical blood vessel cross section following transluminal coronary balloon angioplasty with vessel wall injuries.

Within the past several years, much research has been done to combine transluminal coronary angioplasty with the use of a laser to ablate (or vaporize) the atheromatous plaque. Laser angioplasty provides two improvements over balloon angioplasty by opening blood vessels difficult or nearly impossible to clear, and removing the plaque by vaporization, thus reducing the probability of subsequent restenosis. In a study by Sanborn and Cumberland (Goldsmith, 1987), 34

combined laser-balloon angioplasty procedures were analyzed following a six month period. They found 26 of the 30 vessels recanalized by laser angioplasty remained well-cleared with minimal or no restenosis.

(Goldsmith, 1987) Although the ablative properties of the laser angioplasty makes this procedure an excellent inhibitor of restenosis, it does have a major problem of causing vessel wall perforation.

Summary of Current Angioplasty Research

The laser angioplasty is a relatively new technology and much research has been recently accomplished in search of a more reliable clinical application of this method. For example, much experimental work has been done to characterize various types of laser sources such as the CO₂, Nd-YAG, and argon lasers. In 1982, Abela et al. evaluated the performance of these three laser types in rabbits. In general, they found that approximately 20 to 30 joules of energy were needed to successfully ablate atherosclerotic tissues. They were also able to characterize three zones of thermal damage: (1) complete tissue vaporization, (2) thermal burning, and (3) diffuse tissue disruption. (Abela, 1982). In a 1987 thermographic study of these same lasers, Mnitentag et al. found that the CO₂ laser produced the best heat absorption while the Nd-YAG laser had the best tissue penetration characteristics (Mnitentag et al., 1987).

To minimize the complications of vascular wall perforation and thermal damage, others have experimented with variations to the original laser angioplasty technique. For example, much research and experimentation has been done with laser heated metal tips to better control the laser heating within the blood vessels. In an attempt to

understand ablation phenomena Welch et al. (1987) studied the thermal characteristics of laser probe ablation. Using a thermographic and histologic analysis they found ablation in atheromatous plaques started at 100°C and may exceed temperatures up to 180°C with heating of the adventitial tissue to temperatures in the 70°C range. In addition, ablation was more extensive in atheromatous tissue rather than nonatherosclerotic aortic tissue. Another experimental study done by Morcos, Berns and Henry revealed that the laser heated tip method increased the incidence of plaque coagulation and vasospasm, a sudden but transitory constriction of the blood vessel persisting for several hours after treatment (Morcos et al., 1988). Another variation of the laser angioplasty consists of combining laser heating with the coronary balloon method to mechanically dilate the blood vessel while thermally softening the plaque. Preliminary experimental studies conducted by White et al. demonstrated that this method produced results similar to the heated-tip and free argon laser methods and had no significant advantage over other laser angioplasty techniques due to the lack of selective heating (White et al., 1988). In a 1990 paper published by IEEE, Rosen proposed a similar technique for combining vascular dilation and thermal ablation using a microwave heat source instead of a laser, and conducted experiments using a rabbit model. In his application of this technique, the microwave heat source is used to soften the plaque to prevent vascular restenosis rather than selectively ablate the atheromatous plaque.

While many attempts have been made to develop an effective, long term treatment for atherosclerosis, none of these procedures will selectively ablate atheromas. A better understanding of the thermal

and physical behavior of atheromatous plaques is needed to devise a method that discriminates biological material types and removes abnormal tissues. Thus far, most recent research efforts have been experimental studies characterizing different types of laser sources for fiber optic delivery and their capability for plaque ablation, while studying the arterial response to find ways of controlling the laser to minimize the damage to the normal tissues. The electrical and thermal properties of atheromatous plaques are sketchy at best. Research efforts to evaluate the thermal properties of atheromatous plaques have been limited to studies conducted by Welch et al. at the University of Texas in 1985 where the average thermal conductivity and diffusivity coefficients of various types of plaques were experimentally determined (Welch et al., 1985).

Many numerical studies have been accomplished to study the bioheat equation and its application to predict the heat transfer effects due to blood perfusion in various parts of the body and in the study of hyperthermia to treat malignant tumors. However, numerical modelling of angioplasty procedures to predict the physical behavior in the atheromatous plaques and surrounding vascular tissues has been limited. In 1987, Nickolay Furzikov developed a quantitative estimate for predicting tissue destruction based on laser input power, time exposure, radiation spot size, tissue thermal conductivity, and attenuation coefficient. His thermal model agreed with experimental results although it was a crude approximation due to the lack of reliable data for the physical parameters used in his analysis (Furzikov, 1987). Decker-Dunn, at the University of Utah in 1989, developed a mathematical model to predict normal tissue damage during

laser angioplasty using a finite difference method. The Kubelka-Munk two-flux theory and modified Beer's Law were used to model the laser light incident from the laser tip (Decker-Dunn, 1989). To date, no numerical thermal analysis has been done for the microwave angioplasty technique.

This project investigates the use of a microwave heat source (as opposed to a laser) to ablate the atheromatous plaque in blood vessels. A heat transfer analysis is accomplished using a finite difference numerical analysis in a two-dimensional cylindrical coordinate system to predict the temperature distribution within the blood vessel. The result of this thermal analysis is a first approximation characterizing the thermal behavior of a microwave percutaneous transluminal angioplasty system. An analysis is completed to evaluate atheromatous plaque ablation, therapeutic benefits, possible thermal injuries caused by this technique, and the feasibility of applying this technique clinically in the future.

Further development of the finite difference heat transfer analysis is needed to increase its accuracy for clinical application. Refinements include a three-dimensional solution, detailed analyses of complex thermal and fluid phenomena such as tissue perfusion, metabolic heat generation, and non-Newtonian blood flow effects in the system, and comparative analysis with in vitro experimental results. With these improvements, cardiologists may use this thermal analysis to predict temperature distributions and prescribe the therapeutic microwave doses required to achieve adequate and safe atheromatous plaque ablation prior to surgical procedures.

CHAPTER 2

HEAT TRANSFER THEORY

Description of the Angioplasty Model

The physical system evaluated consists of four layers of dissimilar tissues, which include the blood, atheromatous plaque, blood vessel, and muscle representing the semiinfinite tissue surrounding the blood vessel. A two-dimensional cylindrical coordinate system is applied to the numerical model. As an initial approximation, the model is axially symmetric with the microwave applicator located at the center of the blood vessel. The microwave applicator is used with a balloon to restrict blood flow and prevent the blood from heating up too rapidly relative to the atheromatous plaque. A schematic of the model analyzed is shown in Figure 4.

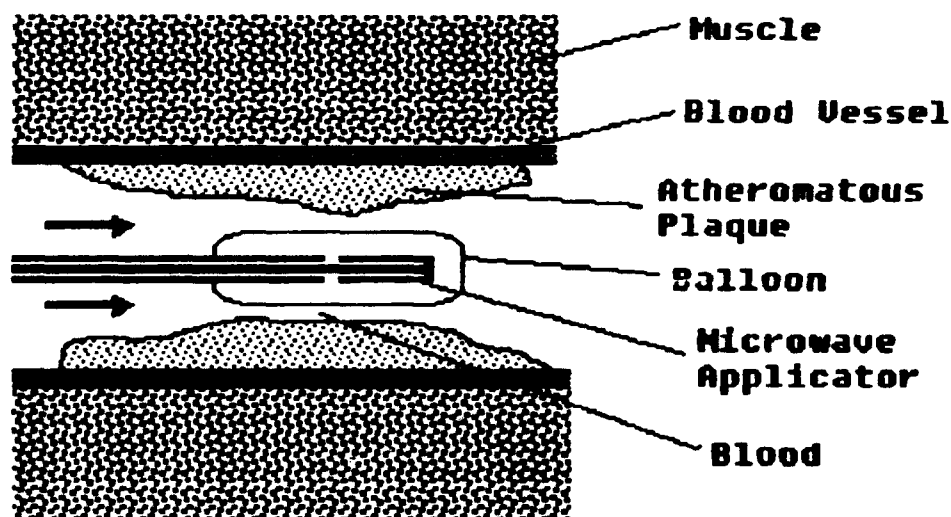


Figure 4. Schematic of the microwave angioplasty model

The Bioheat Equation

In 1948, Pennes derived the bioheat equation to analyze the tissue and blood temperatures in a resting human forearm. The bioheat equation is widely used in the analysis of many heat transfer problems with biomedical applications. The general bioheat equation is (Jain, 1985):

$$\rho c \frac{\partial T}{\partial t} = \nabla(k \nabla T) + q_b + q_m \quad (2-1)$$

where: T = tissue temperature
 c = tissue specific heat capacity
 ρ = tissue density
 k = tissue thermal conductivity
 q_b = rate of heat exchange with the blood
 q_m = rate of metabolic heat generation
 t = time

The bioheat equation is an energy balance equation about a control volume, within a biological system. The term on the left side of the equation represents the transient amount of energy stored by the control volume which produces a temperature distribution change over a period of time, t . The first term on the right side of the equation accounts for the heat being conducted through the various layers of tissues with differing thermal properties using Fourier's Law. For this particular model, conductive heat transfer is calculated for the muscle, blood vessel, and atheromatous plaque.

The second term of the bioheat equation accounts for the heat transfer due to the blood flow (also referred to as perfusion) within the body's circulatory system. In hyperthermia applications, the convective heat transfer term is normally used to account for the net

thermal energy of the arterial blood flow and the venous blood flow. For the angioplasty model, there are two types of heat transfer caused by the blood flow to the region being evaluated: (1) blood flow within the blood vessel and (2) tissue perfusion. Since heat transport for a single blood vessel is of primary interest, this analysis is limited to evaluating the heat transfer caused by the arterial blood flow. In this case, the convective heat transfer boundary conditions of the blood vessel wall/atheromatous plaque and microwave applicator are lumped into the governing bioheat equation for the blood flow. The convective heat transfer term q_b can be expressed in terms of the convective heat transfer coefficients for the vascular wall and plaque, h_p , and microwave applicator, h_a , the differential peripheral surface area of the lumen, dA , and the blood temperature, T_b , surface tissue temperature, T_p , and microwave applicator surface temperature, T_a , as shown in equation (2-2).

$$q_b dV = h_p dA_p (T_b - T_p) + h_a dA_a (T_b - T_a) \quad (2-2)$$

Finally, a third term is used to represent the heat that is generated due to natural metabolic processes in the body and external heat generation sources. The metabolic heat generation refers to the heat produced in the body as a result of oxygen consumption. This form of heat generation is calculated by multiplying the oxygen consumption by the caloric value of the oxygen (Jain, 1985). In this thermal analysis, calculation of the temperature distribution in the atheromatous plaque (which does not produce any metabolic heat generation) is of primary interest. Because the amount of metabolic heat generated in the thermal model is relatively small in comparison

to the heat absorbed by the tissues due the electromagnetic field induced in the system, it be treated as a negligible heat source and is therefore omitted from this analysis.

The major contributor of heat generation in the system is produced by a microwave applicator. The surrounding blood and tissues absorb high-energy electromagnetic waves produced by the applicator, and this energy is converted into thermal energy by the dielectric and resistive losses. The amount of microwave energy generating thermal energy in the tissues is a function of the electrical conductivity of the tissue, σ and the electric field, E (Jain, 1985).

$$Q = \frac{1}{2} \sigma E^2 \quad (2-3)$$

The electric field in equation (2-3) is computed using the Maxwell equations which form the framework of classical electromagnetic theory. For this particular application the finite difference time domain (FDTD) technique was used to solve these equations. Heat generated by the microwave applicator was solved directly using equations (2-4) and (2-5).

$$\nabla \times E = -\mu \frac{\partial H}{\partial t} \quad (2-4)$$

$$\nabla \times H = J + \epsilon \frac{\partial E}{\partial t} \quad (2-5)$$

where: E = electric field

H = magnetic field

μ = material permeability

ϵ = complex permittivity

t = time

In general, microwave diathermy studies applied in hyperthermia treatments have shown that tissues containing high water concentrations such as muscle, skin, and internal organ tissues have high absorption and low depth of penetration characteristics. On the other hand, tissues with low water content such as fat and bone tissue tend to have low absorption and high penetration properties (Jain, 1985).

As a first approximation for applying the bioheat equation to the transluminal microwave angioplasty model, modifications to the basic equations were required. First of all, the heat transfer model was reduced to a two-dimensional axially-symmetric cylindrical coordinate system (r,x) reducing the bioheat equation to the following form.

$$\frac{1}{\alpha} \frac{\partial T}{\partial t} = \frac{\partial^2 T}{\partial r^2} + \frac{1}{r} \frac{\partial T}{\partial r} + \frac{\partial^2 T}{\partial x^2} + \frac{q_a}{k} + \frac{q_b}{k} \quad (2-6)$$

where: q_a = heat generated by the microwave applicator

α = tissue thermal diffusivity

k = tissue thermal conductivity

T = tissue temperature

t = time

q_b = heat transfer of the blood

The Φ term is eliminated from the governing equation since symmetry with respect to the axial direction is assumed, and the temperature distribution does not vary significantly in this direction of the thermal model. In actual situations where the geometry of the atheromatous plaque may be highly irregular, this assumption may not lend itself to an accurate approximation. However,

as an initial analysis to predict the heat distribution of the transluminal microwave angioplasty system and evaluate the feasibility of its application, a two-dimensional system will be analyzed.

Finite Difference Solution Of the Bioheat Equation

Because of the highly irregular geometry of the atheromatous plaques, an analytical solution for the angioplasty model is not available. A finite difference method is applied to solve numerically the bioheat equation. There are three methods for evaluating the time derivative: (1) the pure implicit method, (2) the Crank-Nicolson implicit method, and (3) Euler explicit method. The implicit methods are generally more advantageous because they do not produce the numerical oscillations that may occur if too large a time step is used. However, the explicit method was used in view of its simplicity and fewer number of calculations. Unlike the implicit methods, a gaussian simultaneous equation solver subroutine is not required because the new temperatures are computed directly from the physical formulation equations derived.

To apply the explicit finite difference method, a two dimensional grid was established with semiinfinite and convective boundary conditions as shown in Figure 5.

The finite difference program developed for this thesis project computes the transient heat and mass transport only. Another finite difference program to compute the energy deposition from the microwave applicator developed by Paul McArthur and Wenquan Sui of the University of Utah, Hyperthermia Research Group, Department of Electrical

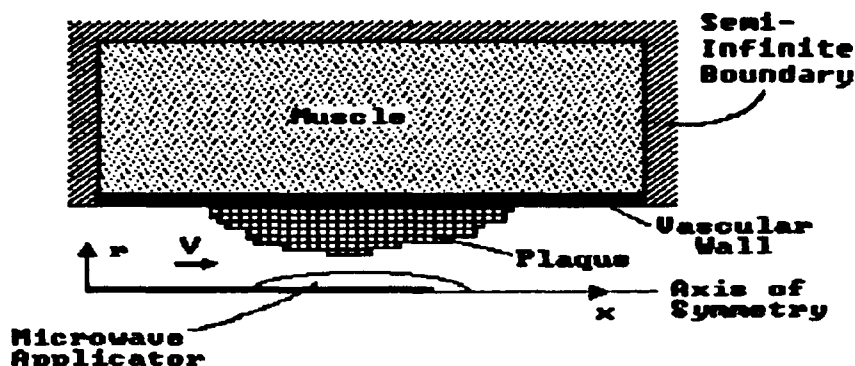


Figure 5. Axisymmetric percutaneous transluminal microwave angioplasty thermal model with semiinfinite boundary conditions.

Engineering was merged with this program to predict the overall temperature distribution of the microwave angioplasty model.

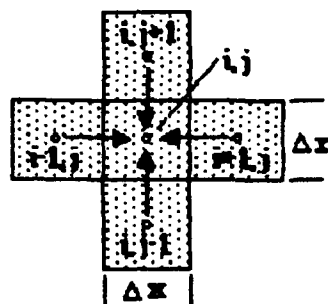
The thermal models analyzed were generated by a model generator program developed by Paul McArthur of the Department of Electrical Engineering. Modifications to the coordinate system were made to accommodate the heat deposition data passed to this program in order to compute the temperatures at the boundary interfaces to solve accurately for temperatures where both conduction and convective heat transfer was occurring at the same node. This was accomplished by shifting the two dimensional cylindrical grid system by $DR/2$ and $DX/2$ in the x and r directions, respectively. The new heat deposition values at these new points were calculated using the cubic spline interpolation method.

The numerical solution consists of twelve different types of finite different nodes to simulate the conduction heat transfer process within the muscle, blood vessel, and atheromatous plaque. Each node type was derived using the physical formulation method to account for the various internal, boundary, and multiproperty nodes modelled in the analysis. Calculations for the coefficients of the temperature at the node being evaluated ($T_{i,j}$) were also done using the Biot and Fourier

Numbers. This calculation was extremely valuable in preventing the occurrence of unstable oscillations in any part of the numerical solution.

The energy balance and finite difference equations for each of the twelve nodes used in the finite difference analysis are shown in Figures 6 through 17 on the following pages. The first set of physical formulations (Figures 6 to 11) represent the finite difference nodes occurring at the insulated and interior layers of tissue in the thermal model. The nodes displayed in Figures 12 to 17 nodes are used at the convective boundary layers of the atheromatous plaque or blood vessel. At the boundary interfaces, semiinfinite conditions were assumed at both ends in the x direction and for relatively large radius values where the muscle tissues are not affected by heat conduction and the high-energy electromagnetic waves. The nodes at these boundaries are approximated as insulated surfaces.

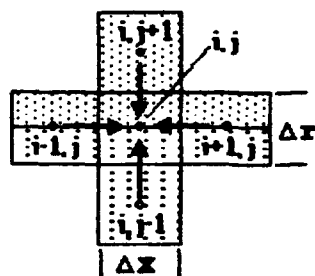
In figures showing more than one configuration the energy balance equation is given for the figure on the left side. The other equation may be easily derived by changing the subscripts for the symmetrical case. For the finite difference cells containing one material type, R_0 refers to the inner radius closed to the microwave applicator and R_1 refers to the outer radius. In cells with two material types, R_0 is again the inner radius, R_1 represents the radius at the interface of the two dissimilar materials, and R_2 refers to the outer radius.



$$\rho c [\pi(r_1^2 - r_0^2) \Delta x] \frac{T'_{i,j} - T_{i,j}}{\Delta t} = \frac{T_{i,j-1} - T_{i,j}}{\frac{\Delta r}{k_2 \pi r_0 \Delta x}} + \frac{T_{i,j+1} - T_{i,j}}{\frac{\Delta r}{k_2 \pi r_1 \Delta x}} +$$

$$\frac{T_{i-1,j} - T_{i,j}}{\frac{\Delta x}{k \pi (r_1^2 - r_0^2)}} + \frac{T_{i+1,j} - T_{i,j}}{\frac{\Delta x}{k \pi (r_1^2 - r_0^2)}} + q_a \pi (r_1^2 - r_0^2) \Delta x \quad (2-7)$$

Figure 6. Interior node of a single medium (Subroutine INTRIOR).



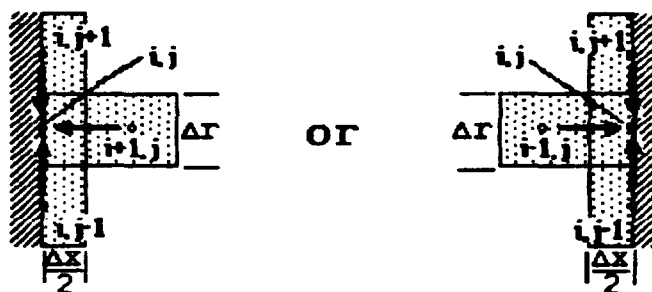
$$\rho_1 c_1 [\pi(r_1^2 - r_0^2) \Delta x] \frac{T'_{i,j} - T_{i,j}}{\Delta t} + \rho_2 c_2 [\pi(r_2^2 - r_1^2) \Delta x] \frac{T'_{i,j} - T_{i,j}}{\Delta t} =$$

$$\frac{T_{i,j-1} - T_{i,j}}{\frac{\Delta r}{k_1 2 \pi r_0 \Delta x}} + \frac{T_{i,j+1} - T_{i,j}}{\frac{\Delta r}{k_2 2 \pi r_2 \Delta x}} + \frac{T_{i-1,j} - T_{i,j}}{\frac{\Delta x}{k_1 \pi (r_1^2 - r_0^2)}} +$$

$$\frac{T_{i-1,j} - T_{i,j}}{\frac{\Delta x}{k_2 \pi (r_2^2 - r_1^2)}} + \frac{T_{i+1,j} - T_{i,j}}{\frac{\Delta x}{k_1 \pi (r_1^2 - r_0^2)}} + \frac{T_{i+1,j} - T_{i,j}}{\frac{\Delta x}{k_2 \pi (r_2^2 - r_1^2)}} +$$

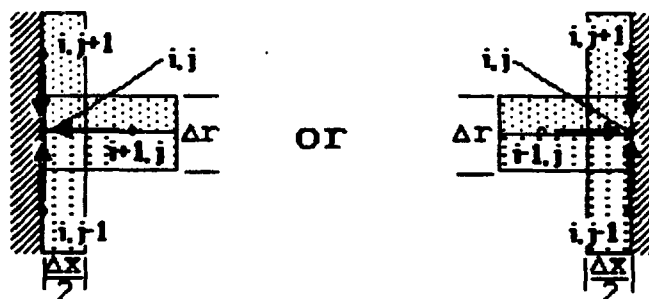
$$+ q_a \pi (r_2^2 - r_0^2) \Delta x \quad (2-8)$$

Figure 7. Interior node with two media (Subroutine R2MATL).



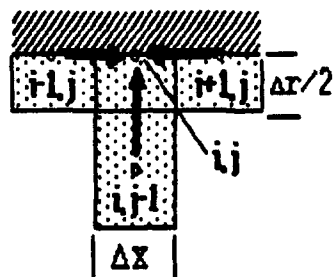
$$\rho c [\pi(r_1^2 - r_0^2) \frac{\Delta x}{2}] \frac{T'_{i,j} - T_{i,j}}{\Delta t} = \frac{T_{i+1,j} - T_{i,j}}{\frac{\Delta x}{k\pi(r_1^2 - r_0^2)}} + \frac{T_{i,j+1} - T_{i,j}}{\frac{\Delta r}{k\pi r_1 \Delta x}} + \frac{T_{i,j-1} - T_{i,j}}{\frac{\Delta r}{k\pi r_0 \Delta x}} + q_a \pi(r_1^2 - r_0^2) \frac{\Delta x}{2} \quad (2-9)$$

Figure 8. Semiinfinite boundary node of a single medium at either end of the model in the x direction (Subroutine SIDE1).



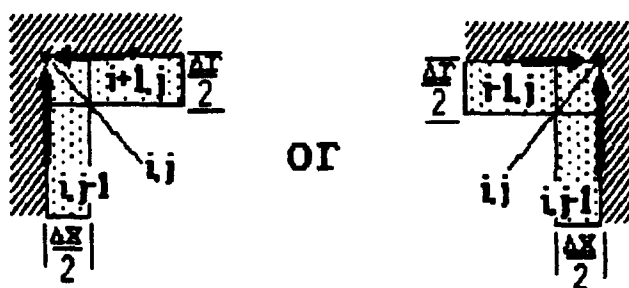
$$\rho_1 c_1 [\pi(r_1^2 - r_0^2) \frac{\Delta x}{2}] \frac{T'_{i,j} - T_{i,j}}{\Delta t} + \rho_2 c_2 [\pi(r_2^2 - r_1^2) \frac{\Delta x}{2}] \frac{T'_{i,j} - T_{i,j}}{\Delta t} = \frac{T_{i+1,j} - T_{i,j}}{\frac{\Delta x}{k_1 \pi(r_1^2 - r_0^2)}} + \frac{T_{i+1,j} - T_{i,j}}{\frac{\Delta x}{k_2 \pi(r_2^2 - r_1^2)}} + \frac{T_{i,j+1} - T_{i,j}}{\frac{\Delta r}{k_2 \pi r_2 \Delta x}} + \frac{T_{i,j-1} - T_{i,j}}{\frac{\Delta r}{k_1 \pi r_0 \Delta x}} + q_a \pi(r_2^2 - r_1^2) \frac{\Delta x}{2} \quad (2-10)$$

Figure 9. Semiinfinite boundary node with two media at either end of the model in the x direction (Subroutine SIDE2).



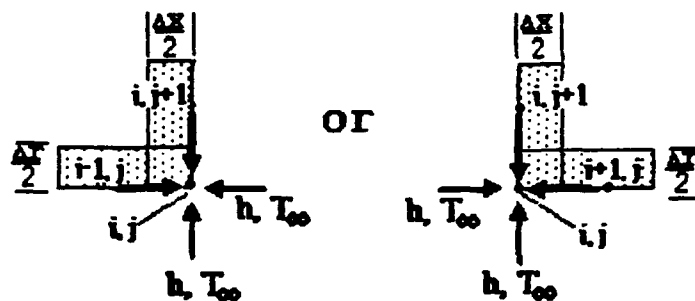
$$\rho c [\pi(r_1^2 - r_0^2) \Delta x] \frac{T_{i,j}^{n+1} - T_{i,j}^n}{\Delta t} = \frac{T_{i,j-1}^n - T_{i,j}^n}{\frac{\Delta r}{k 2 \pi r_0 \Delta x}} + \frac{T_{i-1,j}^n - T_{i,j}^n}{\frac{\Delta x}{k \pi (r_1^2 - r_0^2)}} + \frac{T_{i+1,j}^n - T_{i,j}^n}{\frac{\Delta x}{k \pi (r_1^2 - r_0^2)}} + q_a \pi (r_1^2 - r_0^2) \Delta x \quad (2-11)$$

Figure 10. Semiinfinite boundary interface node in the muscle tissue (Subroutine INSBND).



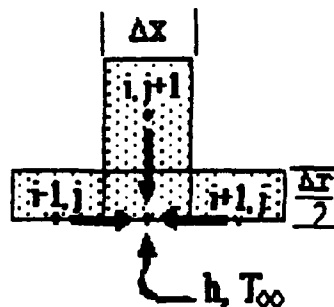
$$\rho c [\pi(r_1^2 - r_0^2) \frac{\Delta x}{2}] \frac{T_{i,j}^{n+1} - T_{i,j}^n}{\Delta t} = \frac{T_{i+1,j}^n - T_{i,j}^n}{\frac{\Delta x}{k \pi (r_1^2 - r_0^2)}} + \frac{T_{i,j-1}^n - T_{i,j}^n}{\frac{\Delta r}{k 2 \pi r_0 \Delta x}} + q_a \pi (r_1^2 - r_0^2) \frac{\Delta x}{2} \quad (2-12)$$

Figure 11. Semiinfinite boundary corner node in the muscle tissue (Subroutine INSCNR).



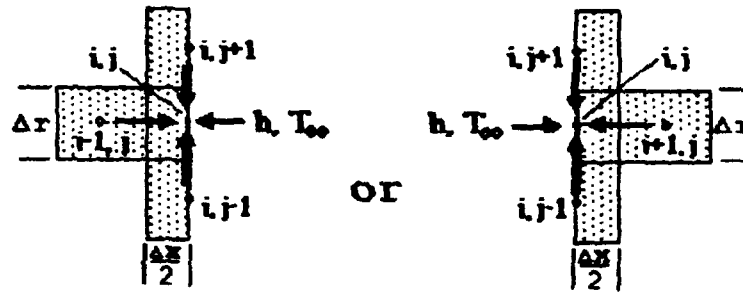
$$\rho c [\pi(r_1^2 - r_0^2) \frac{\Delta x}{2}] \frac{T'_{i,j} - T_{i,j}}{\Delta t} = \frac{T_{i,j+1} - T_{i,j}}{\frac{\Delta r}{k\pi r_1 \Delta x}} + \frac{T_{i+1,j} - T_{i,j}}{\frac{\Delta x}{k\pi(r_1^2 - r_0^2)}} + \frac{T_{\infty} - T_{i,j}}{\frac{1}{h(\pi r_0 \Delta x)}} + q_a \pi(r_1^2 - r_0^2) \frac{\Delta x}{2} \quad (2-13)$$

Figure 12. Convection at the blood vessel corners (Subroutine CONVCLR).



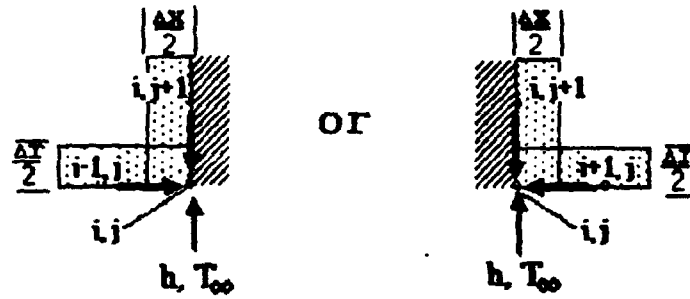
$$\rho c [\pi(r_1^2 - r_0^2) \Delta x] \frac{T'_{i,j} - T_{i,j}}{\Delta t} = \frac{T_{i-1,j} - T_{i,j}}{\frac{\Delta x}{k\pi(r_1^2 - r_0^2)}} + \frac{T_{i+1,j} - T_{i,j}}{\frac{\Delta x}{k\pi(r_1^2 - r_0^2)}} + \frac{T_{i,j+1} - T_{i,j}}{\frac{\Delta r}{k2\pi r_1 \Delta x}} + \frac{T_{\infty} - T_{i,j}}{\frac{1}{h(2\pi r_0 \Delta x)}} + q_a \pi(r_1^2 - r_0^2) \Delta x \quad (2-14)$$

Figure 13. Convection at the blood vessel/blood or plaque/blood interfaces (Subroutine CONVBND).



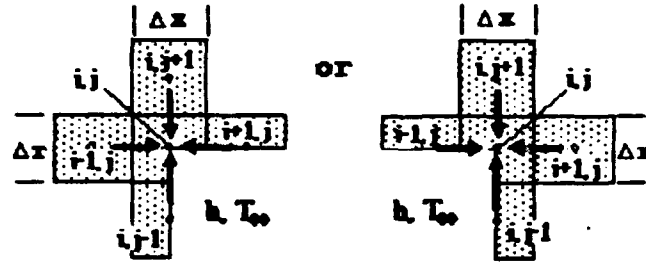
$$\rho c [\pi(r_1^2 - r_0^2) \frac{\Delta x}{2}] \frac{T'_{i,j} - T_{i,j}}{\Delta t} = \frac{T_{i-1,j} - T_{i,j}}{\frac{\Delta x}{k\pi(r_1^2 - r_0^2)}} + \frac{T_{i,j+1} - T_{i,j}}{\frac{\Delta r}{k\pi r_1 \Delta x}} + \frac{T_{i,j-1} - T_{i,j}}{\frac{\Delta r}{k\pi r_0 \Delta x}} + \frac{T_\infty - T_{i,j}}{\frac{1}{h\pi(r_1^2 - r_0^2)}} + q_\infty \pi(r_1^2 - r_0^2) \frac{\Delta x}{2} \quad (2-15)$$

Figure 14. Subroutine CONV3A or CONV3B.



$$\rho c [\pi(r_1^2 - r_0^2) \frac{\Delta x}{2}] \frac{T'_{i,j} - T_{i,j}}{\Delta t} = \frac{T_{i-1,j} - T_{i,j}}{\frac{\Delta x}{k\pi(r_1^2 - r_0^2)}} + \frac{T_{i,j+1} - T_{i,j}}{\frac{\Delta r}{k\pi r_1 \Delta x}} + \frac{T_\infty - T_{i,j}}{\frac{1}{h\pi(r_1^2 - r_0^2)}} + \frac{T_\infty - T_{i,j}}{\frac{1}{h\pi r_0 \Delta x}} + q_\infty \pi(r_1^2 - r_0^2) \frac{\Delta x}{2} \quad (2-16)$$

Figure 15. Subroutine CONV4A or CONV4B.

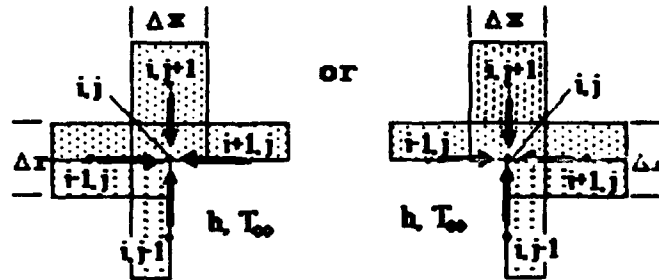


$$\rho c \Delta V \frac{T'_{i,j} - T_{i,j}}{\Delta t} = \frac{T_{i-1,j} - T_{i,j}}{\frac{\Delta x}{k\pi(r_2^2 - r_0^2)}} + \frac{T_{i+1,j} - T_{i,j}}{\frac{\Delta x}{k\pi(r_2^2 - r_1^2)}} + \frac{T_{i,j-1} - T_{i,j}}{\frac{\Delta r}{k\pi r_0 \Delta x}} +$$

$$\frac{T_{i,j+1} - T_{i,j}}{\frac{\Delta r}{k2\pi r_2 \Delta x}} + \frac{T_\infty - T_{i,j}}{\frac{1}{h\pi r_1 \Delta x}} + \frac{T_\infty - T_{i,j}}{\frac{1}{h\pi(r_1^2 - r_0^2)}} + q_\infty \Delta V \quad (2-17)$$

$$\Delta V = \pi(r_2^2 - r_0^2)\Delta x - \pi(r_1^2 - r_0^2)\frac{\Delta x}{2} \quad (2-18)$$

Figure 16. Subroutine CONV5A or CONV5B



$$\left[(\rho c)_1 \pi(r_1^2 - r_0^2) \frac{\Delta x}{2} + (\rho c)_2 \pi(r_2^2 - r_1^2) \Delta x \right] \frac{T'_{i,j} - T_{i,j}}{\Delta t} =$$

$$\frac{T_{i-1,j} - T_{i,j}}{\frac{\Delta x}{k_1 \pi(r_1^2 - r_0^2)}} + \frac{T_{i+1,j} - T_{i,j}}{\frac{\Delta x}{k_2 \pi(r_2^2 - r_1^2)}} + \frac{T_{i,j-1} - T_{i,j}}{\frac{\Delta r}{k_2 \pi(r_2^2 - r_1^2)}} +$$

$$\frac{T_{i,j+1} - T_{i,j}}{\frac{\Delta r}{k_1 \pi r_0 \Delta x}} + \frac{T_{i,j+1} - T_{i,j}}{\frac{\Delta r}{k_2 2\pi r_2 \Delta x}} + \frac{T_\infty - T_{i,j}}{\frac{1}{h\pi(r_1^2 - r_0^2)}} +$$

$$\frac{T_\infty - T_{i,j}}{\frac{1}{h\pi r_1 \Delta x}} + q_\infty \pi \left[(r_2^2 - r_0^2) \Delta x - (r_1^2 - r_0^2) \frac{\Delta x}{2} \right] \quad (2-19)$$

Figure 17. Subroutine CONV6A or CONV6B

Heat transfer to or from the blood flow was calculated in a separate subroutine. As an initial approximation, the convective heat and mass transfer of the blood was solved numerically using a one dimensional finite difference model. The convective heat transfer coefficient was estimated using the two analytical solutions: (1) the solution for a concentric annular pipe which gives the Nusselt Numbers as a function of the ratio of the microwave applicator radius and blood vessel or plaque radius and (2) the solution for circular pipe flow (see equation 2-20). In order to use these solutions, the temperature and velocity profiles of the blood flow were assumed to be steady and fully developed laminar flows. A cubic spline interpolation method was used to calculate the average Nusselt numbers between the values given in Table 1 for the concentric annular pipe solution. The convective heat transfer coefficient is then calculated knowing the hydraulic diameter and thermal conductivity by the following equations.

$$Nu = \frac{hD_h}{k} = 3.66 \quad (2-20)$$

$$D_h = 2(r_o - r_i) \quad (2-21)$$

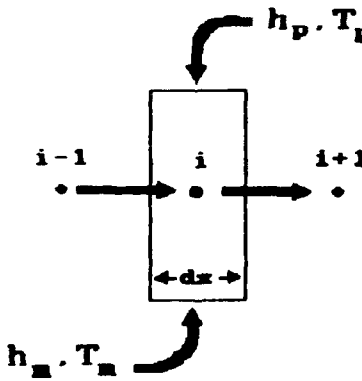
$$h = \frac{Nuk}{D_h} \quad (2-22)$$

A similar derivation of the finite difference energy balance equation for each one-dimensional element was conducted to simulate the heat transfer contribution due to the blood flow in the system. The finite difference equation accounts for the advection of the blood flow through each control volume, the convective heat transfer from the microwave applicator and vascular/plaque boundary conditions, and transient heat storage of the blood. Figure 18 shows a typical one

Table 1. Circular-Tube-Annulus Convective Heat Transfer Solution

r^*	Nu_p	Nu_a
0.00	∞	4.364
0.05	17.81	4.792
0.10	11.91	4.834
0.20	8.499	4.883
0.40	6.583	4.979
0.60	5.912	5.099
0.80	5.58	5.24
1.00	5.385	5.385

Note: Analytical solution for the concentric circular-tube annulus with laminar, fully developed velocity and temperature profiles as a function of $r^*=r_a/r_p$ where the subscript a refers to the microwave applicator and p refers to the plaque or vascular wall. Nu_p and Nu_a represent the respective Nusselt numbers. (Adapted from Kays & Crawford, 1980)



$$\frac{[m c_p (T_{i-1} - T_i) + m c_p (T_{i+1} - T_i)]}{\Delta x} + 2\pi r_a h_a (T_a - T_i) + 2\pi r_p h_p (T_p - T_i) +$$

$$q_a [\pi (r_a^2 - r_p^2)] = \rho c_p \pi (r_a^2 - r_p^2) \frac{(T_i' - T_i)}{\Delta t} \quad (2-22)$$

Figure 18. One-dimensional finite difference node for modelling convective heat transfer due to vascular blood flow.

dimensional finite difference element with its accompanying governing energy equation derived using the physical formulation method.

The maximum possible velocity of the blood was computed assuming an average flow rate of 250 ml/min and dividing by the difference of the cross-sectional area of the lumen and the area of the microwave applicator. Blood mass flow rates vary depending on the rate the heart is pumping and the part of the body where the blood vessel is located. Since this program may be used for applying the microwave angioplasty technique for other parts of the body with lower mass flow rates, the computer code has been written to accommodate other thermal models with slower blood flow rates.

As a first approximation the thermal model of the blood flow does not account for the heat transfer caused by tissue perfusion, the rate of heat exchange occurring in the microvasculature of the surrounding muscle tissues (Shitzer, 1985). Microcirculation provides the means by which heat generated by the microwave applicator is dissipated within the muscle layers. For the transluminal angioplasty model, heat transfer due the microvascular blood flow is negligible relative to the heat being generated in the system and conducted to the blood within the vessel during treatment. The mathematical models using the Beer's Law and Kubelka-Munk two-flux theory developed by Decker-Dunn for the laser angioplasty model also confirms this assumption. Her studies showed that there were no significant theoretical changes by modelling the tissue perfusion contribution in her thermal analysis (Decker-Dunn et al., 1989).

In modelling the blood flow it was assumed the flow throughout the system was laminar. The Reynolds number was calculated using an

average artery diameter of 0.4 cm, total blood flow rate in the human body of 250 ml/min, blood density of 1.057 gm/cm^3 , and a dynamic viscosity of 0.034 gm/cm sec . This yielded a value for the Reynolds number of 412, which is considerably less than the critical Reynolds number of 2000 for laminar flow. With a fifty percent occluded artery (artery diameter of 0.2828 cm) and a microwave applicator diameter of 0.2 cm, using the hydraulic diameter for a concentric annular tube, the calculated Reynolds number is 1991. This is the maximum possible Reynolds number since blood flow in the arteries is usually less than 250 ml/min and varies considerably depending upon the individual and the location of the blood vessel. Although blood is a non-Newtonian fluid since the viscosity of blood varies with the percentage of red blood cells present (the hematocrit), blood viscosity does not change significantly over normal ranges of flow in larger blood vessels (Selkurt, 1982). Therefore, for the purposes of this study a constant viscosity was assumed and the blood flow was treated as a Newtonian fluid.

The explicit finite difference equations with ablation are similarly derived. See Appendix D for a detailed analysis of the development of these equations.

CHAPTER 3

NUMERICAL ANALYSIS AND RESULTS

Investigative Procedures and Graphical Results

The Finite Difference Angioplasty Thermal Analysis (FDATA) program was applied to three different microwave angioplasty models generated by the University of Utah Hyperthermia Research Group. Heat generation data were computed using a Finite Difference Time Domain (FDTD) method to solve for the electric and magnetic fields. These data were read into the FDATA program to compute the temperature distribution for one second heat generation by the microwave applicator. The heat generation data calculated by the Hyperthermia Group assume steady state conditions. Therefore, the heat absorbed by various tissues was calculated independently of the FDATA program. The heat generated at each node is treated as a step function where heat is suddenly turned on and maintained at a constant for one second.

The first two models analyzed are pictured in Figures 19 and 20. A 200 by 30 cylindrical grid system was constructed with a cell size of 0.14286 cm in both the x and r directions. A corresponding time step of 2.5×10^{-4} seconds was used without causing any unstable oscillations in the finite difference solution. Three-dimensional graphs of the initial specific absorption rate or SAR (see Appendix A for a more detailed discussion of selective microwave heating) distribution for Models 1 and 2 are shown in Figures 21 and 22, respectively. The

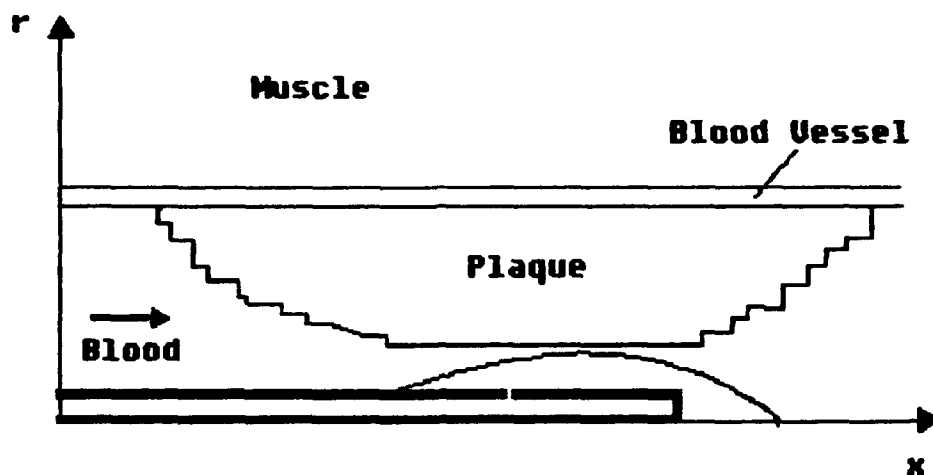


Figure 19. Diagram of Model 1

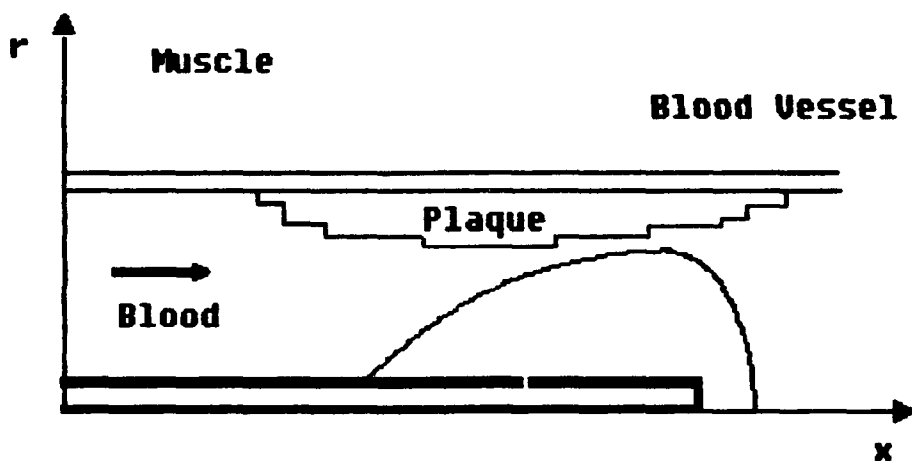


Figure 20. Diagram of Model 2

resulting temperature distributions after one second of microwave heating is exhibited in Figures 23 through 26. The results are displayed as both three-dimensional surface and two-dimensional contour graphs.

A third model was generated to simulate better actual dimensions within the vascular system. The model was generated using typical dimensions for an average artery having a lumen diameter of 0.4 cm and

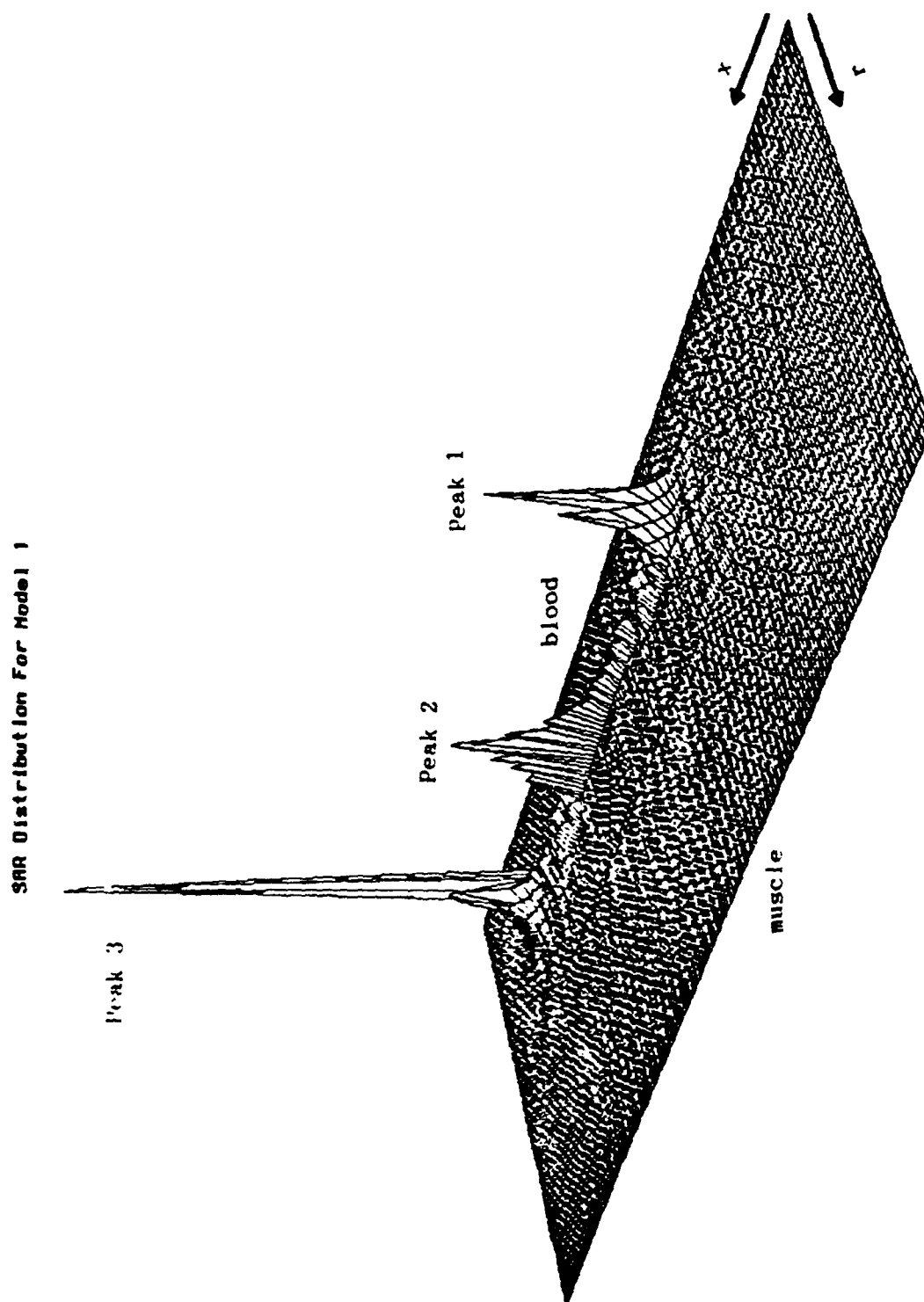


Figure 21. SAR Distribution for Model 1.

Thermal Distribution For Model 1 ($t = 1$ sec)
 $dx=0.001429$ m, $dr=0.001429$ m, $dt=0.00025$ sec, $mult=600000.0$

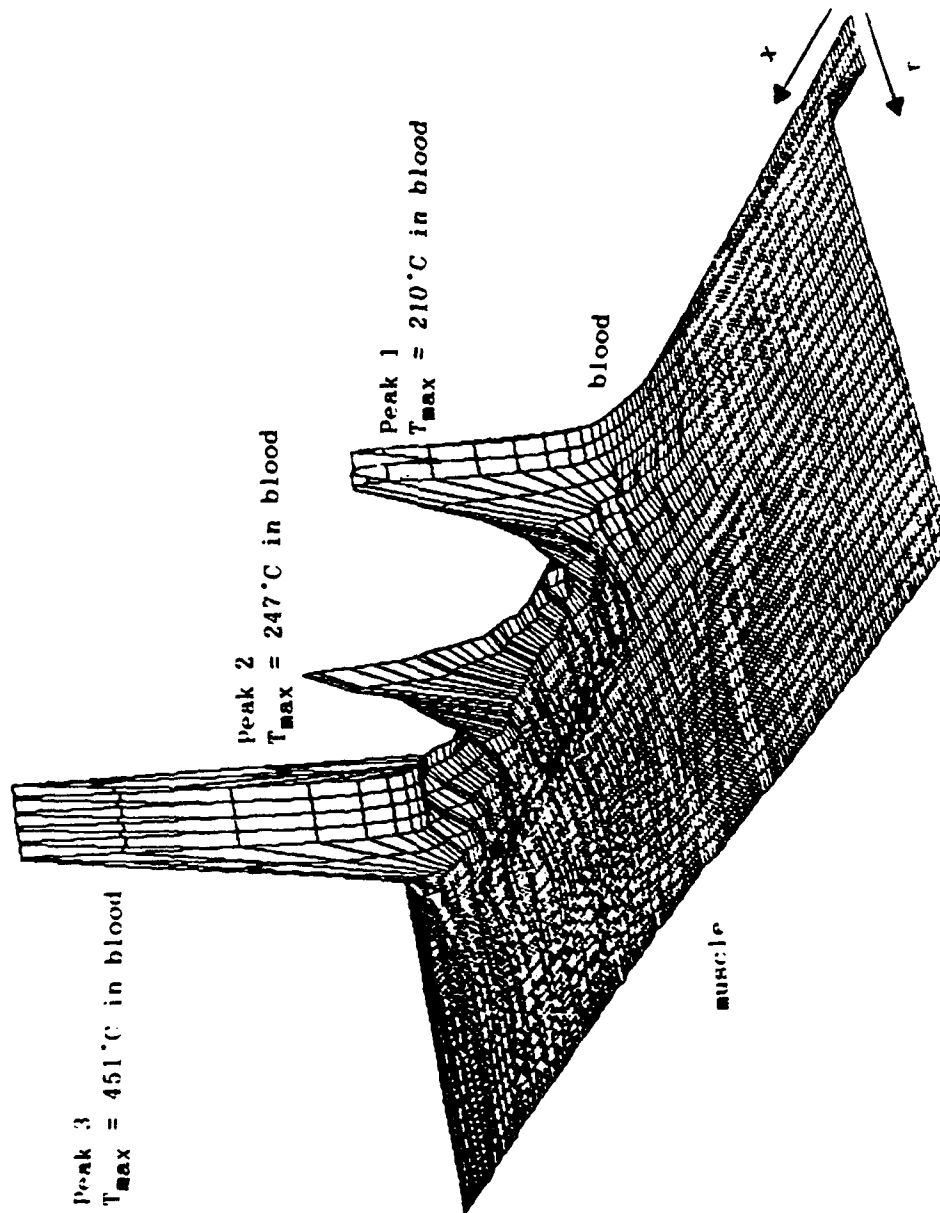


Figure 22. Three-dimensional surface plot of the temperature distribution for Model 1 after one second of heat generation.

Thermal Distribution For Model 1 (at $t=1$ sec)
 $dx=0.001429$ m, $dr=0.001429$ m, $dt=0.00025$ sec, $mult=6000000.0$

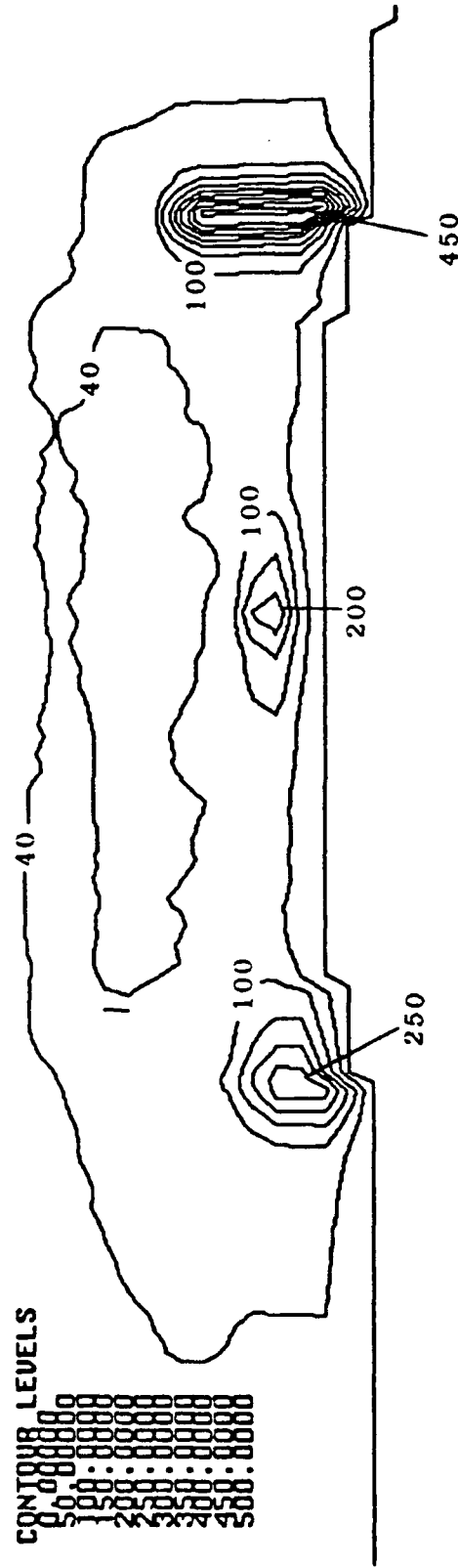


Figure 23. Two-dimensional contour plot of the temperature distribution for Model 1 after one second of heat generation.

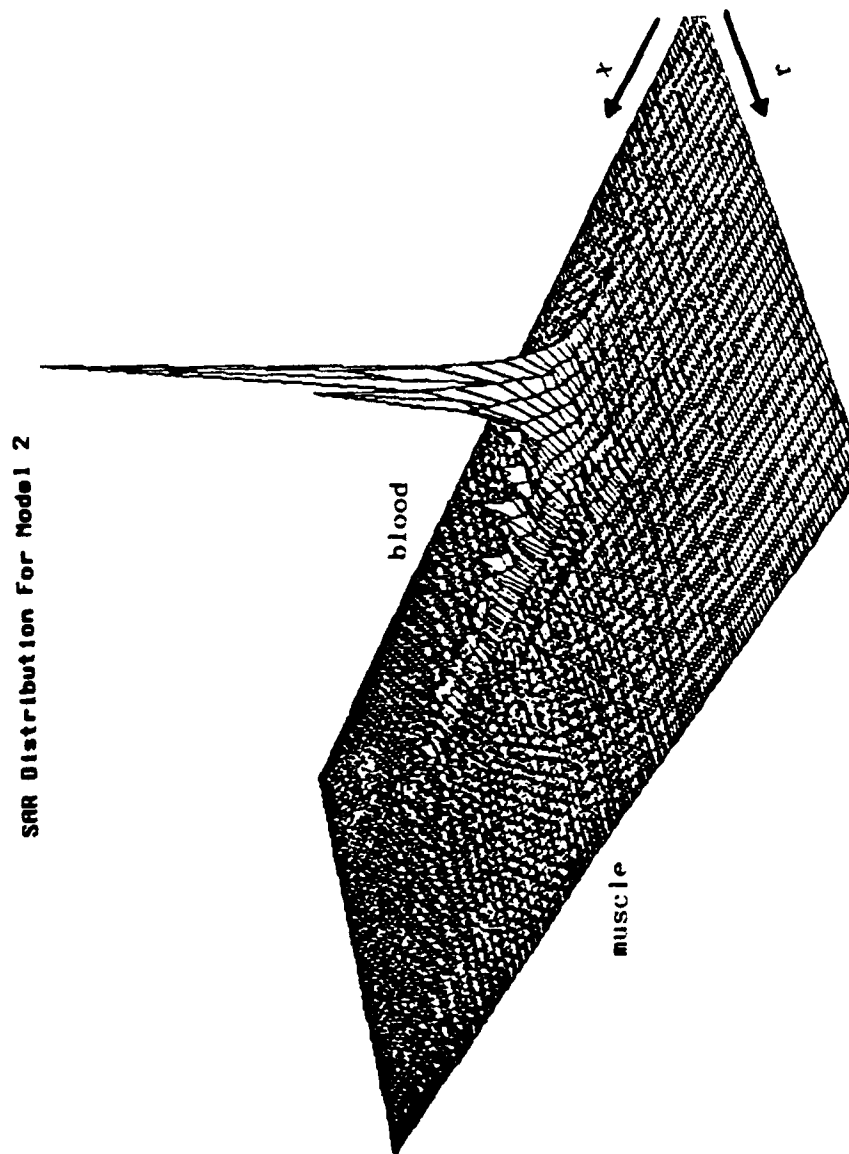


Figure 24. SAR Distribution for Model 2.

Thermal Distribution For Model 2 (at $t=1$ sec)
 $dx=0.001429$ m, $dr=0.001429$ m, $dt=0.00025$ sec, $mult=600000.0$

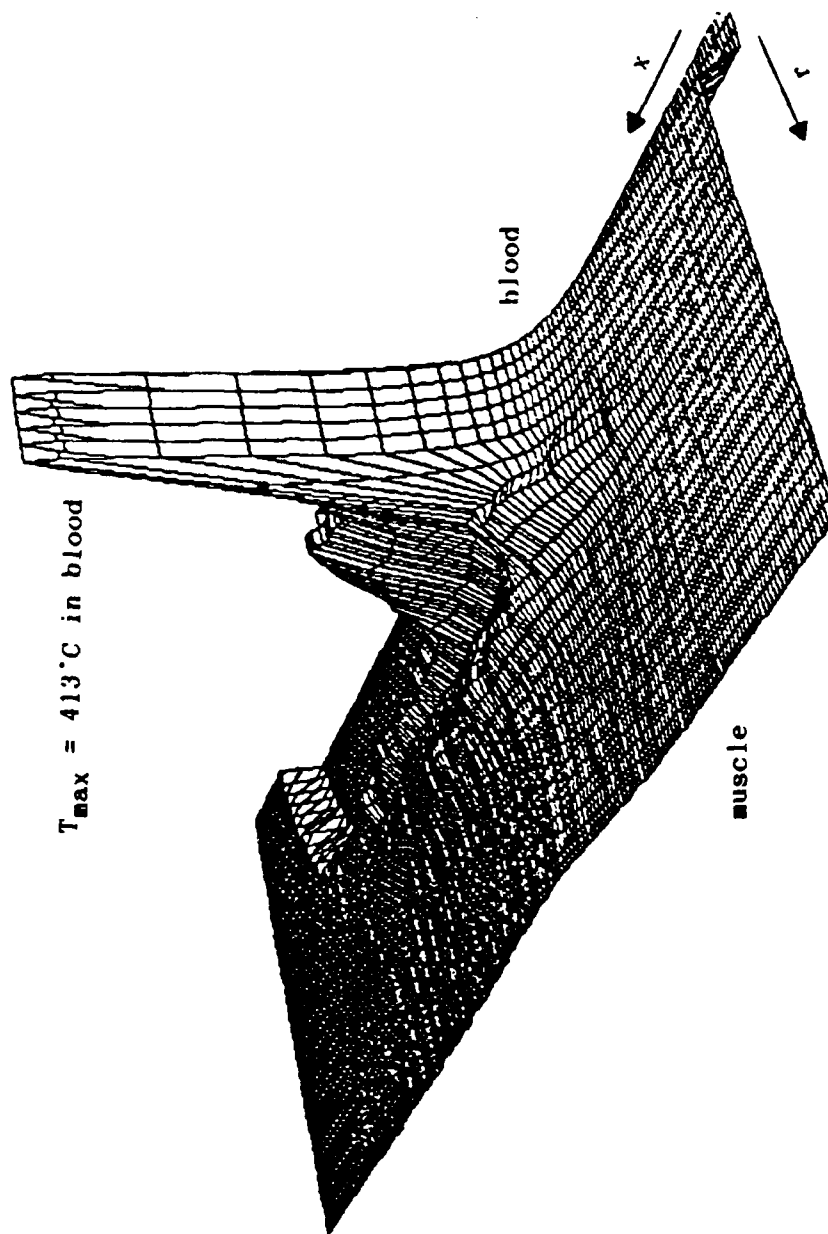


Figure 25. Three-dimensional surface plot of the temperature distribution for Model 2 after one second of heat generation.

Thermal Distribution For Model 2 (at $t=1$ sec)
 $dx=0.001429$ m, $dr=0.001429$ m, $dt=0.00025$ sec, $mult=6000000.0$

CONTOUR LEVELS
 0.000000
 50.000000
 100.000000
 150.000000
 200.000000
 250.000000
 300.000000
 350.000000
 400.000000
 450.000000

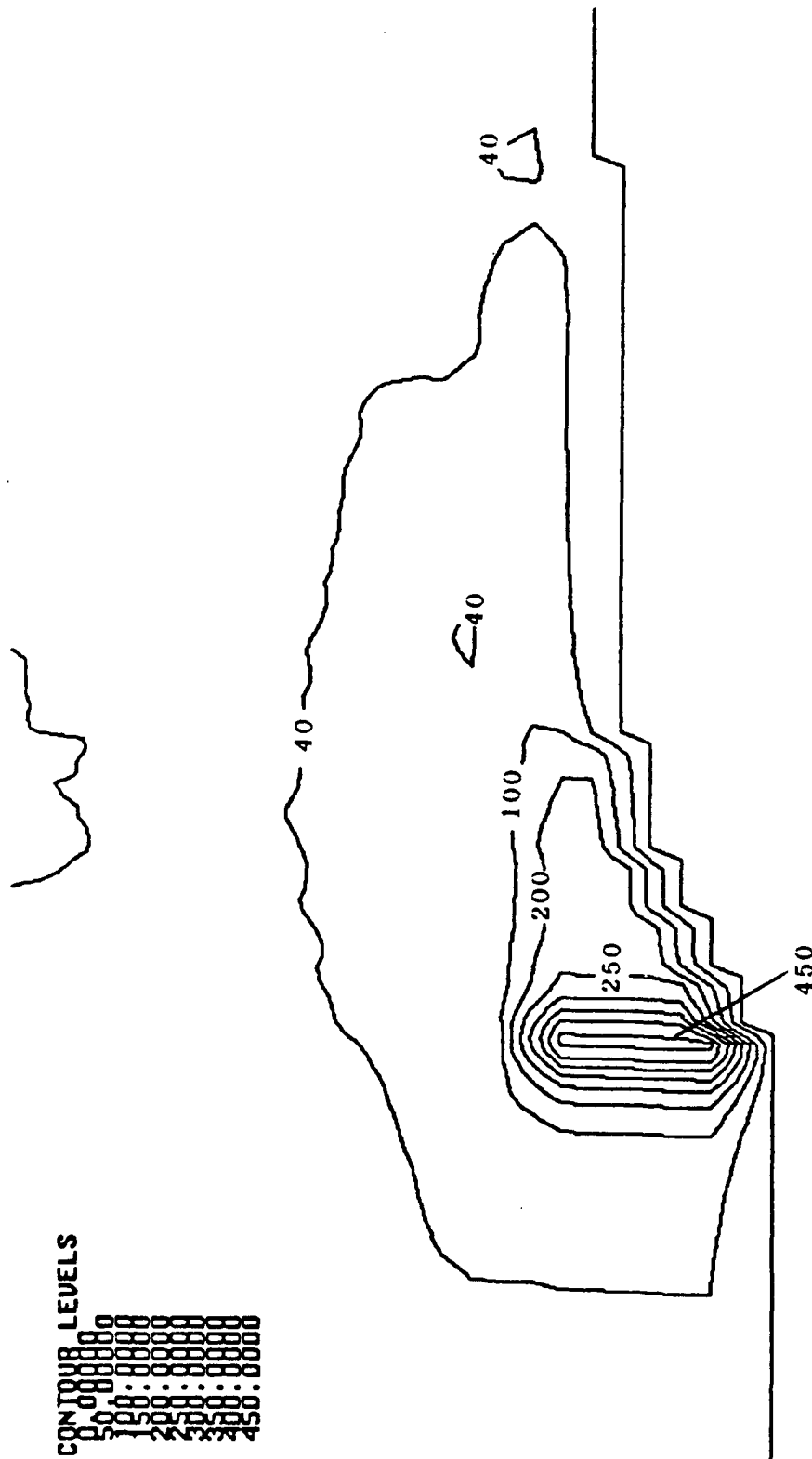


Figure 26. Two-dimensional contour plot of the temperature distribution for Model 2 after one second of heat generation.

wall thickness of 1 mm. The maximum thickness of the plaque layer used in this model was 0.5 mm. The microwave angioplasty model was imposed on a 200 by 80 cylindrical grid system with a uniform cell size of 1 mm in both x and r directions. To meet stability criteria, the thermal transient solution was obtained with a time step of 2.5×10^{-5} seconds. Although the smaller cell size increased the number of iterations and computational time it allowed for a more detailed analysis of thermal diffusion within the blood vessel wall. A diagram depicting the third model is shown in Figure 27. The initial SAR calculated by the electromagnetic FDTD program and final temperature distribution results are shown in Figures 28, 29, and 30, respectively.

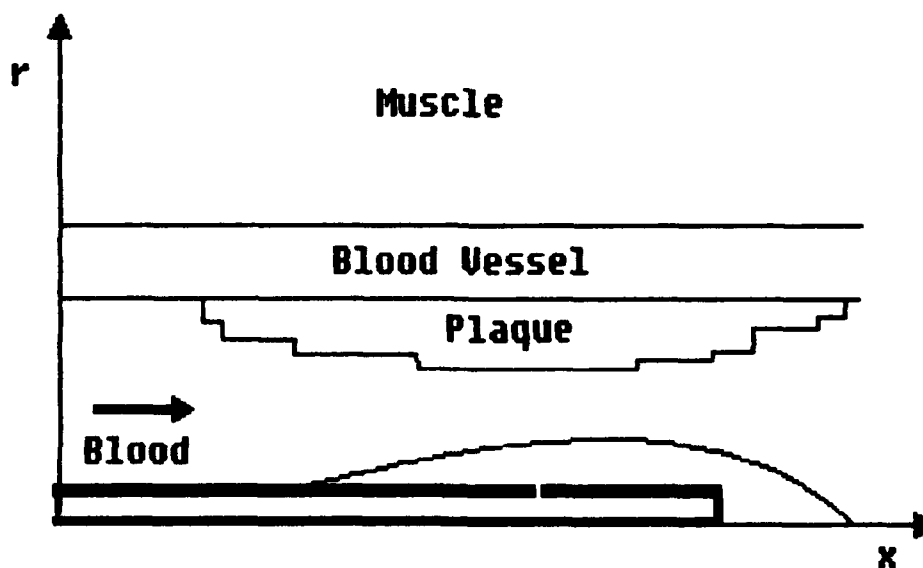
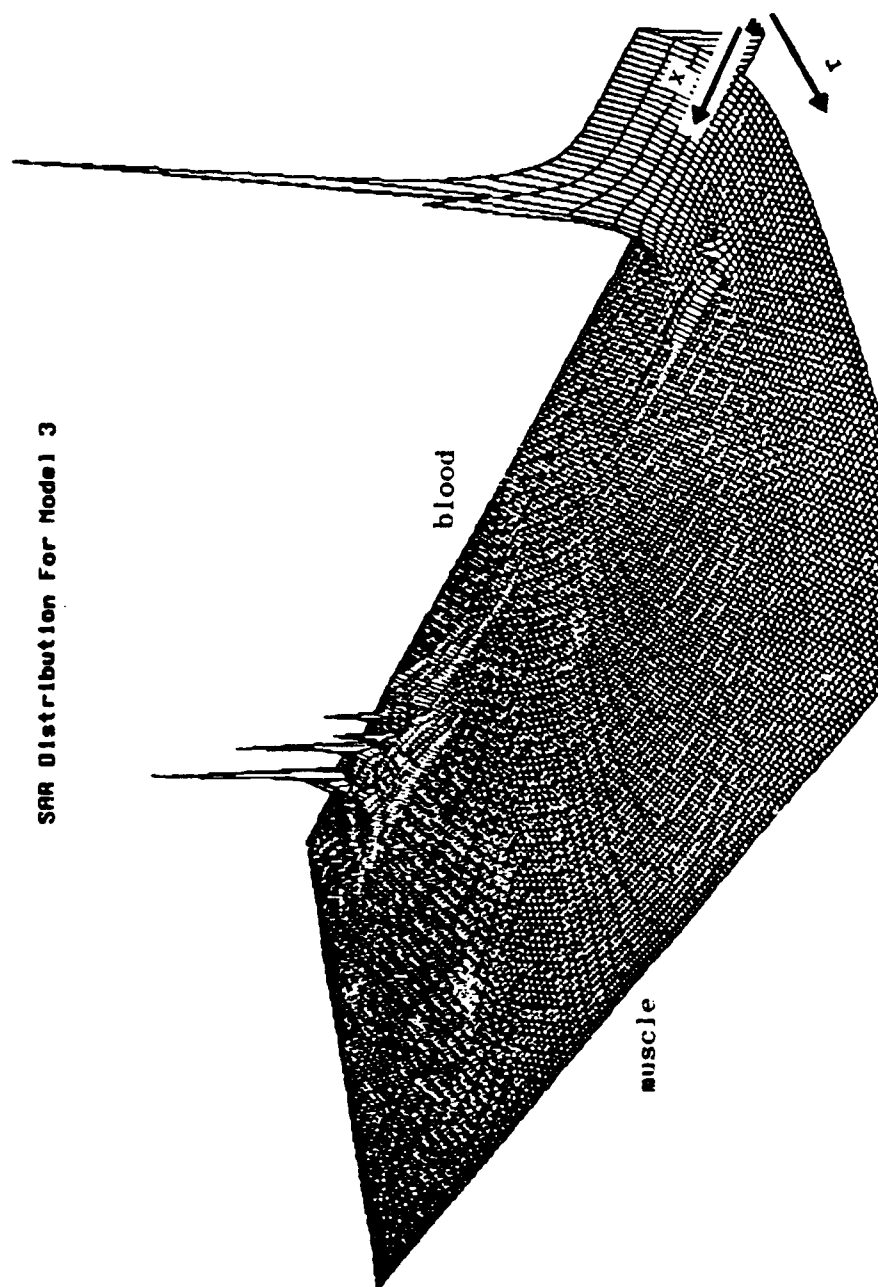


Figure 27. Diagram of Model 3



Thermal Distribution For Model 3 (at $t=1$ sec)
 $dx=0.0001$ m, $dr=0.0001$ m, $dt=0.000025$ sec, $mult=250000000.0$

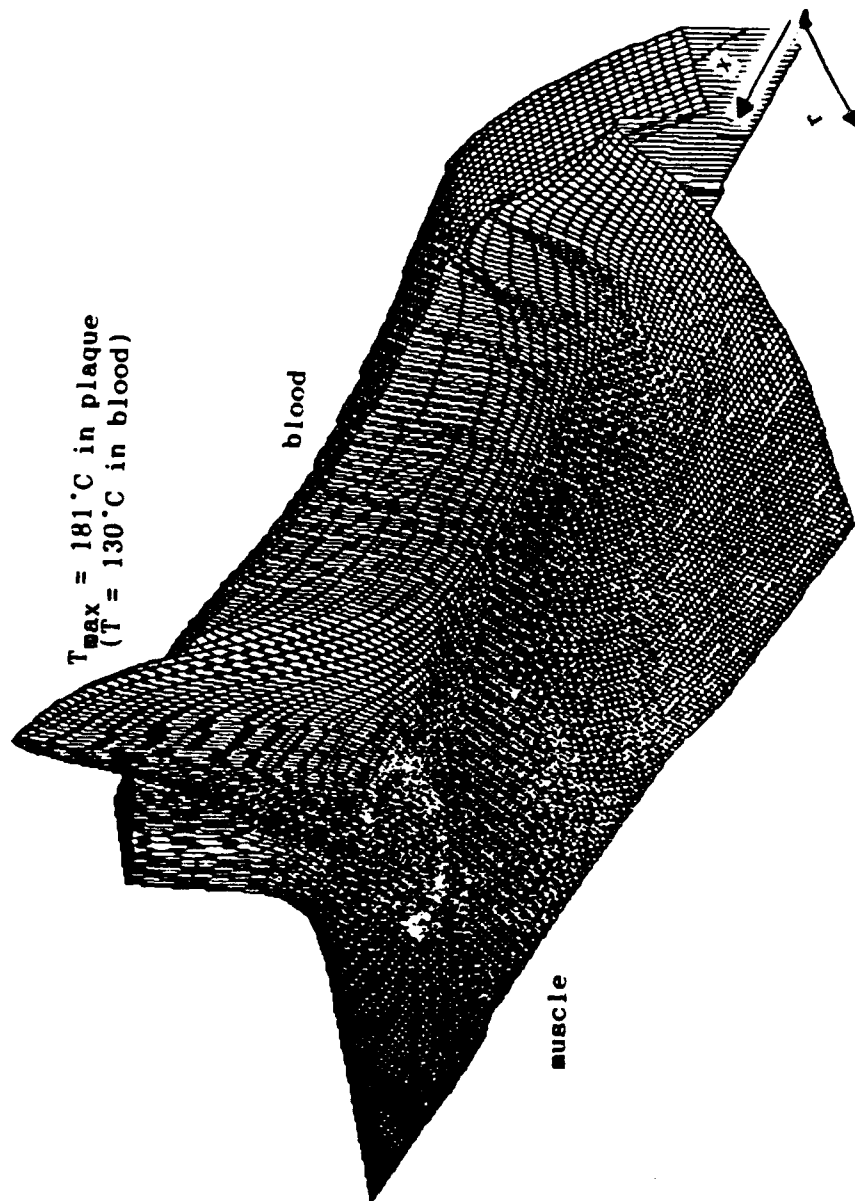


Figure 29. Three-dimensional surface plot of the temperature distribution for Model 3 after one second of heat generation.

Thermal Distribution For Model 3 (at $t=1$ sec)
 $dx=0.0001$ m, $dr=0.0001$ m, $dt=0.000025$ sec, $mult=250000000.0$

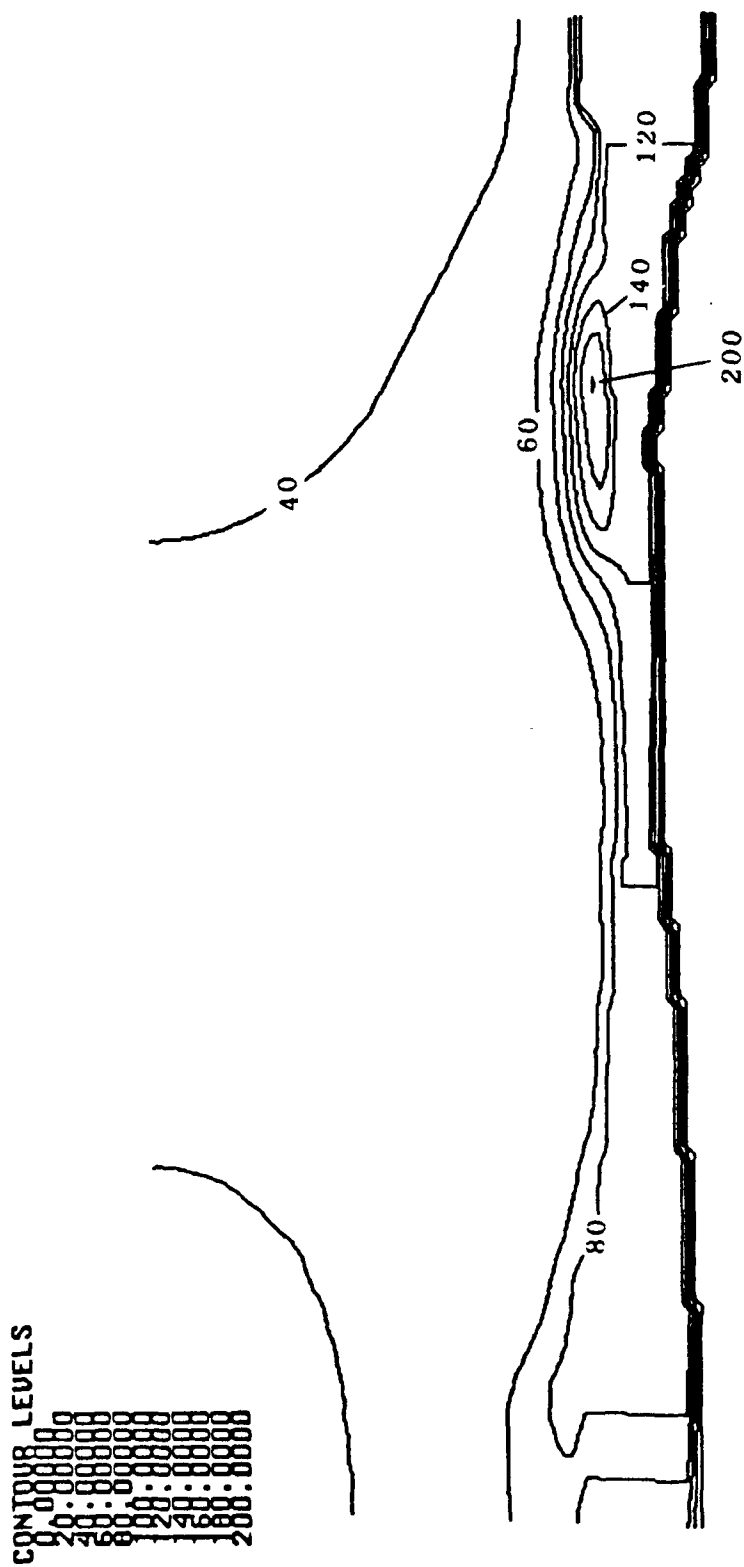


Figure 30. Two-dimensional contour plot of the temperature distribution for Model 3 after one second of heat generation.

Analysis of Thermal Results

The success of the microwave angioplasty techniques is dependent on three major criteria. The first criterion is to heat the atheromatous plaque to a high enough temperature for removal by melting or vaporization. Most biological tissues contain high concentrations of water relative to other chemicals. Previous studies with laser angioplasty techniques have shown that tissue ablations starts at temperatures higher than 100°C , which is closely associated with the boiling point of water (Welch et al., 1985). Tissue ablation occurs after the water in tissues is initially vaporized and is accompanied by a rapid rise in the plaque temperature. The rapid temperature rise in tissues is caused by a reduction in the specific heat and conductivity as the tissue is dehydrated. As mentioned previously, there are three different types of atheromatous plaques. Depending on the type of plaque predominantly present, effective ablation in tissue occurs in a temperature ranges of 160 to 310°C (Welch et al., 1985).

Second, the prevention of significant thermal injury to normal vascular and muscle tissue is of primary concern in applying the microwave angioplasty technique. Thermal tissue damage is defined as loss of biological function in cells or extracellular fluid (Welch, 1985). Tissue damage is dependent on the amount of time the tissues are exposed to increased temperature in addition to their temperature rise. In the case of hyperthermia, the body can withstand temperatures up to a range of 42 to 43°C for a period of 60 minutes before thermal injury occurs. At higher temperatures the body's resistance for thermal damage is decreased and cellular necrosis occurs at much shorter periods of exposure to abnormally high temperatures. The

mathematical relationship to predict the thermal damage to tissue as a time-dependent rate process was derived by Henriques and Moritz (Henriques and Moritz, 1947; Welch, 1985).

$$\frac{d\Omega(r,z,t)}{dt} = A \exp \left[\frac{E}{RT(r,z,t)} \right] \quad (3-1)$$

where: Ω = damage function

A = a constant

E = activation energy for a reaction

R = universal gas constant

T = absolute temperature

t = time

By numerically integrating this equation, the thermal damage can be predicted with experimental evaluation of the constant, A, and activation energy, E. Although these values have not been determined for the microwave angioplasty model, the results for cellular necrosis due to thermal radiation in tissues (Figure 31) can be used to determine whether thermal injury will occur in blood vessel and muscle tissue. For example, skin tissues at 75°C will reach the threshold damage of 1.0 within 10^{-5} second.

Blood temperature increase caused by the absorption of thermal energy induced by the electromagnetic field also deserves some consideration. Previous studies have demonstrated that prolonged temperatures greater than 48°C will result in hemolysis of the blood and increased red cell osmotic fragility (Wilson, Knauf, and Iserson, 1987). Furthermore, the body is an excellent thermoregulator at temperatures below 45°C, but it becomes less efficient for significant

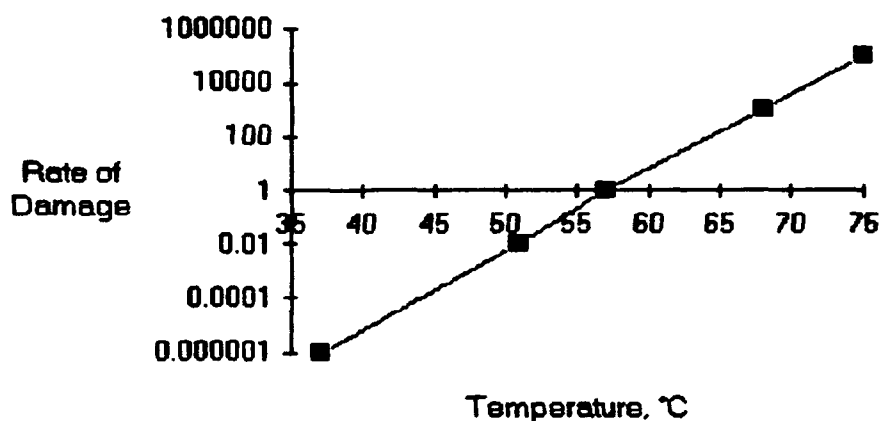


Figure 31. Rate of accumulation of damage in skin tissue as a function of increase in tissue temperature. This graph is used to estimate the number of seconds required before threshold damage occurs. (Adapted from Welch, 1985)

increases in blood temperature. Since the amount of microwave exposure is anticipated to be extremely short fraction of a second, hemolysis of the blood may not be detrimental to the welfare of the patient. On the other hand, extremely high heat generation in blood may cause a substantial imbalance in the body's thermal regulatory system if the overall body temperature is raised above 45°C. Therefore, some evaluation of the body's natural ability to dissipate the generated heat and maintain close to normal body temperatures should also be considered.

The electromagnetic fields produced by the microwave applicator generated one to three sharp spikes of extremely high SAR. The sharp increases in the thermal energy absorbed by the tissues are located either near the area surrounding the gap in the outer conductor of the microwave applicator or where the electric vector field intersects the balloon surface in a normal direction. In the latter case, the difference in the complex permittivity and electrical conductivity

properties between blood and air results in a significant increase in the SAR for blood. (A more thorough discussion of this concept is covered in Appendix A.) Therefore, the occurrence of a spike is dependent upon the microwave applicator design and the shape of the electric field. The location of this spike is typically at the ends of the balloon.

The temperature distribution after heating the angioplasty model for one second yielded a heating pattern similar to the SAR output. Results of the finite difference thermal analysis generally showed atheromatous plaque heating due to two effects: (1) selective heating and (2) convective heat transfer. In the former case, plaque was selectively heated by the microwave applicator in the area closest to the gap of the outer conductor. Convective heat transport is also present because of the fluid flow and temperature difference between the blood and plaque.

In Model 1, plaque heating is accomplished by three SAR spikes produced by the microwave applicator. Consequently three areas of high heat intensity were created. In each of these three areas, most of the heating occurred in the blood and the plaque layers closest to the blood. One second of heat generation in the plaque resulted in peak plaque temperatures in the 100°C range for the SAR spike closest to the incoming blood flow, 200°C in the center, and 65°C at the downstream end of the applicator. In all three cases, blood temperatures were, on the average, approximately two times higher than the plaque temperatures. The dissipation of heat into the neighboring blood vessel resulted in relatively high vascular temperatures of 50°C. At the downstream end of the balloon, some plaque heating is caused by

convective heat transfer rather than selective heating. In this case, the SAR spike generates extremely high blood temperatures in the 300 to 400°C range. Although the convective heat transfer raised the plaque temperatures by approximately 28°C, it was not sufficient to promote ablation. Figures 32 to 34 depicts the temperature distributions in each of the three SAR spikes as a function of the radius, r . The temperatures are shown for the blood, plaque, vascular, and muscle tissues, excluding the microwave applicator.

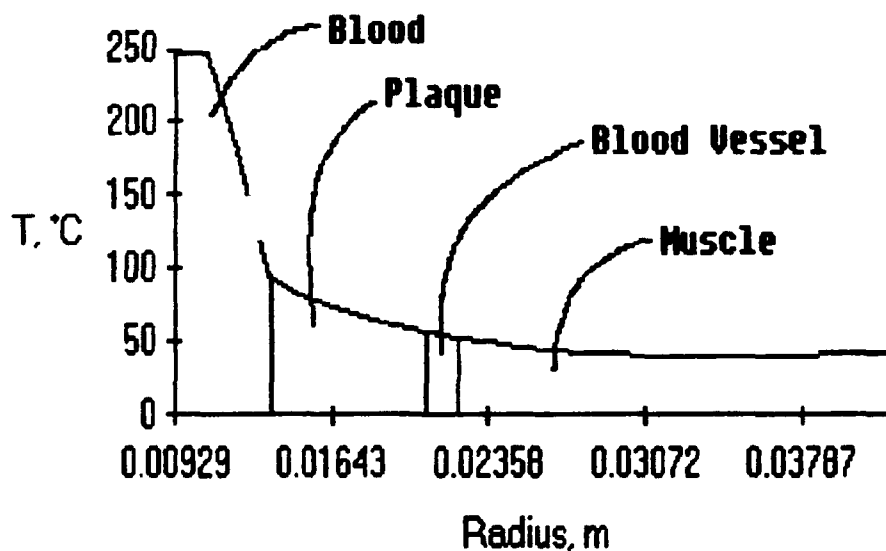


Figure 32. Temperature distribution for various materials in Model 1 at Peak 1. Heat generation on the upstream end of the microwave applicator was caused by the permittivity difference between air and blood. Results are shown for a one second microwave pulse at $t = 1.0$ second.

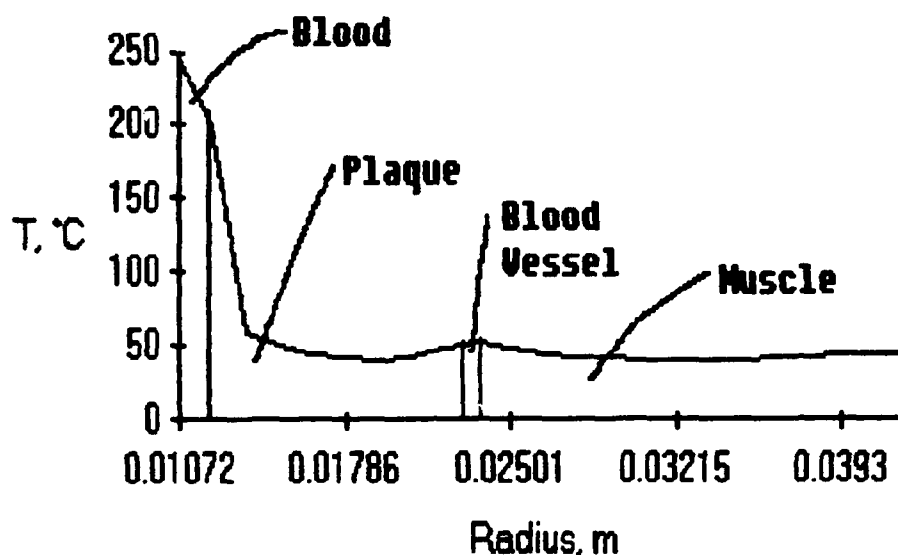


Figure 33. Temperature distribution for various materials in Model 1 at Peak 2. Heat generation was produced by the microwave applicator gap located in the middle of the thermal model. Results are shown for a one second microwave pulse at $t = 1.0$ second.

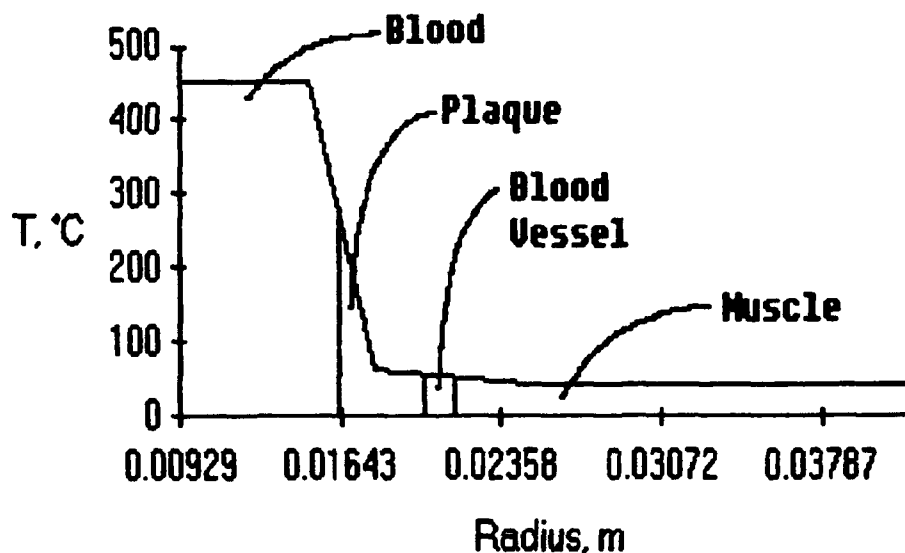


Figure 34. Temperature distribution for various materials in Model 1 at Peak 3. Heat generation on the downstream end of the microwave applicator was caused by the permittivity difference between air and blood. Results are shown for a one second microwave pulse at $t = 1.0$ second.

Angioplasty Model 2 produced a single SAR spike. Unlike the first model, temperatures in the atheromatous plaque after one second of heat generation were not high enough to initiate ablation. Most of the thermal energy was absorbed by the blood rather than plaque. Blood temperatures ranged from 300 to 380°C with corresponding plaque temperatures of approximately 70 to 97°C in the area of the SAR spike location. Despite the lack of adequate heating in the plaque, blood vessel temperatures also increased to about 60 to 67°C. The temperature distribution at the site of peak SAR for Model 2 is shown in Figure 35.

Although two SAR spikes were generated by the microwave applicator in the third model, only one provided any significant heating in either the blood or atheromatous plaque. Much of the heat generated in the blood by the first spike is cooled by the incoming

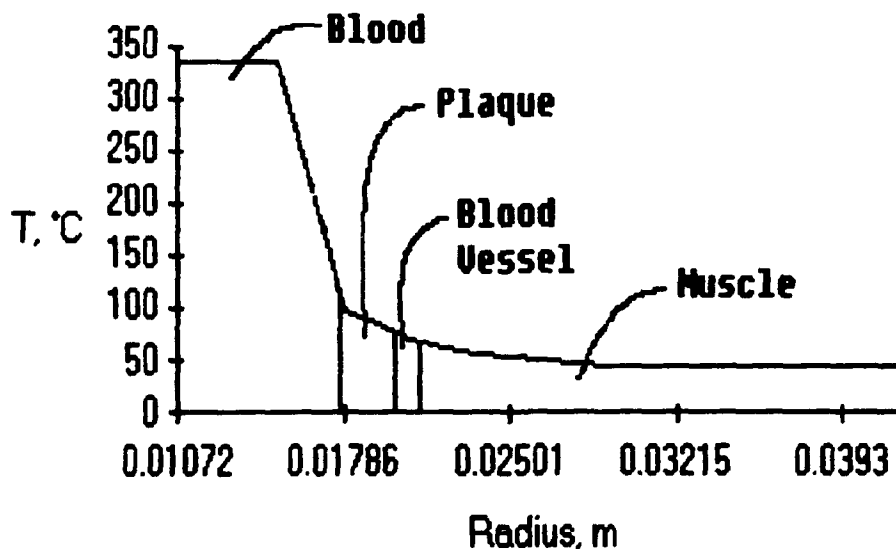


Figure 35. Temperature distribution for various materials at peak heat generation for Model 2. Results are shown for a one second microwave pulse at $t = 1.0$ second.

blood flow. Blood temperature increases were kept to a minimum as indicated by relatively low average blood temperatures of 40 to 45°C for this region. Some thermal energy was also absorbed in the blood vessel and muscle. Therefore, undesirable temperature increases in the vascular tissues were seen next to the entrance region. The average tissue temperatures in this region were in the 70°C range.

The second SAR peak in Model 3 provided sufficient thermal heat generation in the atheromatous plaque to cause ablation to occur. The microwave applicator was successful in delivering more heat generation in the plaque layers instead of the blood. The maximum plaque temperature in this region of the model was 181°C. Temperatures in the blood were lower than those for plaque by an average of 50°C. Although this model was more successful in achieving selective plaque ablation, extremely high tissue temperatures were found in the vascular tissue. The amount of heat in the 1.0 mm thick blood vessel was conducted away quite rapidly. For example, the temperature of the blood vessel cell next to the plaque was 127°C. For the outermost blood vessel cell, the temperature dropped to 46.1°C. A temperature distribution for this region of the model is shown in Figure 36.

Because many simplifying assumptions were made to model the fluid flow and convective heat transfer in this thermal analysis, a simple numerical experiment was conducted to determine the importance of this contribution. The subroutine to calculate the convective heat transfer coefficients was bypassed and all coefficients were set to zero. As seen in Figure 37, the blood temperatures for the case with convection nearly overlaps the temperature distribution without convective heat transfer after one second of constant microwave heat generation. There

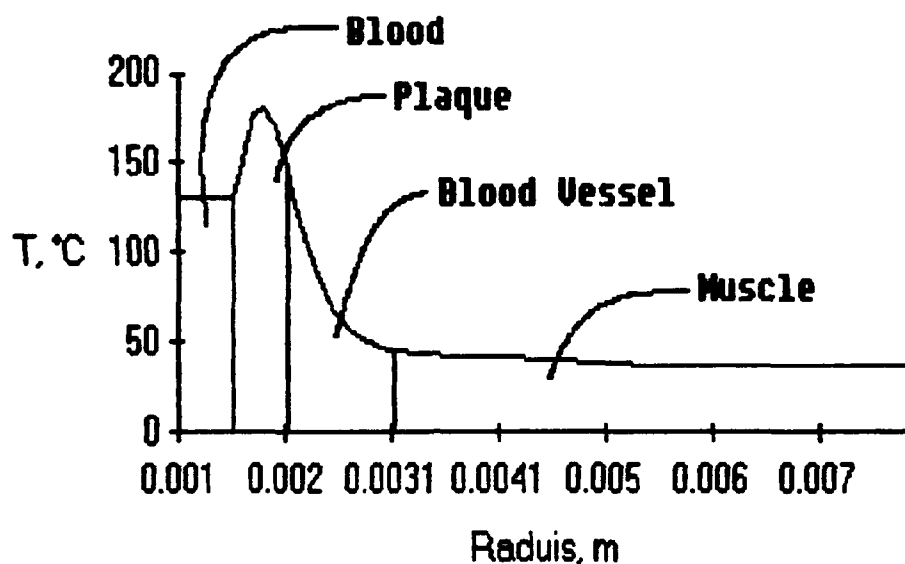


Figure 36. Temperature distribution of various materials at peak heat generation for Model 3. Results are shown for a one second microwave pulse at $t = 1.0$ second.

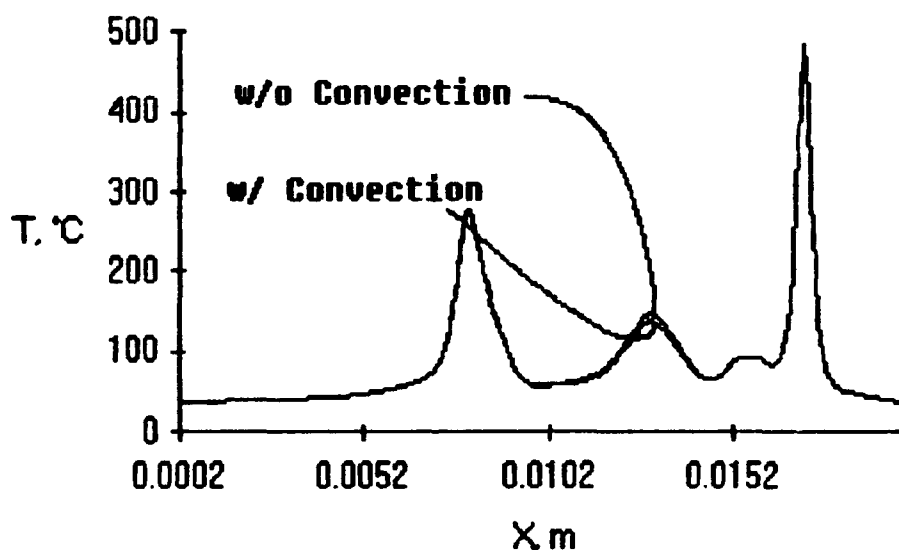


Figure 37. Comparison of the effects of convective heat transfer in blood temperatures using Model 1. Results are shown for a one second pulse at $t = 1$ second. Both curves overlap in most areas of the curve. Therefore, convection is not of significant importance during short periods of microwave heating.

is a small region in the center where a small difference exists, however, this variation did not alter the results of this thermal analysis during short time periods of constant heat generation.

As Model 1 was allowed to cool for three additional seconds after one second of heat generation, an increased difference was observed between the case with convective heat transfer and the same model calculated without convection. These results are graphically shown in Figure 38. These results demonstrate the importance of developing a better numerical model for the blood flow, especially during the cooling process and possibly between microwave pulses.

In all of the models analyzed, blood and vascular tissue temperatures rose above the limits for preventing thermal injury. As a possible resolution to this problem, a limited study of microwave pulsing was also conducted. By inducing a short high microwave energy

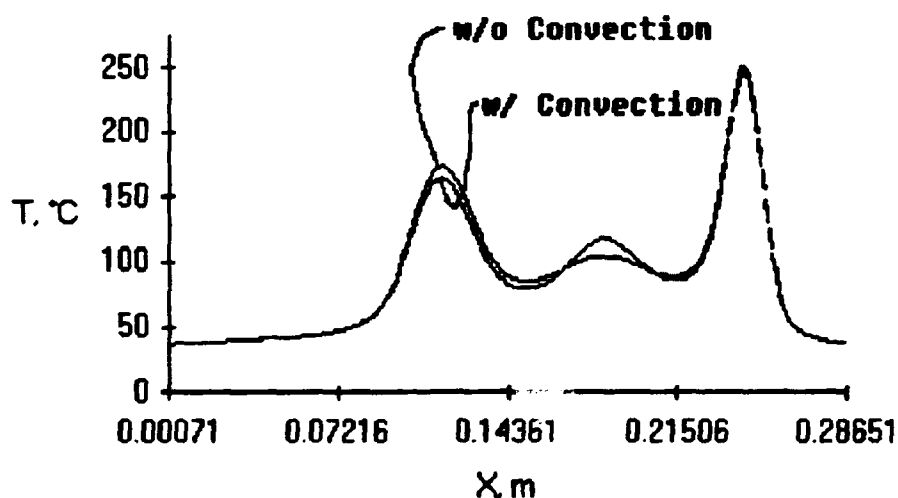


Figure 38. Comparison of the effects of convective heat transfer in blood temperatures using Model 1 after a one second pulse of heat generation plus three additional seconds of cooling ($t = 4$ sec). After a few seconds of cooling the convective heat transfer due to fluid flow becomes more significant in the thermal analysis.

input to the system and turning it off, temperatures high enough to initiate ablation could be achieved while letting the thermal system cool to avoid permanent thermal damage.

To test the thermal effect of microwave pulsing, a 0.20 second pulse was applied to Model 3. The intensity of the SAR distribution was doubled in order to achieve plaque ablation within 0.20 seconds. The model was allowed to cool up to 3 seconds. The result of this analysis is exhibited in Figures 39 and 40. The temperatures in the blood vessel layers increased because the direction of heat dissipation is toward the cooler muscle tissue. Since temperatures in the blood were usually higher than those for plaque, more heat was being added to the plaque which eventually conducted into the blood vessel and muscle layers. Temperatures in the vascular tissues did exceed 45°C especially in the layers next to the plaque and blood vessel interface due to conduction into the muscle tissue. These temperatures were slightly higher immediately following heat generation. For example, at a specific location in the blood vessel having a temperature of 60.4°C after a 0.20 second pulse of microwave heat generation, the temperature rose up to 68.5°C one second after turning off the heat source. Hot spots caused by the electrical field crossing the air-blood interface created significant heating of the blood. In Model 1 blood temperatures reached as high as 245°C. Although blood temperatures in Model 3 at the peak site of heat generation were less than plaque temperatures, the amount of heat convected to blood was minimal in comparison to conduction in the tissues.

The thermal properties of atheromatous plaques used in all models discussed above were based on a combined average of property value for

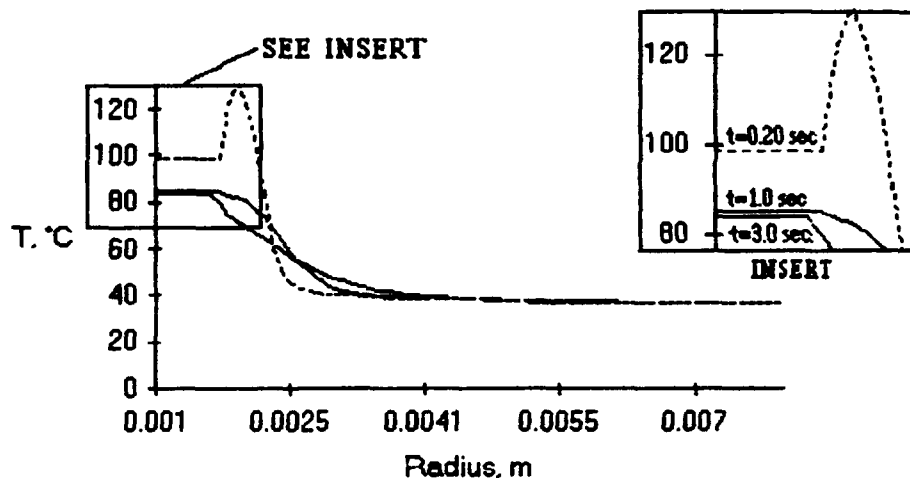


Figure 39. Heat dissipation after a 0.20 second pulse of microwave heat generation using Model 3. Temperature distributions are shown for $t=0.20$ sec, $t=1$ sec, and $t=3$ sec.

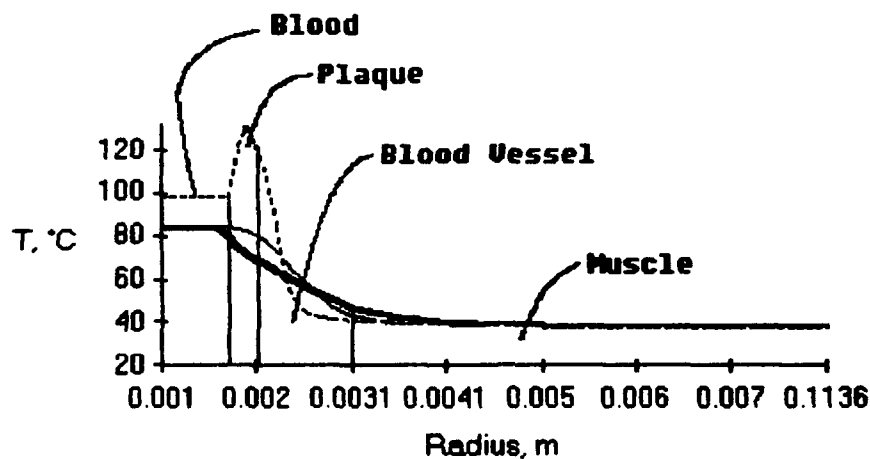


Figure 40. Temperature distribution in tissues after a 0.20 second pulse of microwave heat generation using Model 3. Temperatures are shown for $t=0.20$ sec, $t=1$ sec and $t=3$ sec as in Figure 39.

fatty, fibrous, and calcified plaques (Welch, 1985). In different parts of the body, certain predominant types of plaques are more likely to be deposited on the blood vessel linings. For example, calcified plaques are more commonly found in the blood vessels of the leg and limbs whereas fatty and fibrofatty plaques are usually deposited in the coronary arteries. Further numerical experiments were performed to

determine whether certain types of plaques would have a higher affinity for selective plaque ablation.

The amount of thermal energy absorbed in the plaque varied according to the predominant plaque type in the angioplasty model. Because of the higher water content, the thermal conductivity and specific heat values for fatty plaques were the highest. Applying an equal amounts of microwave heat generation to Model 3 for all three cases resulted in consistently higher temperature rises for fatty plaques. As shown in Figure 41 fatty plaques are followed by fibrous then calcified types in their ability to absorb thermal energy. The variance between plaque types is not enormous. At site of peak plaque temperature the fatty plaque was about 15.5 percent higher than the calcified type. The difference was much less for fibrous plaque with a three percent difference in comparison to the fatty plaque. Therefore, application of this angioplasty technique is not limited to the removal of fatty plaques alone. Plaques normally consist of a mixture of various plaque types. Since the variance in results was not significant, the thermal analysis averaging all three types of plaques was not a bad approximation for calculating the overall plaque thermal properties.

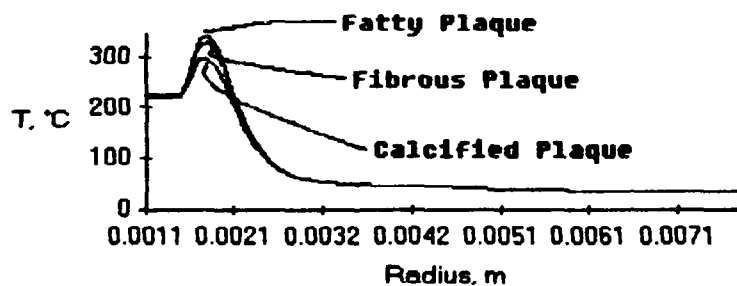


Figure 41. Temperature distributions for various plaque types. Fatty plaques absorb less than 15.5 percent more thermal energy than other types. Results are shown for a one second microwave pulse at $t=1$ sec.

Discussion Of the Results

Although the results of this thermal analysis have not been checked experimentally, similar results were obtained in ablation studies for the laser angioplasty technique. In research work done by Welch et al. a laser probe was applied to an atherosclerotic human aorta with a wall thickness of 1.5 mm. The atheromatous plaque was heated up to 180°C to induce ablation and the adventitial temperatures reached 70°C during the ablation process (Welch et al., 1987). The heat transport mechanisms for both laser and microwave angioplasty techniques are comparable since both methods attempt to heat the plaque to the same temperature levels. Heat in both cases is dissipated radially outward toward the cooler muscle tissue. The blood vessel temperatures in the thermal models analyzed by this study reached the 60 to 80°C range. In Model 3 a maximum temperature of 127°C was observed at the plaque and vessel wall interface. The similarities in these analyses provides a fair amount of confidence in the validity of this thermal model.

During the development of the finite difference code several adjustments and approximations were made to allow the use of SAR data generated by the Department of Electrical Engineering. For one, the data obtained provided relative SAR data rather than actual heat generation values. Results from the FDTD program produced SARs having an order of magnitude of 10^{-6} for heat generated by the microwave. Over a wide range of the microwave exposures, the SARs linearly increase with increasing power input. Therefore, to show effective heating in the thermal model, a multiplier was estimated to increase SAR values to a level where the plaque ablation could take place.

Further studies to include the plaque ablation portion of finite difference code will require a correction of this discrepancy to allow simultaneous execution of both FDTD and FDATA programs.

Additionally, the relative SAR data were calculated at the center of each finite difference cell rather than the boundary interfaces. Because both conductive and convective phenomena takes place in this thermal analysis, the SAR data required recalculations to shift the coordinate system by a half interval in both the x and r directions. Therefore, a cubic spline interpolation subroutine the SAR values was implemented to calculate this change. Models 1 and 2 were originally generated by the Department of Electrical Engineering to test various applicator designs numerically. The coordinate mesh in these to models was too coarse (0.1429 cm) and the cubic spline interpolation produced unrealistic numbers where large fluctuations in the SAR data were observed. This problem was eliminated by using a linear interpolation subroutine instead. Therefore, a 5 to 10 percent error in this solution may be present as a result of the coordinate system changes between the FDTD and FDATA programs.

It is important to note that Models 1 and 2 do not reflect the actual dimensions of the vascular system. For example, the model data shows the blood vessel starting 15 cells away from the centerline. For the cell size of 0.1429 cm in the r direction this equates to a 4 cm lumen diameter. The largest blood vessel in the human body is 2.5 cm in diameter. The blood vessel was also modelled as being only one cell thick. Model 3 was developed to account for this discrepancy and to better evaluate the heat distribution within the vascular tissues. Therefore, Models 1 and 2 are useful in determining whether or not

selective plaque ablation can be achieved but they do not represent the actual physical system.

In Model 3 the SAR spike at the entrance region of the model was not anticipated. The insulative boundary conditions in this case did not accurately represent semiinfinite conditions because of the build up of heat in this region. Therefore, the high adventitial temperatures observed in this study are probably lower than the calculated values. Boundary condition problems of this nature can be alleviated by changing the dimensions of the cell size. By generating a cylindrical grid where the dx dimension is two or three times greater than dr, the semiinfinite boundary conditions can be met without increasing the matrix size and computational iterations. As an alternative method for modelling the boundary conditions, the boundary temperatures could be held constant at normal body temperature (37°C).

The extent of permanent thermal damage to the vascular tissues can not be clearly defined at this time. Other thermographic and histological studies with laser angioplasty techniques have demonstrated that actual ablation of normal vascular tissue requires temperatures exceeding 180°C. Tissue dehydration and shrinkage starts at temperatures of 60°C or greater (Welch et al., 1987). For small increments of time, the tissues are able to tolerate different levels of heating without causing irreversible permanent damage. Therefore, although high temperatures in the blood vessel tissues were observed in this thermal analysis, short exposures to the elevated temperatures may not cause a significant amount of thermal destruction.

In this thermal analysis, hemolysis of the blood appeared to be a potential problem. However, the extent of adverse thermoregulation

alteration and blood loss is expected to be minimal for short exposures of microwave heat generation. The circulatory system stores an average of 8 liters of blood within its vast system of arteries, veins and capillaries. The amount of heated blood is anticipated to be far less than the total blood volume available. This assumption holds true for the laser angioplasty technique. With improvements to the present applicator design to eliminate the hot spots in the blood created by the air-blood interface, blood hemolysis should not be a major concern.

Pulsing applications of the microwave angioplasty technique provided better results than the constant heat generation models. High plaque heating for ablation could be accomplished while minimizing temperature rises in the blood vessel and muscle tissues. Further numerical optimizing experiments with high heat generation at multiple time exposures may provide more desirable temperature profiles.

This thermal analysis was a first attempt for approximating the conductive and convective heat transfer contributions to the microwave angioplasty model. Increasing the complexity of this analysis by eliminating many of the simplifying assumptions will greatly improve the accuracy of the results obtained here.

As previously mentioned, tissue perfusion and metabolic heat generation were omitted from this thermal analysis. In the muscle tissue the omission of tissue perfusion may not be such a good approximation since this is the body's only means of heat removal. An inclusion of the perfusion term in the bioheat equation will allow the heat to dissipate at a faster rate than observed for the blood vessels of this first approximation.

A better treatment of the fluid flow and solution for the convective heat transfer coefficient is also required. Preliminary observations showed some significance of convective heat transfer over long periods of time during cooling. These results should be verified by conducting a more detailed analysis of the blood flow. Further development of the thermal model should include non-Newtonian and pulsating blood flow effects as well as account for the curvature and elasticity in the blood vessels. Because of the complex geometry of the system, the fluid flows do not have fully developed velocity and temperature profiles. Entrance region effects should be carefully examined and included in the model. Development of a numerical solution to take these effects into consideration may alter the convective heat transfer coefficients used in the analysis.

In addition, plaque deposition in arteries is generally nonuniform. Therefore, a three-dimensional thermal analysis is also required to handle the eccentricity of plaque distribution within the blood vessel.

Thermal properties in tissues are not constant at different temperatures and pressures as modelled in this analysis. Additional studies should make some provisions for estimating the actual thermal properties as a function of temperature. This is highly recommended for the blood and atheromatous plaque layers where the greatest temperature gradients occur in the model.

A phase change portion of the thermal analysis should be added to the numerical solution. The results presented here provide temperature distributions with the ablated plaque still in place. By removing the plaque from the model and recalculating the SAR distribution

accordingly, temperatures in the blood vessels may be lower than the result obtained in this study. As ablation takes place the latent heat is carried away by the blood flow. Therefore, plaque temperatures would be cooler when the heat source is turned off and less heat will be conducted to the blood vessel. Heat will be convected to the outer layers of plaque due to the increased blood temperature, but this heat input is expected to be relatively small.

Extremely high temperatures in the blood were not initially anticipated. However, the heat intensities observed in this study indicated that blood vaporization would probably occur in a real model. Some treatment of the phase change in blood is needed to increase the accuracy of the thermal model.

Additional thermal studies are required for improving the modelling techniques. For example, the ablation properties of atheromatous plaques are not known. Future experimental work should include measurements for the latent heat of fusion, vaporization, and sublimation in atheromatous plaques and is essential to accurately model the ablation aspect of the thermal model. The rate at which the plaque melts or vaporizes also requires evaluation.

In addition, further studies to determine the thermal destruction thresholds for vascular tissues are needed to evaluate the feasibility for applying this angioplasty technique clinically. Studies similar to those accomplished for skin burns are required to calculate burn injury criteria and to find a correlation for the damage constant as a function of time.

Although the results in this study show vascular tissue damage and hemolysis might have occurred during treatment, further development

in applicator design may alleviate these problems. Design improvements for the microwave applicator should include a heat exchanger system for the blood. By keeping blood temperatures lower than those of the plaque, heat flows into the blood vessel will be reduced if heat can be convected away by the blood. Injection of blood cooler than normal body temperature during microwave heating may help to minimize blood temperature increases.

The microwave applicator design should also include a means for directing the electromagnetic field better. Plaque distributions in blood vessels are not axisymmetric. Future microwave applicator designs should be capable of heating the blood vessels in sections to avoid heating of the blood vessel. Undesirable heating at the air-blood interface of the applicator ends should be eliminated by optimizing the applicator balloon shape with the solution of the electromagnetic field.

Of the many deficiencies identified here, the most important improvement is the quantifying of ablation characteristics in the atheromatous plaques through in vitro experimental studies. The success of the microwave angioplasty method is entirely dependent upon the ablation process in plaques. Adequate atheromatous plaque removal depends on the rate in which the plaque melts or vaporizes as well as the latent heat required to initiate a phase change. Therefore, to accurately simulate the heat transfer in an angioplasty model, the phase change phenomena must be added to the thermal analysis. In this study temperatures were allowed to rise constantly as heat dissipated into the vascular and muscle tissues. Differences in temperature distributions for studies including the ablation phenomena are

anticipated since blood and plaque temperatures are held constant during the phase change process. The estimated power required to remove the remaining plaque through a series of subsequent microwave pulses will also be affected by ablation. These experimental studies will moreover provide a means of validating the thermal results obtained numerically. Further development of the microwave applicator design would be meaningless without additional analyses of the plaque ablation process.

The future of the microwave angioplasty technique is promising. Implementation of the improvements described above may lead to the practical application of this technique clinically. Thermal conductivity from the plaque to blood vessel may present a problem if the blood vessel cells are found to be less resistant to biological dysfunction due to abnormal temperature rises. The application of this numerical thermal analysis will assist in predicting the occurrence of thermal injury for new applicator designs. In the clinic it may be useful in helping physicians estimate the microwave dosimetry required to achieve safe and effective atheromatous plaque ablation.

CHAPTER 4

CONCLUSION AND RECOMMENDATIONS

Conclusion

In this study a finite difference thermal model was developed as a first approximation to predict the temperature distribution in three percutaneous transluminal microwave angioplasty models. The temperature distributions in each model were examined to determine whether successful atheromatous plaque ablation could be achieved without causing extensive thermal injuries to surrounding vascular tissue and muscle.

The results of this thermal analysis show that the microwave angioplasty technique has a good potential for application in a clinical environment in the treatment of atherosclerosis. Selective atheromatous plaque heating was achieved initially and temperatures well above 100°C were attained for plaque ablation.

High temperatures in the surrounding tissues and blood indicated a high probability for the onset of thermal injuries during application of the microwave angioplasty technique. Temperatures in the vascular tissues did exceed 45°C especially in the layers next to the plaque and blood vessel interface due to conduction into the muscle tissue. These temperatures were slightly higher immediately following heat generation. Vascular tissue temperatures were in the 60 to 80°C range one second after the microwave applicator was turned off. Some thermal

damage such as dehydration and shrinkage to the tissues would occur at this elevated temperature level, however, temperatures of 180°C or greater are needed to initiate tissue vaporization. In addition, there is a high potential for hemolysis to occur in the blood as a result of the hot spots caused by the electrical field crossing the air-blood interface created significant heating of the blood. In Model 1 blood temperatures reached as high as 245°C.

The microwave angioplasty technique performed best in fatty plaques. Higher temperatures were observed in the fatty plaque model for identical amounts of heat generation applied to all three plaque types. However, a difference in maximum temperatures between all three plaque types was not prominent. Therefore, the microwave angioplasty technique will be of comparable effectiveness in removing all plaque types.

Recommendations For Further Study

Although this thermal analysis provides a good first approximation of the heat transfer phenomena present in the microwave angioplasty system, many improvements are needed. Further studies to analyze the phase change process in atheromatous plaques are most important since ablation is the primary means of plaque removal using this technique. Additionally, to provide a more exact solution of the thermal model many of the simplifying assumptions made here should be eliminated. The results previously discussed showed that convective heat transfer does have an important effect on the thermal analysis over long periods of cooling and potentially between microwave pulses. A more accurate method of analyzing the blood flow in the problem is

therefore required. Further studies should include the non-Newtonian, pulsating, and entrance region fluid flow effects. The solution should also account for curvature and elasticity of the blood vessels. Additional studies to include the heat transfer effects due to tissue perfusion and running the phase change version of the FDATA program will greatly improve the accuracy of these results.

Other indirect studies are needed to evaluate the safety and possible clinical application of this technique. These studies should include experimental studies of phase change properties in plaque and thermal destruction thresholds for vascular tissues.

Further development of the applicator design may also provide more controlled heating in the plaque layers alone. Examples of these improvements consist of adding a heat exchanger system to regulate blood temperatures, better applicator design to prevent undesirable heating at the air-blood boundary, and a means of directing the electromagnetic field for non-axisymmetric thermal models.

APPENDIX A

THE MICROWAVE ANGIOPLASTY METHOD

Microwave Applicator Design

The microwave angioplasty technique for treating atherosclerosis is similar to the balloon and laser methods since all three methods employ a catheter system to deliver the plaque removal device. The microwave applicator located at the tip of the catheter consists of an extremely fine and flexible coaxial cable encased in a thin metal tube and shorted at the end of the applicator. The coaxial cable is connected to an external microwave generator. A radial gap in the metal casing close to the end of the applicator is designed to create an electrical potential difference between the inner coaxial conductor (which includes the coaxial wire and shorted end of the tube) and the outer coaxial conductor as shown in Figure 42. This potential

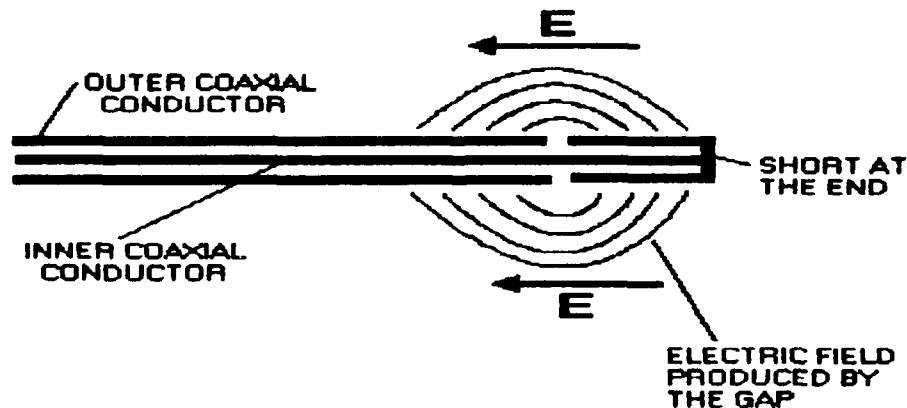


Figure 42. Microwave applicator as designed by the University of Utah Department of Electrical Engineering.

difference between the inner and outer coaxial conductors produces an electromagnetic field. The surrounding blood, plaque, vascular, and muscle tissue absorbs the thermal energy induced by the high-energy electromagnetic field as a function of the electrical properties of each layer of tissue.

Concept of Selective Plaque Ablation

A balloon is used in conjunction with the microwave applicator; however, its function is quite different than its use in the coronary balloon angioplasty method and microwave angioplasty applicator proposed by Rosen (1990). In hyperthermia studies conducted by the Christensen and Durney (1981) of the University of Utah, it was found that separating the fat-muscle layer and electric dipole by an air gap caused the fat to overheat. Since the muscle has a relatively high electrical conductivity in comparison to the fat and muscle, this causes the system to behave as two capacitors in series with two dielectric layers as shown in Figure 43.

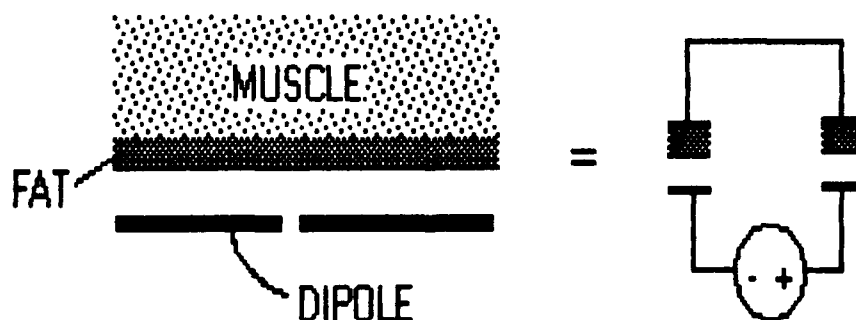


Figure 43. The electrical conductivity in the muscle-fat-air system is analogous to an equivalent electrical circuit with two capacitors in series.

Assuming the electrical and thermal properties of fat are similar to that of atheromatous plaques, this physical phenomenon is applied to the microwave angioplasty model to selectively heat and ablate intravascular atheromata while minimizing thermal injury to the surrounding tissue.

Selective heating of the fat in the hyperthermia model also occurs because of the difference in the complex permittivity of the fat and muscle tissues. By definition, permittivity is the electrical property of a material measuring the electromagnetic field interactions which produce thermal energy in tissues. These interactions include the orientation of the electric dipoles in the atoms and molecules of the tissues, polarization of the atoms and molecules, and displacement of conductive electrons and ions in tissues (Christensen and Durney, 1981). The heat generated within the tissues is caused by the frictional losses due to the movement of atoms and molecules undergoing orientation and polarization interactions and the collisions of moving atoms and molecules with stationary ones during the displacement interaction.

If two capacitor plates are placed on either side of two layers of fat and muscle as shown in Figure 43, a strong electric field perpendicular to the plates is produced. A much weaker magnetic field is also produced but its effect is not significant in the heat generation of the tissues. At the interface of the fat and muscle, a boundary condition (see Figure 44) relating the permittivities of each tissue type and their respective electric fields is given as:

$$\epsilon_1 E_1 = \epsilon_2 E_2 \quad (A-1)$$

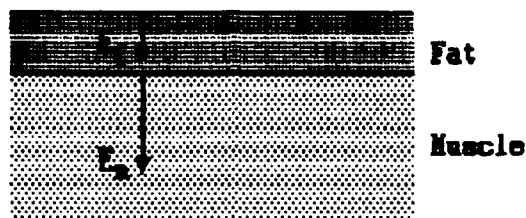


Figure 44. Boundary condition at the fat and muscle tissues. The plaque having similar properties of fat can absorb about seven times more heat generated by the electromagnetic field than the muscle and vascular tissues.

The amount of heat absorbed by the tissues, also known as the specific absorption rate (SAR) is a function of the the electrical conductivity and electromagnetic field. By calculating the SAR ratio of fat to muscle the relationship in equation (A-3) is obtained.

$$SAR = \frac{1}{2} \frac{\sigma |E|^2}{\rho} \quad (A-2)$$

$$\frac{SAR_f}{SAR_m} = \frac{\rho_m \sigma_f |E_f|^2}{\rho_f \sigma_m |E_m|^2} \quad (A-3)$$

By substituting the boundary condition for the fat/muscle interface into equation (A-3), the SAR ratio is reduced to equation (A-4). Known values for the electrical conductivities and complex permittivities of fat and muscle are substituted into this equation giving a calculated ratio of about 7.

$$\frac{SAR_f}{SAR_m} = \frac{\rho_m \sigma_f |\epsilon_m|^2}{\rho_f \sigma_m |\epsilon_f|^2} = 7 \quad (A-4)$$

Published values for the electrical properties in atheromatous plaques are unavailable. However, the University of Utah Hyperthermia Research Group was able to obtain experimental measurements for plaque. Their measurements for plaque were similar to that of documented values

for fatty tissues. For example, the experimental relative permittivity, ϵ and electrical conductivity, σ values for plaque were 36 and 0.068 S/m, respectively. These values are relatively close to the values for relative permittivity, 40 and electrical conductivity, 0.019 S/m in fatty tissues (Hahn et al., 1980). Performing the same calculations with the experimental measurements for plaque, the SAR ratio is 7.55 for a 10 MHz microwave heat source. Both documented electrical properties for fatty tissues and experimental measurements for plaque demonstrates the high potential for selective heating because fatty tissues absorb approximately seven times more heat than the vascular and muscle tissues.

APPENDIX B

THERMAL PROPERTIES OF BIOLOGICAL TISSUES

Tissue Type	Thermal Conductivity [W/(m°C)]	Thermal Diffusivity [m ² /sec]	Heat Capacity [W·sec/(m ² sec)]
Average Plaque (1)	0.4912	1.265x10 ⁻⁷	3.878x10 ⁶
Fatty Plaque (1)	0.4312	1.241x10 ⁻⁷	3.476x10 ⁶
Fibrous Plaque (1)	0.4760	1.295x10 ⁻⁷	3.677x10 ⁶
Calcified Plaque (1)	0.5667	1.364x10 ⁻⁷	4.480x10 ⁶
Blood Vessel Wall (1)	0.4320	1.220x10 ⁻⁷	3.541x10 ⁶
Muscle (2)	0.5100	1.800x10 ⁻⁷	2.833x10 ⁶
Blood (3)	0.6270	1.545x10 ⁻⁷	4.059x10 ⁶

References:

- (1) Velch et al., 1985
- (2) Shitzer and Eberhart, 1985
- (3) Bluestein, Harvey and Robinson, 1968

APPENDIX C

FINITE DIFFERENCE ANGIOPLASTY THERMAL ANALYSIS PROGRAM

Description of Nomenclature

ALPHA - array storing the thermal diffusivities for each tissue type
[m^2/sec]

C2 - common coefficient used by several subroutine

DR - differential cell radius in the r direction [m]

DT - differential time step [sec]

DX - differential cell length in the x direction [m]

HP - convective heat transfer coefficient for the plaque [$\text{W}/(\text{m}^2\cdot\text{C})$]

HM - convective heat transfer coefficient for the microwave applicator
[$\text{W}/(\text{m}^2\cdot\text{C})$]

IFIN - maximum number of columns in MODEL

IOFF - integer indicating end of microwave pulse duration $\text{INT}(\text{TIME}/\text{DX})$

IPRT - counter for intermediate printouts of the result

ISTART - minimum number of columns in MODEL

JFIN - maximum number of rows in MODEL

JRPL - integer corresponding to the location where the plaque starts
for a given x location.

JEPR - integer corresponding to the location where the microwave probe
starts for a given x location.

JSTART - minimum number of row in MODEL

K - array storing thermal conductivities for each tissue type [$\text{W}/\text{m}\cdot\text{C}$]

MODEL - matrix storing the model parameters.

- 1 - refers to air
- 2 - refers to the metal of the microwave applicator
- 3 - refers to the muscle tissue
- 4 - refers to the atheromatous plaque
- 5 - refers to the blood
- 6 - refers to the blood vessel

POWER - SAR results from FDTD program [W/m^3]

QAVE - average blood flow rate, default value is 250 ml/min

QM - matrix storing the heat generated by the microwave applicator [W/m^3]

QB - array storing the lumped heat generated in the blood for the one dimension convection analysis [W/m^3]

RO - radius of the finite difference cell closest to the microwave applicator [m]

RHOC - array storing the heat capacity (density multiplied by the specific heat) for various tissue types [$\text{W}\cdot\text{sec}/(\text{m}^3\cdot\text{C})$]

RPLX - array storing the radii values at the plaque layer [m]

RPRX - array storing the radii values at the microwave probe [m]

SEC - total time for running the FDATA program [sec]

SUM - summation of four model nodes to determine which finite difference subroutine to execute

TEMP - matrix storing the initial temperature increases computed by the FDTD program [$^{\circ}\text{C}$]

TEST - matrix to check whether the program is executing the correct finite difference subroutine for the plaque geometry given

TIME - current time during finite difference calculation

TMAX - maximum temperature found in the final results; used for normalizing temperature matrix TN and allowing its use with EE programs [$^{\circ}\text{C}$]

TMP - matrix storing the interpolated temperatures from TEMP [$^{\circ}\text{C}$]

TO - matrix for storing the old temperature distribution [$^{\circ}\text{C}$]

TN - matrix for storing the new temperature distribution [$^{\circ}\text{C}$]

TP - array for storing the microwave probe surface temperatures [$^{\circ}\text{C}$]

V - average blood velocity based on QAVE [m/sec]

Summary of FDATA Program Steps

1. Input the total number of seconds to evaluate the temperature distribution in the angioplasty model (SEC).
2. Input the alternate value for average blood flow rate in ml/min or use the default value 250 ml/min.
3. Read in formatted data from the FDTD program. Data includes POWER, TEMP, and MODEL matrices.
4. Initialize all temperature matrices and arrays (TC, TB) to normal body temperature, 37.0°C.
5. Interpolate POWER and TEMP to compute the amount of heat generation at the boundary interfaces. The interpolated data are stored in QM and TMP matrices.
6. Compute the radii along the model length of the microwave applicator and plaque/blood vessel layer using MODEL. Store surface temperatures for the microwave applicator from TMP into TP.
7. For each finite difference cell along the axial direction, compute the amount of heat in the blood by lumping the heat generation, QM in the radial direction per unit volume. These numbers are stored in QB.
8. Calculate the convective heat transfer coefficients using cubic spline interpolation to evaluate points between values given in Kays and Crawford, 1980.
9. From DX to SEC, in steps of DX, do the following steps.
 - a. Use the summation of MODEL(I,J), MODEL(I+1,J), MODEL(I,J+1), and MODEL(I+1,J+1) to determine which finite subroutine to execute (SUM). The new temperatures calculated from matrix TO are stored in matrix TN.
 - i. If SUM=20, run R2MATL.
 - ii. If SUM=18 or 22, run CONVBND or CONV3A/CONV3B.
 - iii. If SUM=16, run INTRIOR.
 - iv. If SUM=17, run CONV5A/CONV5B.
 - v. If SUM=19, run CONV4A/CONV4B.
 - vi. If SUM=21, run CONV6A/CONV6B.
 - b. Compare MODEL(I,J) with MODEL (I,J+1) to run either INTRIOR or R2MATL subroutines.
 - c. For the last row of muscle in MODEL, run INSBND.

d. Run subroutines CONVCR, INSCNR, SIDE1, and SIDE2 along the edges of the thermal model.

e. Compute the finite difference temperatures for the blood flow using subroutine BFLOW.

f. Replace TO with TN for the next iteration.

10. Normalize final results for future use with the Department of Electrical Engineering graphics program and format output.

11. Print formatted output.


```

*****
C  THESIS PROJECT - A FINITE DIFFERENCE HEAT TRANSFER ANALYSIS OF
C  ATHEROMATOUS PLAQUE FOR PERCUTANEOUS TRANSLUMINAL MICROWAVE
C  ANGIOPLASTY IN BLOOD VESSELS.
*****
C
C  FINITE DIFFERENCE ANGIOPLASTY THERMAL ANALYSIS (FDATA) PROGRAM
C
      include 'head.h'
      parameter(m=200,n=200,nt=6)
      REAL*8 TO(0:M,0:N),ALPHA(6),RHOC(6),DX,DR,DT,TIME,QAVE,
      .      C2(6),K(6),TN(0:M,0:N),RO,COEFF,QM(0:M,0:N),TP(0:M),V(0:M),
      .      TB(0:M+2),QB(0:M),RPLX(0:M),RPRX(0:M),HM(0:M),HP(0:M),SEC,
      .      POWER(M,N),TEMP(M,N),TMP(0:M,0:N),TMAX
      INTEGER IPRT,MODEL(M,N),JRPR(0:M),SUM,JFIN,IFN,IPRT2,IOFF,
      .      ITMP(M,N),ISTART,IFIN,JSTART,TEST(0:M,0:N),JRPL(0:M)
      CHARACTER*1 STATUS
      CHARACTER*40 TITLE
C
C  INITIALIZE PARAMETERS
C
      COMMON TO,TN,QM
      COMMON /DAT/POWER,TEMP,MODEL,ISTART,IFIN,JSTART,JFIN
      DATA ALPHA(3),ALPHA(6),ALPHA(4),ALPHA(5)/1.8E-7,1.22E-7,
      .      1.265E-7,1.54476E-7/
      DATA RHOC(3),RHOC(6),RHOC(4),RHOC(5) /2.833E6,3.541E6,
      .      3.878E6,4.05888E6/
      DATA K(3),K(6),K(4),K(5) /.51,.432,.4912,0.53/
      DATA DT,DX,DR /2.5E-5,1.0000E-4,1.0000E-4/
      IPRT=1
      IPRT2=1
      IFN=40
      IOFF=8000
C
      PRINT*,'THIS IS THE NONABLATION VERSION OF THE FDATA PROGRAM.'
      PRINT*,' '
C
C  INPUT THE NUMBER OF SECONDS TO EVALUATE TEMPERATURE CHANGE
      PRINT*,'INPUT THE NUMBER OF SECONDS TO EVALUATE TEMP CHANGES'
      READ*,SEC
C
      PRINT*,'DO YOU WANT TO INPUT NEW VALUES FOR BLOOD FLOW RATE? TYPE
      .Y TO INPUT NEW VALUES OR N TO USE A DEFAULT VALUE OF 250 ML/MIN.'
      READ*,STATUS
      IF (STATUS.EQ.'Y') THEN
          PRINT*,'INPUT QAVE IN ML/MIN'
          READ*, QAVE
      ELSE
          QAVE=250.0
      ENDIF
C
      OPEN (7,FILE='ang9t.dat',status='unknown')
      OPEN (8,FILE='mod9.dat',status='unknown')
      OPEN (9,FILE='ang9fg.dat',status='unknown')

```

```

OPEN (10,FILE='ang9i.dat',status='unknown')
C
C READ IN SPECIFIC ABSORPTION RATE, TEMPERATURE, AND MODEL DATA
C FROM EE FDTD PROGRAM.
C
CALL DATIN
TITLE='SPECIFIC ABSORPTION RATE DATA'
CALL PDATA2(8,POWER,TITLE)
TITLE='E-M FIELD TEMPERATURE DATA '
CALL PDATA2(8,TEMP,TITLE)
C
C ESTABLISH INITIAL TEMPERATURES IN THE TO MATRIX AND TB ARRAY
C - FOR THIS INITIAL CASE, ASSUME ALL TEMPERATURES IN EACH LAYER ARE
C THE EQUAL TO THE NORMAL BODY TEMPERATURE OF 37 C
C
DO 10 I=ISTART-1,IFIN
  TB(I)=37.0
  DO 20 J=JSTART-1,JFIN
    TO(I,J)=37.0
20  CONTINUE
10  CONTINUE
  TB(IFIN+1)=TB(IFIN)
  TB(IFIN+2)=TB(IFIN+1)
C
DO 15 I=3,NT
  C2(I)=COEFF(ALPHA,DT,DX,I)
15  CONTINUE
C
C SHIFT POWER MATRIX BY DR/2 AND DX/2 TO CALCULATE THE MICROWAVE HEAT
C INPUT AT THE BOUNDARY AND INTERFACE NODES.
C
CALL INTRP1(1,QM,DR,DX)
TITLE='INTERPOLATED QM DATA'
CALL PDATA1(10,QM,TITLE,TIME)
CALL INTRP1(2,TMP,DR,DX)
TITLE='INTERPOLATED TEMP DATA'
CALL PDATA1(10,TMP,TITLE,TIME)
CLOSE(UNIT=10)
C
C FIND THE RADII ALONG THE MODEL LENGTH OF THE MICROWAVE PROBE AND
C PLAQUE LAYER.
C
DO 30 I=ISTART,IFIN
  DO 40 J=JSTART+1,JFIN-1
    IF ((MODEL(I,J).EQ.5).AND.(MODEL(I,J+1).NE.5)) THEN
      RPLX(I)=(J*DR)
      JRPL(I)=J
    ENDIF
    IF ((MODEL(I,J).EQ.5).AND.(MODEL(I,J-1).NE.5)) THEN
      TP(I)=TMP(I,J-1)
      JRPR(I)=J-1
      RPRX(I)=JRPR(I)*DR
    ENDIF
  END DO
END DO

```

```

40     CONTINUE
30     CONTINUE
      TP(0)=TP(1)
C
C   ADJUST PLAQUE STARTING J POINT TO ACCOUNT FOR AN INCREASE IN PLAQUE
C   THICKNESS AS THE BLOOD APPROACHES THE BOUNDARY LAYER.
C
      DO 41 I=ISTART,IFIN-1
        IF (JRPL(I).GT.JRPL(I+1)) JRPL(I)=JRPL(I+1)
41     CONTINUE
C
C   FIND THE AVERAGE RADII IF THE COORDINATE SYSTEM IS SHIFTED TO THE
C   RIGHT BY DX/2.
C
      DO 35 I=ISTART,IFIN-1
        RPLX(I)=(RPLX(I)+RPLX(I+1))/2.0
        RPRX(I)=(RPRX(I)+RPRX(I+1))/2.0
35     CONTINUE
      RPLX(0)=RPLX(1)
      RPLX(IFIN)=RPLX(IFIN-1)
      RPRX(0)=RPRX(1)
      RPRX(IFIN)=RPRX(IFIN-1)
      JRPL(0)=JRPL(1)
      JRPR(0)=JRPR(1)
C
C   LUMP MICROWAVE HEAT INPUT IN THE R DIRECTION FOR EACH LENGTH OF DX
C   TO REPRESENT THE TOTAL HEAT ADDED TO THE BLOOD PER UNIT VOLUME.
C
      DO 45 I=ISTART,IFIN
        KK=(JRPL(I)-1)-(JRPR(I)+1)
        IF (KK.EQ.0) THEN
          QB(I)=0.5*QM(I,JRPL(I))
          GO TO 45
        ELSE
          DO 46 J=JRPR(I)+1,JRPL(I)-1
            R1=DR*J+DR/2.0
            R0=DR*J-DR/2.0
            QB(I)=QB(I)+QM(I,J)*(R1**2-R0**2)
46          CONTINUE
            R1=JRPL(I)*DR-DR/2.0
            R0=JRPR(I)*DR+DR/2.0
            QB(I)=QB(I)/(R1**2-R0**2)+0.5*QM(I,JRPR(I))
          ENDIF
45     CONTINUE
      QB(0)=QB(1)
C
C   COMPUTE THE AVERAGE CONVECTIVE HEAT TRANSFER COEFFICIENTS
C
      CALL HTC(RPLX,RPRX,IFIN,HP,HM,K)
C
C   DETERMINE WHETHER THE NODE BEING EVALUATED IS AN INTERIOR NODE OR
C   ONE WITH BOUNDARY CONDITIONS AND APPLY THE APPROPRIATE SUBROUTINE.
C

```

```

DO 25 TIME=DT,SEC,DT
C
C   TURN OFF HEAT GENERATION AT THE END OF MICROWAVE PULSE DURATION
C
      IF (INT(TIME/DX).EQ.10FF) THEN
      DO 48 II=0,IFIN
      QB(II)=0.0
      DO 47 JJ=0,JFIN
      QM(II,JJ)=0.0
47    CONTINUE
48    CONTINUE
      ENDIF
C
      DO 50 I=ISTART,IFIN-1
      R0=JRPL(I)*DR
      DO 60 J=JRPR(I),JFIN-1
      IF ((MODEL(I,J).EQ.1).OR.(MODEL(I,J).EQ.2)) GO TO 60
C
C   COMPUTE THE SUM OF THE MODEL NODES TO DETERMINE WHICH CONVECTIVE
C   HEAT TRANSFER BOUNDARY CONDITION TO APPLY FOR THE PLAQUE.
C
      SUM=MODEL(I,J)+MODEL(I,J+1)+MODEL(I+1,J)+MODEL(I+1,J+1)
      IF (SUM.EQ.20) THEN
      IF(MODEL(I,J).EQ.4) GO TO 62
      GO TO 60
      ENDIF
      IF (SUM.EQ.18).OR.(SUM.EQ.22)) THEN
      IF (MODEL(I,J).EQ.6) GO TO 62
      IF (MODEL(I,J).EQ.MODEL(I+1,J)) THEN
      TEST(I,J)=8
      IF (SUM.EQ.18) TYPE=4
      IF (SUM.EQ.22) TYPE=6
      CALL CONV3B(HP,ALPHA,RHOC,DR,DT,TYPE,I,J,TB,C2,R0)
      R0=R0+DR/2.0
      GO TO 60
      ELSE
      IF (MODEL(I,J).EQ.5) THEN
      TEST(I,J)=9
      CALL CONV3B(HP,ALPHA,RHOC,DR,DX,DT,4,I,J,TB,C2,R0)
      GO TO 61
      ELSE
      TEST(I,J)=10
      CALL CONV3A(HP,ALPHA,RHOC,DR,DX,DT,4,I,J,TB,C2,R0)
      GO TO 61
      ENDIF
      ENDIF
      ENDIF
      IF (SUM.EQ.16) THEN
      TEST(I,J)=1
      CALL INTRIOR(ALPHA,RHOC,DR,DT,4,I,J,C2,R0)
      GO TO 61
      ENDIF
      IF (SUM.EQ.17) THEN
      IF (MODEL(I,J).EQ.5) THEN

```

```

TEST(I,J)=11
CALL CONV5B(HP,ALPHA,RHOC,DR,DX,DT,4,I,J,TB,R0)
GO TO 61
ELSE
TEST(I,J)=12
CALL CONV5A(HP,ALPHA,RHOC,DR,DX,DT,4,I,J,TB,R0)
GO TO 61
ENDIF
ENDIF
IF (SUM.EQ.19) THEN
IF (MODEL(I,J+1).EQ.5) THEN
TEST(I,J)=13
CALL CONV4A(HP,ALPHA,RHOC,DR,DX,DT,4,I,J,TB,C2,R0)
R0=R0+DR/2.0
GO TO 60
ELSE
TEST(I,J)=14
CALL CONV4B(HP,ALPHA,RHOC,DR,DX,DT,4,I,J,TB,C2,R0)
R0=R0+DR/2.0
GO TO 60
ENDIF
ENDIF
IF (SUM.EQ.21) THEN
IF (MODEL(I,J).EQ.5) THEN
TEST(I,J)=15
CALL CONV6B(HP,K,RHOC,DR,DX,DT,4,6,I,J,TB,R0)
GO TO 61
ELSE
TEST(I,J)=16
CALL CONV6A(HP,K,RHOC,DR,DX,DT,4,6,I,J,TB,R0)
GO TO 61
ENDIF
ENDIF
ENDIF
C
C COMPUTE NEW TEMPERATURE DISTRIBUTION USING THE APPROPRIATE THE
C INTERIOR NODES.
C
62 IF (I.EQ.1) THEN
L=2
ELSE
L=I
ENDIF
IF ((MODEL(L-1,J).EQ.MODEL(L+1,J)).AND.(MODEL(L,J).EQ.
MODEL(L,J+1))) THEN
TEST(I,J)=1
CALL INTRIOR(ALPHA,RHOC,DR,DT,MODEL(I,J),I,J,C2,R0)
GO TO 61
ENDIF
IF (MODEL(L,J).NE.MODEL(L,J+1).AND.(SUM.NE.10)) THEN
TEST(I,J)=2
CALL R2MATL(K,RHOC,DX,DR,DT,MODEL(I,J),MODEL
(I,J+1),I,J,R0)
ENDIF
61 R0=R0+DR

```

```

60     CONTINUE
50     CONTINUE
      DO 70 I=ISTART,IFIN-1
          RO=JFIN*DR-DR/2.0
          TEST(I,JFIN)=3
          CALL INSBND(ALPHA,RHOC,DR,DT,3,I,J,C2,RO)
70     CONTINUE
C
C     COMPUTE NEW TEMPERATURE DISTRIBUTION AT THE ENDS OF THE MODEL.
C
      DO 90 I=ISTART-1,IFIN,IFIN
          IF (I.EQ.0) L=1
          IF (I.EQ.IFIN) L=IFIN
          RO=RPLX(I)
          DO 80 J=JRPL(I),JFIN
              IF (J.EQ.JFIN) THEN
                  TEST(I,J)=4
                  CALL INSCNR(ALPHA,RHOC,DR,DT,I,J,3,C2,RO,IFIN,C2,RO,IFIN)
                  GO TO 80
              ENDIF
              IF (MODEL(L,J).NE.5) THEN
                  IF (MODEL(L,J).NE.MODEL(L,J+1)) THEN
                      TEST(I,J)=5
                      CALL SIDE2(K,RHOC,DX,DR,DT,MODEL(L,J),MODEL(L,J+1),
                          I,J,RO,IFIN)
                      GO TO 81
                  ENDIF
                  IF ((MODEL(L,J).EQ.MODEL(L,J+1))) THEN
                      TEST(I,J)=6
                      CALL SIDE1(ALPHA,RHOC,MODEL(L,J),DR,DT,,J,C2,RO,IFIN)
                      GO TO 81
                  ENDIF
              ELSE
                  IF (MODEL(L,J).EQ.MODEL(L,J+1)) GO TO 80
                  TEST(I,J)=7
                  CALL CONVNR(HP,ALPHA,RHOC,DR,DX,MODEL(L,J+1),I,
                      J,TB,C2,RO,IFIN)
                  RO=RO+DR/2.0
                  GO TO 80
              ENDIF
          ENDIF
81     RO=RO+DR
80     CONTINUE
90     CONTINUE
          IF (TIME.EQ.DT) THEN
              TITLE='TEST FILE'
              CALL ARR2(8,TEST,M,30,100,0,0,IFIN,JFIN,TITLE)
              CLOSE (UNIT=8)
          ENDIF
C
C     CALCULATE THE AVERAGE BLOOD FLOW VELOCITY THEN CALCULATE THE
C     TEMPERATURE DISTRIBUTION OF THE BLOOD
C
      CALL BFLOW(TB,QB,RHOC,5,HP,HM,RPLX,RPRX,DX,DT,TP,V,
          IFIN,JRPR,JRPL,QAVE)

```

```

C
C STORE NEW TEMPERATURE DISTRIBUTION INTO THE OLD TEMPERATURE MATRIX
C FOR THE NEXT ITERATION.
C
      DO 140 J=0,JFIN
        DO 130 I=0,IFIN
          TO(I,J)=TN(I,J)
130      CONTINUE
140      CONTINUE
C
C PRINT NEW TEMPERATURE DISTRIBUTION FOR THE 1000TH TIME STEP.
C
      IF (IPRT.EQ.2000) THEN
        IPRT=1
        TITLE='NEW TEMP PROFILE '
        CALL PDATA1(IFN,TN,TITLE,TIME)
        CLOSE (UNIT=IFN)
        IFN=IFN+1
      ELSE
        IPRT=IPRT+1
      ENDIF
25 CONTINUE
C
C NORMALIZE FINAL TEMPERATURE DISTRIBUTION OUTPUT FOR USE WITH THE EE
C GRAPHICS OUTPUT PROGRAM. (FIND TMAX FOR TN(M,N); DIVIDE TN(M,N) BY
C TMAX; MULTIPLY BY A FACTOR OF 1000; CONVERT DATA TO AN INTEGER
C MATRIX)
C
      DO 350 I=ISTART-1,IFIN-1
        DO 360 J=JSTART-1,JFIN-1
          TEMP(I+1,J+1)=(TN(I,J)+TN(I+1,J)+TN(I,J+1)+TN(I+1,J+1))/4.0
360      CONTINUE
350      CONTINUE
        TITLE='NEW TEMP PROFILE '
        CALL PDATA2(7,TEMP,TITLE,TIME)
        CLOSE (UNIT=7)
        TMAX=0.0
        DO 310 I=ISTART-1,IFIN
          DO 320 J=JSTART-1,JFIN
            IF (TEMP(I,J).GT.TMAX) TMAX=TEMP(I,J)
320          CONTINUE
310        CONTINUE
        DO 330 I=ISTART,IFIN
          DO 340 J=JSTART,JFIN
            ITMP(I,J)=INT((FLOAT(TEMP(I,J))/FLOAT(TMAX))*1000)
340          CONTINUE
330        CONTINUE
        TITLE='FINAL NORMALIZED TEMPERATURE OUTPUT'
        CALL ARRAYOUT(9,ITMP,M,30,100,ISTART,JSTART,IFIN,JFIN,TITLE)
        TITLE='MODEL GENERATED BY EE'
        CALL ARRAYOUT(9,MODEL,M,30,100,ISTART,JSTART,IFIN,JFIN,TITLE)
        STOP
      END
C

```

C SUBROUTINE TO CALCULATE TPRIME (STORED IN MATRIX X) AT DT FOR AN
C INTERIOR NODE.

C

```

SUBROUTINE INTRIOR(ALPHA,RHOC,DR,DT,TYPE,I,J,C2,R0)
INCLUDE 'head.h'
INTEGER TYPE,I,J
REAL*8 TO(0:M,0:N),TN(0:M,0:N),ALPHA(NT),RHOC(NT),DR,DT,C1
REAL*8 R0,R1,C2(NT),C,QM(0:M,0:N)
COMMON TO,TN,QM
R1=R0+DR
C1=2.0*ALPHA(TYPE)*DT/((R1**2-R0**2)*DR)
C=1.0-C1*R0-C1*R1-2.0*C2(TYPE)
IF (C.LT.0.0) THEN
  PRINT*,'INTR UNSTABLE CONDITION; C=',C
ENDIF
TN(I,J)=C1*(R0*TO(I,J-1)+R1*TO(I,J+1))+C2(TYPE)*
.   (TO(I-1,J)+TO(I+1,J))+C*TO(I,J)+QM(I,J)*DT/RHOC(TYPE)
RETURN
END

```

C

C

C SUBROUTINE TO CALCULATE TPRIME (STORED IN T) AT DT FOR A NODE
C AT A BOUNDARY LAYER WITH TWO MATERIAL TYPES.

C

```

SUBROUTINE R2MATL(K,RHOC,DX,DR,DT,TYP1,TYP2,I,J,R0)
INCLUDE 'head.h'
INTEGER I,J,TYP1,TYP2
REAL*8 TO(0:M,0:N),TN(0:M,0:N),K(NT),RHOC(NT),DX,DR,DT
REAL*8 C,C1,C2,C3,C4,CXX,R0,R1,R2,QM(0:M,0:N)
COMMON TO,TN,QM
R1=R0+DR/2.0
R2=R0+DR
CXX=RHOC(TYP1)*(R1**2-R0**2)+RHOC(TYP2)*(R2**2-R1**2)
C1=2.0*K(TYP1)*DT/(CXX*DR)
C2=2.0*K(TYP2)*DT/(CXX*DR)
C3=K(TYP1)*(R1**2-R0**2)*DT/(CXX*DX**2)
C4=K(TYP2)*(R2**2-R1**2)*DT/(CXX*DX**2)
C=1.0-C1*R0-C2*R2-2.0*C3-2.0*C4
IF (C.LT.0.0) THEN
  PRINT*,'R2MATL UNSTABLE CONDITION; C=',C
ENDIF
TN(I,J)=C1*R0*TO(I,J-1)+C2*R2*TO(I,J+1)+C3*(TO(I-1,J)
.   +TO(I+1,J))+C4*(TO(I-1,J)+TO(I+1,J))+QM(I,J)*(R2**2
.   -R0**2)*DT/CXX+C*TO(I,J)
RETURN
END

```

C

C SUBROUTINE TO ACCOUNT FOR INSULATIVE SIDE BOUNDARY CONDITIONS FOR A
C SINGE ELEMENT NODE.

C

```

SUBROUTINE SIDE1(ALPHA,RHOC,TYPE,DR,DT,I,J,C2,R0,IFIN)
INCLUDE 'head.h'
INTEGER I,J,TYPE,IFIN
REAL*8 TO(0:M,0:N),TN(0:M,0:N),ALPHA(NT),RHOC(TYPE),DR,DT

```



```

REAL*8 C,C1,C2(NT),R0,R1,QM(0:M,0:N)
COMMON TO,TN,QM
R1=R0+DR
C1=2.0*ALPHA(TYPE)*DT/((R1**2-R0**2)*DR)
C=1.0-C1*R1-C1*R0-2.0*C2(TYPE)
IF (C.LT.0.0) THEN
  PRINT*, 'SIDE1 UNSTABLE CONDITION; C=',C
ENDIF
IF (I.EQ.0) K=I+1
IF (I.EQ.IFIN) K=I-1
TN(I,J)=C1*R1*TO(I,J+1)+C1*R0*TO(I,J-1)+C2(TYPE)*2.0*
  TO(K,J)+QM(I,J)*DT/RHOC(TYPE)+C*TO(I,J)
RETURN
END

```

```

C
C SUBROUTINE TO ACCOUNT FOR THE INSULATIVE SIDE BOUNDARY CONDITIONS
C FOR A NODE CONTAINING TWO DIFFERENT MATERIALS
C

```

```

SUBROUTINE SIDE2(K,RHOC,DX,DR,DT,TYP1,TYP2,I,J,R0,IFIN)
INCLUDE 'head.h'
INTEGER TYP1,TYP2,I,J,KK,IFIN
REAL*8 TO(0:M,0:N),TN(0:M,0:N),RHOC(NT),K(NT),DX,DR,DT
REAL*8 CXX,C,C1,C2,C3,C4,R0,R1,R2,QM(0:M,0:N)
COMMON TO,TN,QM
R1=R0+DR/2.0
R2=R0+DR
CXX=RHOC(TYP1)*(R1**2-R0**2)+RHOC(TYP2)*(R2**2-R1**2)
C1=2.0*K(TYP1)*DT/(CXX*DR)
C2=2.0*K(TYP2)*DT/(CXX*DR)
C3=K(TYP1)*(R1**2-R0**2)*DT/(CXX*DX**2)
C4=K(TYP2)*(R2**2-R1**2)*DT/(CXX*DX**2)
IF (I.EQ.0) KK=I+1
IF (I.EQ.IFIN) KK=I-1
C=1.0-C1*R0-C2*R2-2.0*C3-2.0*C4
IF (C.LT.0.0) THEN
  PRINT*, 'SIDE2 UNSTABLE CONDITION; C=',C
ENDIF
TN(I,J)=C1*R0*TO(I,J-1)+C2*R2*TO(I,J+1)+2.0*C3*
  TO(KK,J)+2.0*C4*TO(KK,J)+QM(I,J)*(R2**2-R0**2)*DT
  /CXX+C*TO(I,J)
RETURN
END

```

```

C
C SUBROUTINE TO CALCULATE THE TEMPERATURE EFFECTS AT THE INSULATED
C CORNERS REPRESENTING THE SEMI-INFINITE BOUNDARY CONDITIONS OF
C THE MUSCLE TISSUE.
C

```

```

SUBROUTINE INSCNR(ALPHA,RHOC,DR,DT,I,J,TYPE,C2,R0,IFIN)
INCLUDE 'head.h'
INTEGER I,J,TYPE,IFIN
REAL*8 TO(0:M,0:N),TN(0:M,0:N),ALPHA(NT),RHOC(NT)
REAL*8 C,C1,C2(NT),R0,R1,DR,DT,QM(0:M,0:N)
COMMON TO,TN,QM
R1=R0+DR/2.0

```

```

      C1=2.0*ALPHA(TYPE)*DT/((R1**2-R0**2)*DR)
      C=1.0-C1*R0-2.0*C2(TYPE)
      IF (C.LT.0.0) THEN
        PRINT*, 'INSCNR UNSTABLE CONDITION; C=', C
      ENDIF
      IF (I.EQ.0) K=I+1
      IF (I.EQ.IFIN) K=I-1
      TN(I,J)=C1*R0*TO(I,J-1)+2.0*C2(TYPE)*TO(K,J)+QM(I,J)*
        DT/RHOC(TYPE)+C*TO(I,J)
      RETURN
    END

```

C

C SUBROUTINE TO ACCOUNT FOR THE INSULATIVE MUSCLE LAYER

```

      SUBROUTINE INSBND(ALPHA,RHOC,DR,DT,TYPE,I,J,C2,R0)
      INCLUDE 'head.h'
      INTEGER TYPE,I,J
      REAL*8 TO(0:M,0:N),TN(0:M,0:N),ALPHA(NT),RHOC(NT),DR,DT
      REAL*8 C,C1,C2(NT),R0,R1,QM(0:M,0:N)
      COMMON TO,TN,QM
      R1=R0+DR/2.0
      C1=2.0*ALPHA(TYPE)*DT/((R1**2-R0**2)*DR)
      C=1.0-C1*R0-2.0*C2(TYPE)
      IF (C.LT.0.0) THEN
        PRINT*, 'INSBND UNSTABLE CONDITION; C=', C
      ENDIF
      TN(I,J)=C1*R0*TO(I,J-1)+C2(TYPE)*(TO(I-1,J)+TO(I+1,J))+
        C*TO(I,J)+QM(I,J)*DT/RHOC(TYPE)
      RETURN
    END

```

C

C SUBROUTINE TO ACCOUNT FOR THE INSULATIVE CORNER BOUNDARY CONDITIONS
C WHERE CONVECTION OCCURS AT THE BLOOD/PLAQUE INTERFACE

C

```

      SUBROUTINE CONVCONR(H,ALPHA,RHOC,DR,DT,TYPE,
        I,J,TB,C2,R0,IFIN)
      INCLUDE 'head.h'
      INTEGER TYPE,I,J,K,IFIN
      REAL*8 TO(0:M,0:N),TN(0:M,0:N),ALPHA(NT),RHOC(NT),DR,DT
      REAL*8 H(0:M),C,C1,C2(NT),C3,R1,R0,TB(0:M+2),QM(0:M,0:N)
      COMMON TO,TN,QM
      R1=R0+DR/2.0
      IF (I.EQ.0) K=I+1
      IF (I.EQ.IFIN) K=I-1
      C1=2.0*ALPHA(TYPE)*DT/((R1**2-R0**2)*DR)
      C3=2.0*H(I)*R0*DT/(RHOC(TYPE)*(R1**2-R0**2))
      C=1.0-C1*R1-2.0*C2(TYPE)-C3
      IF (C.LT.0.0) THEN
        PRINT*, 'CONVCNR UNSTABLE CONDITION; C=', C
      ENDIF
      TN(I,J)=C1*R1*TO(I,J+1)+2.0*C2(TYPE)*TO(K,J)+C*TO(I,J)
        +C3*TB(I+1)+(QM(I,J)/RHOC(TYPE))*DT
      RETURN
    END

```

```

C
C SUBROUTINE TO CALCULATE TPRIME AT DT FOR A NODE LYING ON A
C CONVECTIVE BOUNDARY LAYER (PLAQUE/BLOOD)
C
      SUBROUTINE CONVBND(H, ALPHA, RHOC, DR, DT, TYPE, I, J, TB, C2, R0)
      INCLUDE 'head.h'
      INTEGER I, J, TYPE
      REAL*8 TO(0:M, 0:N), TN(0:M, 0:N), H(0:M), ALPHA(NT), RHOC(NT),
      .      QM(0:M, 0:N), C2(NT), C, DR, DT, C1, C3, R0, R1, TB(0:M+2)
      COMMON TO, TN, QM
      R1=R0+DR/2.0
      C1=2.0*ALPHA(TYPE)*DT/((R1**2-R0**2)*DR)
      C3=2.0*H(I)*R0*DT/(RHOC(TYPE)*(R1**2-R0**2))
      C=1.0-C1*R1-2.0*C2(TYPE)-C3
      IF (C.LT.0.0) THEN
        PRINT*, 'CONVBND UNSTABLE CONDITION; C=', C
      ENDIF
      TN(I, J)=C1*R1*TO(I, J+1)+C2(TYPE)*(TO(I-1, J)+TO(I+1, J))
      .      +C3*TB(I+1)+C*TO(I, J)+QM(I, J)*DT/RHOC(TYPE)
      RETURN
      END

C
C SUBROUTINES FOR THE VARIOUS CONVECTIVE BOUNDARY LAYER CONDITIONS IN
C THE PLAQUE LAYER OF VARYING RADII.
C
      SUBROUTINE CONV3A(H, ALPHA, RHOC, DR, DX, DT, TYPE, I, J, TB, CC, R0)
      INCLUDE 'head.h'
      INTEGER I, J, TYPE
      REAL*8 TO(0:M, 0:N), TN(0:M, 0:N), H(0:M), ALPHA(NT), RHOC(NT),
      .      QM(0:M, 0:N), C2, C, DR, DT, C1, C3, R0, R1, TB(0:M+2), CC(NT), DX
      COMMON TO, TN, QM
      R1=R0+DR
      C1=2.0*CC(TYPE)
      C2=2.0*ALPHA(TYPE)*DT/(DR*(R1**2-R0**2))
      C3=2.0*H(I)*DT/(RHOC(TYPE)*DX)
      C=1.0-C1-C2*R1-C2*R0-C3
      IF (C.LT.0.0) THEN
        PRINT*, 'CONV3A UNSTABLE CONDITION; C=', C
      ENDIF
      TN(I, J)=C1*TO(I-1, J)+C2*R1*TO(I, J+1)+C2*R0*TO(I, J-1)
      .      +C3*TB(I+2)+C*TO(I, J)+QM(I, J)*DT/RHOC(TYPE)
      RETURN
      END

C
C
      SUBROUTINE CONV3B(H, ALPHA, RHOC, DR, DX, DT, TYPE, I, J, TB, CC, R0)
      INCLUDE 'head.h'
      INTEGER I, J, TYPE
      REAL*8 TO(0:M, 0:N), TN(0:M, 0:N), H(0:M), ALPHA(NT), RHOC(NT),
      .      QM(0:M, 0:N), C2, C, DR, DT, C1, C3, R0, R1, TB(0:M+2), CC(NT), DX
      COMMON TO, TN, QM
      R1=R0+DR
      C1=2.0*CC(TYPE)
      C2=2.0*ALPHA(TYPE)*DT/(DR*(R1**2-R0**2))

```

```

C3=2.0*H(I)*DT/(RHOC(TYPE)*DX)
C=1.0-C1-C2*R1-C2*R0-C3
IF (C.LT.0.0) THEN
  PRINT*, 'CONV3B UNSTABLE CONDITION; C=', C
ENDIF
TN(I,J)=C1*TO(I+1,J)+C2*R1*TO(I,J+1)+C2*R0*TO(I,J-1)
  +C3*TB(I)+C*TO(I,J)+QM(I,J)*DT/RHOC(TYPE)
RETURN
END

```

C
C

```

SUBROUTINE CONV4A(H, ALPHA, RHOC, DR, DX, DT, TYPE, I, J, TB, CC, R0)
INCLUDE 'head.h'
INTEGER I, J, TYPE
REAL*8 TO(0:M, 0:N), TN(0:M, 0:N), H(0:M), ALPHA(NT), RHOC(NT), DX
  , QM(0:M, 0:N), C2, C, DR, DT, C1, C3, C4, R0, R1, TB(0:M+2), CC(NT), CR
COMMON TO, TN, QM
R1=R0+DR/2.0
CR=R1**2-R0**2
C1=2.0*CC(TYPE)
C2=2.0*ALPHA(TYPE)*DT*R1/(DR*CR)
C3=2.0*H(I)*DT/(RHOC(TYPE)*DX)
C4=2.0*H(I)*R0*DT/(RHOC(TYPE)*CR)
C=1.0-C1-C2-C3-C4
IF (C.LT.0.0) THEN
  PRINT*, 'CONV4A UNSTABLE CONDITION; C=', C
ENDIF
TN(I,J)=C1*TO(I+1,J)+C2*TO(I,J+1)+C3*TB(I)+C4*TB(I+1)+C*
  TO(I,J)+QM(I,J)*DT/RHOC(TYPE)
RETURN
END

```

C
C

```

SUBROUTINE CONV4B(H, ALPHA, RHOC, DR, DX, DT, TYPE, I, J, TB, CC, R0)
INCLUDE 'head.h'
INTEGER I, J, TYPE
REAL*8 TO(0:M, 0:N), TN(0:M, 0:N), H(0:M), ALPHA(NT), RHOC(NT), DX
  , QM(0:M, 0:N), C2, C, DR, DT, C1, C3, C4, R0, R1, TB(0:M+2), CC(NT), CR
COMMON TO, TN, QM
R1=R0+DR/2.0
CR=R1**2-R0**2
C1=2.0*CC(TYPE)
C2=2.0*ALPHA(TYPE)*DT*R1/(DR*CR)
C3=2.0*H(I)*DT/(RHOC(TYPE)*DX)
C4=2.0*H(I)*R0*DT/(RHOC(TYPE)*CR)
C=1.0-C1-C2-C3-C4
IF (C.LT.0.0) THEN
  PRINT*, 'CONV4B UNSTABLE CONDITION; C=', C
ENDIF
TN(I,J)=C1*TO(I-1,J)+C2*TO(I,J+1)+C3*TB(I+2)+C4*TB(I+1)+C*
  TO(I,J)+QM(I,J)*DT/RHOC(TYPE)
RETURN
END

```

C

C

```

SUBROUTINE CONV5A(H,ALPHA,RHOC,DR,DX,DT,TYPE,I,J,TB,R0)
INCLUDE 'head.h'
INTEGER I,J,TYPE
REAL*8 TO(0:M,0:N),TN(0:M,0:N),H(0:M),ALPHA(NT),RHOC(NT),
.      C2,DR,DT,C1,C3,C4,R0,R1,R2,TB(0:M+2),C5,C6,VOL,PI,CR2,DX,C
.      ,QM(0:M,0:N),CR1
COMMON TO,TN,QM
PI=3.141592654
R1=R0+DR/2.0
R2=R0+DR
CR1=R2**2-R1**2
CR2=R2**2-R0**2
VOL=PI*(CR2*DX-CR1*DX/2.0)
C1=ALPHA(TYPE)*PI*CR2*DT/(VOL*DX)
C2=ALPHA(TYPE)*PI*CR1*DT/(VOL*DX)
C3=ALPHA(TYPE)*PI*R0*DX*DT/(VOL*DR)
C4=ALPHA(TYPE)*2.0*PI*R2*DX*DT/(VOL*DR)
C5=H(I)*PI*R1*DX*DT/(VOL*RHOC(TYPE))
C6=H(I)*PI*CR1*DT/(VOL*RHOC(TYPE))
C=1.0-C1-C2-C3-C4-C5-C6
IF (C.LT.0.0) THEN
  PRINT*, 'CONV5A UNSTABLE CONDITION; C=',C
ENDIF
TN(I,J)=C1*TO(I-1,J)+C2*TO(I+1,J)+C3*TO(I,J-1)+C4*TO(I,J+1)
.      +C5*TB(I+1)+C6*TB(I+2)+C*TO(I,J)+QM(I,J)*DT/RHOC(TYPE)
RETURN
END

```

C

```

SUBROUTINE CONV5B(H,ALPHA,RHOC,DR,DX,DT,TYPE,I,J,TB,R0)
INCLUDE 'head.h'
INTEGER I,J,TYPE
REAL*8 TO(0:M,0:N),TN(0:M,0:N),H(0:M),ALPHA(NT),RHOC(NT),
.      C2,DR,DT,C1,C3,C4,R0,R1,R2,TB(0:M+2),C5,C6,VOL,PI,CR2,DX,C
.      ,QM(0:M,0:N),CR1
COMMON TO,TN,QM
PI=3.141592654
R1=R0+DR/2.0
R2=R0+DR
CR1=R2**2-R1**2
CR2=R2**2-R0**2
VOL=PI*(CR2*DX-(R1**2-R0**2)*DX/2.0)
C1=ALPHA(TYPE)*PI*CR2*DT/(VOL*DX)
C2=ALPHA(TYPE)*PI*CR1*DT/(VOL*DX)
C3=ALPHA(TYPE)*PI*R0*DX*DT/(VOL*DR)
C4=ALPHA(TYPE)*2.0*PI*R2*DX*DT/(VOL*DR)
C5=H(I)*PI*R1*DX*DT/(VOL*RHOC(TYPE))
C6=H(I)*PI*(R1**2-R0**2)*DT/(VOL*RHOC(TYPE))
C=1.0-C1-C2-C3-C4-C5-C6
IF (C.LT.0.0) THEN
  PRINT*, 'CONV5B UNSTABLE CONDITION; C=',C
ENDIF
TN(I,J)=C1*TO(I+1,J)+C2*TO(I-1,J)+C3*TO(I,J-1)+C4*TO(I,J+1)
.      +C5*TB(I+1)+C6*TB(I)+C*TO(I,J)+QM(I,J)*DT/RHOC(TYPE)

```

RETURN
END

C

```

SUBROUTINE CONV6A(H,K,RHOC,DR,DX,DT,TYP1,TYP2,I,J,TB,R0)
INCLUDE 'head.h'
INTEGER TYP1,TYP2,I,J
REAL*8 TO(0:M,0:N),TN(0:M,0:N),H(0:M),K(NT),RHOC(NT),
.      DR,DX,DT,R0,R1,R2,C,VOL,PI,CR1,CR2,C1,C2,C3,C4,C5,C6,C7,
.      QM(0:M,0:N),TB(0:M+2)
COMMON TO,TN,QM
PI=3.141592654
R1=R0+DR/2.0
R2=R0+DR
CR1=R2**2-R1**2
CR2=R1**2-R0**2
VOL=PI*((R2**2-R0**2)*DX-CR2*DX/2.0)
C1=(PI*(RHOC(TYP1)*CR2*DX/2.0+RHOC(TYP2)*CR1*DX))/DT
C2=K(TYP1)*PI*CR2/(DX*C1)
C3=K(TYP2)*PI*CR1/(DX*C1)
C4=K(TYP1)*PI*R0*DX/(DR*C1)
C5=2.0*K(TYP2)*PI*R2*DX/(DR*C1)
C6=H(I)*PI*R1*DX/C1
C7=H(I)*PI*CR2/C1
C=1.0-C2-2.0*C3-C4-C5-C6-C7
IF (C.LT.0.0) THEN
  PRINT*, 'CONV6A UNSTABLE CONDITION; C=',C
ENDIF
TN(I,J)=C2*TO(I-1,J)+C3*(TO(I-1,J)+TO(I+1,J))+C4*TO(I,J-1)
. +C5*TO(I,J+1)+C6*TB(I+1)+C7*TB(I+2)+C*TO(I,J)+QM(I,J)*VOL/C1
RETURN
END

```

C
C

```

SUBROUTINE CONV6B(H,K,RHOC,DR,DX,DT,TYP1,TYP2,I,J,TB,R0)
INCLUDE 'head.h'
INTEGER TYP1,TYP2,I,J
REAL*8 TO(0:M,0:N),TN(0:M,0:N),H(0:M),K(NT),RHOC(NT),
.      DR,DX,DT,R0,R1,R2,C,VOL,PI,CR1,CR2,C1,C2,C3,C4,C5,C6,C7,
.      QM(0:M,0:N),TB(0:M+2)
COMMON TO,TN,QM
PI=3.141592654
R1=R0+DR/2.0
R2=R0+DR
CR1=R2**2-R1**2
CR2=R1**2-R0**2
VOL=PI*((R2**2-R0**2)*DX-CR2*DX/2.0)
C1=(PI*(RHOC(TYP1)*CR2*DX/2.0+RHOC(TYP2)*CR1*DX))/DT
C2=K(TYP1)*PI*CR2/(DX*C1)
C3=K(TYP2)*PI*CR1/(DX*C1)
C4=K(TYP1)*PI*R0*DX/(DR*C1)
C5=2.0*K(TYP2)*PI*R2*DX/(DR*C1)
C6=H(I)*PI*R1*DX/C1
C7=H(I)*PI*CR2*DX/C1
C=1.0-C2-2.0*C3-C4-C5-C6-C7

```

```

      IF (C.LT.0.0) THEN
        PRINT*, 'CONV6B UNSTABLE CONDITION; C=', C
      ENDIF
      TN(I,J)=C2*TO(I+1,J)+C3*(TO(I+1,J)+TO(I-1,J))+C4*TO(I,J-1)
      .+C5*TO(I,J+1)+C6*TB(I+1)+C7*TB(I)+C*TO(I,J)+QM(I,J)*VOL/C1
      RETURN
    END

```

C
C

```

      DOUBLE PRECISION FUNCTION COEFF(ALPHA,DT,DX,TYPE)
      include 'head.h'
      INTEGER TYPE
      REAL*8 ALPHA(NT),DT,DX
      COEFF=ALPHA(TYPE)*DT/DX**2
      RETURN
    END

```

C
C
C
C
C
C

```

      CUBIC SPLINE INTERPOLATION SUBROUTINE FOR CALCULATING THE AVERAGE
      CONVECTIVE HEAT TRANSFER COEFFICIENTS AND ENERGY DEPOSITION FROM THE
      MICROWAVE APPLICATOR AT THE NODE INTERFACES.

```

C

```

      SUBROUTINE CUBSPL(X,FX,F,XBAR,NN,NX)
      INCLUDE 'head.h'
      INTEGER NN,NX
      PARAMETER (NO=200)
      REAL*8 X(0:NN),F(0:NN),XBAR(0:NX),FX(0:NX)
      REAL*8 ALPHA(NO),B(0:NO),C(0:NO),D(0:NO),H(0:NO)
      .,L(0:NO),MU(0:NO),Z(0:NO),X1
      DO 10 I=0,NN-1
        H(I)=X(I+1)-X(I)
10      CONTINUE
      DO 20 I=1,NN-1
        ALPHA(I)=3.0*(F(I+1)*H(I-1)-F(I)*(X(I+1)-X(I-1))+F(I-1)*H(I))
        ./(H(I-1)*H(I))
20      CONTINUE
      L(0)=1.0
      MU(0)=0.0
      Z(0)=0.0
      DO 30 I=1,NN-1
        L(I)=2.0*(X(I+1)-X(I-1))-H(I-1)*MU(I-1)
        MU(I)=H(I)/L(I)
        Z(I)=(ALPHA(I)-H(I-1)*Z(I-1))/L(I)
30      CONTINUE
      L(NN)=1.0
      Z(NN)=0.0
      C(NN)=0.0
      DO 40 I=NN-1,0,-1
        C(I)=Z(I)-MU(I)*C(I+1)
        B(I)=(F(I+1)-F(I))/H(I)-H(I)*(C(I+1)+2.0*C(I))/3.0
        D(I)=(C(I+1)-C(I))/(3.0*H(I))
40      CONTINUE
      DO 50 I=0,NX
        J=0

```

```

      IF (XBAR(I).LT.X(0)) THEN
        FX(I)=F(0)
        GO TO 50
      ENDIF
      IF (XBAR(I).GT.X(NN)) THEN
        FX(I)=F(NN)
        GO TO 50
      ENDIF

      DO 55 K=1,NN
        IF ((XBAR(I).LT.X(K)).AND.(XBAR(I).GE.X(K-1))) J=K-1
55    CONTINUE
        IF (F(J).EQ.F(J+1)) THEN
          FX(I)=F(J)
          GO TO 50
        ENDIF
        X1=XBAR(I)-X(J)
        FX(I)=F(J)+B(J)*X1+C(J)*(X1**2)+D(J)*(X1**3)
50    CONTINUE
      RETURN
      END

C
C SUBROUTINE TO ESTIMATE THE CONVECTIVE HEAT TRANSFER COEFFICIENTS
C OF THE BLOOD VESSEL WALL AND MICROWAVE APPLICATOR USING A CUBIC
C SPLINE APPROXIMATION FOR THE ANALYTICAL SOLUTION OF A CONCENTRIC
C ANNULAR CIRCULAR PIPE.
C
      SUBROUTINE HTC(RPLX,RPRX,IFIN,HP,HM,K)
      INCLUDE 'head.h'
      INTEGER IFIN,I
      PARAMETER (NO=200,TYPE=5)
      REAL*8 RSTR1(0:6),RSTR2(0:7),NU1(0:6),NU2(0:7),RPRX(0:M),
      .      NU(0:NO),RBAR(0:NO),K(NT),HP(0:M),HM(0:M),DH,RPLX(0:M)
      DATA (RSTR1(I),I=0,6)/.05,.10,.20,.40,.60,.80,1.00/
      DATA (NU1(I),I=0,6)/17.81,11.91,8.499,6.583,5.912,5.58,5.385/
      DATA (RSTR2(I),I=0,7)/0.0,.05,.10,.20,.40,.60,.80,1.00/
      DATA (NU2(I),I=0,7)/4.364,4.792,4.834,4.883,4.979,5.099,
      .      5.24,5.385/
      DO 10 I=0,IFIN
        RBAR(I)=RPRX(I)/RPLX(I)
10    CONTINUE
      CALL CUBSPL(RSTR1,NU,NU1,RBAR,6,IFIN)
      DO 20 I=0,IFIN
        IF (RPRX(I).EQ.0.0) THEN
          HM(I)=0.0
        ELSE
          DH=2.0*(RPLX(I)-RPRX(I))
          HM(I)=NU(I)*K(TYPE)/DH
        ENDIF
20    CONTINUE
      CALL CUBSPL(RSTR2,NU,NU2,RBAR,7,IFIN)
      DO 30 I=0,IFIN
        IF (RPRX(I).EQ.0.0) THEN

```



```

        DH=2.0*RPLX(I)
        NU=3.66
        HP(I)=NU*K(TYPE)/DH
    ELSE
        DH=2.0*(RPLX(I)-RPRX(I))
        HP(I)=NU(I)*K(TYPE)/DH
C      PRINT*, 'H, NU 1 ', HP(I), NU(I)
    ENDIF
30  CONTINUE
    RETURN
    END

C
C  SUBROUTINE TO CALCULATE THE HEAT DISTRIBUTION IN THE BLOOD LAYER
C  DUE TO ONE-DIMENSIONAL CONVECTIVE HEAT TRANSFER
C
    SUBROUTINE BFLOW(TB1,QB,RHOC,TYPE,HPL,HPR,RPL,RPR,
.      DX,DT,TP,V,IFIN,JRPR,JRPL,QAVE)
    INCLUDE 'head.h'
    INTEGER TYPE,IFIN,L,JRPR(0:M),JRPL(0:M)
    REAL*8 TN(0:M,0:N),TB1(0:M+2),RPL(0:M),RPR(0:M),QB(0:M),
.      HPL(0:M),HPR(0:M),V(0:M),DX,DT,C,C1,C2,C3,C4,TB2(0:452)
.      ,RHOC(NT),TP(0:M),QAVE,QM(0:M,0:N),TO(0:M,0:N)
    COMMON TO,TN,QM
    DO 10 I=0,IFIN
        C1=2.0*DT/(RHOC(TYPE)*(RPL(I)**2-RPR(I)**2))
        C2=HPR(I)*RPR(I)*C1
        C3=HPL(I)*RPL(I)*C1
        V(I)=QAVE*5.3051647E-9/(RPL(I)**2-RPR(I)**2)
        C4=V(I)*DT/DX
        C=1.0-2.0*C4-C2-C3
        IF (C.LT.0.0) THEN
            PRINT*, 'BFLOW UNSTABLE CONDITION,; C=',C
        ENDIF
        TB2(I+1)=C4*(TB1(I)+TB1(I+2))+C2*TP(I)+C3*TN(I,JRPL(I))+C*
.      TB1(I+1)+QB(I)*DT/RHOC(TYPE)
10  CONTINUE
        TB1(IFIN+2)=TB2(IFIN+1)
        DO 20 I=1,IFIN+1
            TB1(I)=TB2(I)
20  CONTINUE
        DO 40 I=0,IFIN
            DO 30 J=JRPR(I),JRPL(I)-1
                TN(I,J)=TB1(I+1)
30  CONTINUE
40  CONTINUE
    RETURN
    END

C
C  SUBROUTINE TO RECALCULATE THE POWER GENERATED BY THE MICROWAVE
C  APPLICATOR AT THE INTERFACE OF THE NODES USING THE CUBIC SPLINE
C  SUBROUTINE.
C
    SUBROUTINE INTRP1(IFLAG,AOUT,DR,DX)
    INCLUDE 'head.h'

```

```

      INTEGER I,J,ISTART,IFIN,JSTART,JFIN,MODEL(M,N),NN1,NN2
      INTEGER NX1,NX2
      REAL*8 AOUT(0:M,0:N),X(0:200),F(0:200),FX(0:200),DR,DX
      REAL*8 XBAR(0:200),RBAR(0:200),TEMP(M,N)
      REAL*8 POWER(M,N),QM(0:M,0:N),TO(0:M,0:N),TN(0:M,0:N)
      COMMON TO,TN,QM
      COMMON /DAT/POWER,TEMP,MODEL,ISTART,IFIN,JSTART,JFIN
      NN1=IFIN-ISTART
      NN2=JFIN-JSTART
      NX1=IFIN
      NX2=JFIN
      DO 10 J=JSTART,JFIN
        DO 20 I=ISTART,IFIN
          IF (IFLAG.EQ.1) THEN
            F(I-1)=POWER(I,J)
          ELSE
            F(I-1)=TEMP(I,J)
          ENDIF
          X(I-1)=I*DX-DX/2.0
          XBAR(I-1)=(I-1)*DX
20      CONTINUE
          XBAR(IFIN)=XBAR(IFIN-1)+DX
          CALL CUBSPL(X,FX,F,XBAR,NN1,NX1)
          DO 30 I=ISTART-1,IFIN
            AOUT(I,J)=FX(I)
30      CONTINUE
10     CONTINUE
        DO 40 I=ISTART-1,IFIN
          DO 50 J=JSTART,JFIN
            F(J-1)=AOUT(I,J)
            X(J-1)=J*DR-DR/2.0
            RBAR(J-1)=(J-1)*DR
50      CONTINUE
            RBAR(JFIN)=RBAR(JFIN-1)+DR
            CALL CUBSPL(X,FX,F,RBAR,NN2,NX2)
            DO 60 J=JSTART-1,JFIN
              AOUT(I,J)=FX(J)
60      CONTINUE
40     CONTINUE
      RETURN
      END

C
C  ALTERNATIVE INTERPOLATION SUBROUTINE FOR COURSE MESH ANGIOPLASTY
C  MODELS WHERE LARGE DIFFERENCES IN SAR VALUES OCCUR IN THE EE DATA
C  GENERATED.  SUCH LARGE DIFFERENCES DO NOT PERMIT ACCURATE
C  APPLICATION OF THE CUBIC SPLINE SUBROUTINE
C
      SUBROUTINE INTRP2(IFLAG,AOUT,DR,DX)
      INCLUDE 'head.h'
      INTEGER I,J,ISTART,IFIN,JFIN,MODEL(M,N)
      REAL*8 AOUT(0:M,0:N),DR,DX,TEMP(M,N),POWER(M,N),QM(0:M,0:N)
      REAL*8 TO(0:M,0:N),TN(0:M,0:N);AIN(M,N)
      COMMON TO,TN,QM
      COMMON /DAT/POWER,TEMP,MODEL,ISTART,IFIN,JSTART,JFIN

```

```

DO 10 J=JSTART,JFIN
  DO 20 I=ISTART,IFIN
    IF (IFLAG.EQ.1) THEN
      AIN(I,J)=POWER(I,J)
    ELSE
      AIN(I,J)=TEMP(I,J)
    ENDIF
20  CONTINUE
10  CONTINUE
DO 30 I=ISTART,IFIN-1
  DO 40 J=JSTART,JFIN-1
    AOUT(I,J)=(AIN(I,J)+AIN(I+1,J)+AIN(I,J+1)+AIN(I+1,J+1))/4.0
40  CONTINUE
30  CONTINUE
DO 50 I=0,IFIN,IFIN
  IF (I.EQ.0) L=1
  IF (I.EQ.IFIN) L=IFIN
  DO 60 J=JSTART,JFIN
    AOUT(I,J)=(AIN(L,J)+AIN(L,J+1))/2.0
60  CONTINUE
50  CONTINUE
DO 70 J=0,JFIN,JFIN
  IF (J.EQ.0) L=1
  IF (J.EQ.JFIN) L=JFIN
  DO 80 I=ISTART,IFIN
    AOUT(I,J)=(AIN(I,L)+AIN(I+1,L))/2.0
80  CONTINUE
70  CONTINUE
AOUT(0,0)=(AOUT(0,1)+AOUT(1,0))/2.0
AOUT(IFIN,JFIN)=(AOUT(IFIN-1,JFIN)+AOUT(IFIN,JFIN-1))/2.0
AOUT(0,JFIN)=(AOUT(0,JFIN-1)+AOUT(1,JFIN))/2.0
AOUT(IFIN,0)=(AOUT(IFIN-1,0)+AOUT(IFIN,1))/2.0
999 RETURN
END

```

C

C SUBROUTINES PDATA1 AND PDATA2 FORMAT DATA OUTPUT

C

```

SUBROUTINE PDATA1(IFN,OUTP1,TITLE,TIME)
  INCLUDE 'head.h'
  PARAMETER (LINES=17,COLM=12)
  INTEGER I,J,ISTART,IFIN,JSTART,JFIN,MODEL(M,N),K,I1,I2,IFN
  REAL*8 POWER(M,N),QM(0:M,0:N),TO(0:M,0:N),TN(0:M,0:N)
  ,TEMP(M,N),OUTP1(0:M,0:N),TIME
  CHARACTER*40 TITLE
  COMMON/DAT/POWER,TEMP,MODEL,ISTART,IFIN,JSTART,JFIN
  COMMON TO,TN,QM
  WRITE (IFN,300) TIME,TITLE
300  FORMAT (1X,'TIME=',E10.3,2X,40A)
  DO 100 K=1,LINES
    I1=COLM*(K-1)
    I2=I1+COLM-1
    IF (K.EQ.LINES) I2=IFIN
    WRITE (IFN,400) (I,I=I1,I2)
400  FORMAT (1X,12 I10)

```

```

      DO 200 J=JSTART-1,JFIN
        WRITE (IFN,500) J,(OUTP1(I,J),I=I1,I2)
500    FORMAT(1X,I3,1X,12 E10.3)
200    CONTINUE
100    CONTINUE
      RETURN
      END

      SUBROUTINE PDATA2(IFN,OUTP2,TITLE)
      INCLUDE 'head.h'
      PARAMETER (LINES=17,COLM=12)
      INTEGER I,J,ISTART,IFIN,JSTART,JFIN,MODEL(M,N),K,I1,I2,IFN
      REAL*8 POWER(M,N),QM(0:M,0:N),TO(0:M,0:N),TN(0:M,0:N)
      ,TEMP(M,N),OUTP2(M,N)
      CHARACTER*40 TITLE
      COMMON/DAT/POWER,TEMP,MODEL,ISTART,IFIN,JSTART,JFIN
      COMMON TO,TN,QM
      WRITE (IFN,300) TITLE
300    FORMAT (1X,40A)
      DO 100 K=1,LINES
        I1=COLM*(K-1)+1
        I2=I1+COLM-1
        IF (K.EQ.LINES) I2=IFIN
        WRITE (IFN,400) (I,I=I1,I2)
400    FORMAT(1X,12 I10)
      DO 200 J=JSTART,JFIN
        WRITE (IFN,500) J,(OUTP2(I,J),I=I1,I2)
500    FORMAT(1X,I3,1X,12 E10.3)
200    CONTINUE
100    CONTINUE
      RETURN
      END

```

APPENDIX D

THERMAL ANALYSIS FOR ATHEROMATOUS PLAQUE ABLATION

The primary means of plaque ablation using the microwave angioplasty technique is through a phase change of the plaque. As the fatty tissue is heated to temperatures above 100°C, the plaque starts to melt or vaporize. During a phase change the temperature remains constant while the substance is in equilibrium at its melting or vaporization point. When the latent heat of fusion, vaporization or sublimation, h_{fg} is reached, some of the plaque mass is lost due to melting or vaporization. Assuming all phase changes in the plaque takes place next to the blood and plaque boundary, the latent heat is absorbed by the blood (if its temperature is less than that of the plaque).

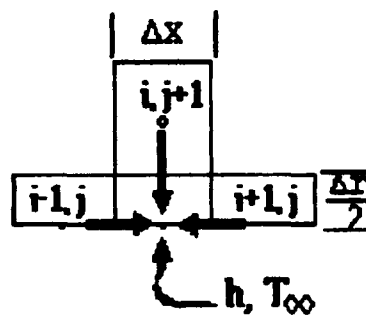
The bioheat governing equation can be modified to include the effects of atheromatous plaque ablation by eliminating the transient term and replacing it with a latent heat accumulation term. Elimination of the transient term during ablation simulates the temperature being constant until latent heat level required to achieve plaque ablation is reached.

$$\rho c \frac{\partial T}{\partial t} = \nabla(k \nabla T) + q_b + q_a \quad (D-1)$$

$$h_{fg} \frac{\partial M}{\partial t} = \nabla(k \nabla T) + q_b + q_a \quad (D-2)$$

The differential equation can be rewritten into an explicit finite difference equation as previously discussed in Chapter 2. Again, the ablation equations are derived by performing an energy balance on each finite difference cell and using the physical formulation method. As an example, the explicit finite difference energy balance equation for the general convective boundary method is shown in Figure 45. Other finite difference equations at the various boundary and interior nodes are similarly derived.

As the plaque is removed from the model, energy is conserved by dumping the heat into the blood. This increase in energy is



$$q_{acc} = h_{fc} \frac{\Delta M}{\Delta t} = \frac{T_{i-1,j} - T_{i,j}}{\frac{\Delta x}{k\pi(r_1^2 - r_0^2)}} + \frac{T_{i+1,j} - T_{i,j}}{\frac{\Delta x}{k\pi(r_1^2 - r_0^2)}} + \frac{T_{i,j+1} - T_{i,j}}{\frac{\Delta r}{k2\pi r_1 \Delta x}} + \frac{T_{\infty} - T_{i,j}}{\frac{1}{h(2\pi r_0 \Delta x)}} \quad (D-3)$$

$$\Delta M = \rho \Delta V \quad (D-4)$$

$$\Delta V = \pi(r_1^2 - r_0^2) \Delta x \quad (D-5)$$

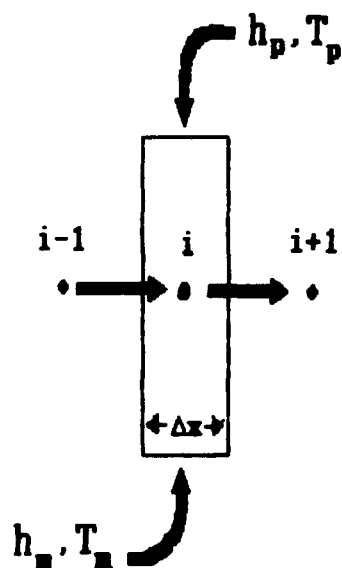
Figure 45. Derivation of the plaque ablation explicit finite difference equation for the convective boundary node (Subroutine ABLCONV)

represented by an increase in blood temperatures. Some heat may be conducted further into the plaque layer; however, this amount is assumed to be relatively small since the melted or vaporized plaque will be carried away by the blood flow. In cases where only one-half to three-fourths of the plaque in a model node exceeds the critical latent heat, the temperatures will be allowed to increase until the entire node can be eliminated.

The type of phase change occurring in the plaque is dependent upon the rate of heating. The critical rate of heating to distinguish between melting and heating has not been studied. Estimates for the latent heat of fusion and vaporization were made using the thermal properties for fat or lipids. As future experimental studies of atheromatous plaques are completed, provisions have been made in the FDATA computer code to alter the default values for fat.

For the one dimensional fluid flow phase changes in the blood can be modelled in a similar model as shown in Figure 46. This subroutine has not yet been added to the ablation program because high heat generation within the blood was not initially anticipated until the results from the FDTD program were obtained.

Like the ablation subroutine, blood temperatures are held constant until the heat stored in the cell is greater or equal to the latent heat of vaporization. The blood temperatures are then allowed to increase as more heat is added to the blood by microwave heat generation or plaque ablation.



$$q_{acc} = h_{fe} \frac{\Delta M}{\Delta t} = \frac{[mc_p(T_{i-1} - T_i) - mc_p(T_{i+1} - T_i)]}{\Delta x} + 2\pi r_0 h_n (T_n - T_i) + 2\pi r_i h_p (T_p - T_i) + q_n [\pi(r_0^2 - r_i^2)] \quad (D-6)$$

$$\Delta M = \rho \Delta V = \rho \pi (r_p^2 - r_n^2) \Delta x \quad (D-7)$$

Figure 46. Derivation of the explicit finite difference equation for the blood vaporization.

APPENDIX E

GLOSSARY OF MEDICAL TERMS (Miller and Keane, 1987)

ablation: removal, especially by cutting. In the case of the microwave angioplasty, plaque removal is accomplished by heating tissues to the point where a phase change such as vaporization or melting occurs.

adventitia: the outer coat of an organ or structure, especially the outer coat of an artery.

angina pectoris: acute pain in the chest caused by interference with the supply of oxygen to the heart.

angioplasty: plastic repair of blood vessels or lymphatic channels.

aorta: the largest artery arising from the left ventricle of the heart.

arteriosclerosis: thickening and loss of elasticity of the coats of the arteries, with inflammatory changes caused by fibrous and mineral deposits in the middle layer of the artery wall.

artery: a vessel through which the blood passes away from the heart to various parts of the body. The wall of an artery consist typically of an outer coat (tunica adventitial), a middle coat (tunica media) and inner coat (tunica intima).

atheroma: an abnormal mass of fatty or lipid material existing as a discrete deposit in an arterial wall.

atheromatous plaque: a deposit of predominantly fatty material in the lining of blood vessels occurring in atherosclerosis.

atherosclerosis: a condition characterized by degeneration and hardening of the walls of the arteries and sometimes the valves of the heart, related especially to thickening of the tunica intima (intimal layer) due to an accumulation of atheromatous plaques.

blood: the fluid that circulates through the heart, arteries and veins. It is the chief means of transport within the body.

catheter: a tubular instrument of rubber, plastic, metal or other material, normally used for draining or injecting fluids through a body

passage. For coronary angioplasties they serve as a means of delivering the plaque removal device to the site of occlusion.

cerebral vascular accident: a disorder of the blood vessels of the brain resulting in impaired blood supply to parts of the brain; also called a stroke.

cholesterol: the principle animal sterol, occurring in faintly yellow, pearly leaflets or granules in all animal tissues.

coronary: a term referring to the vessels, ligaments, etc.

coronary arteries: two large arteries that branch from the ascending portion of the aorta and supply all of the heart muscle with blood.

coronary thrombosis: formation of a clot in a coronary artery.

femoral: pertaining to the femur or to the thigh.

hemoglobin: the oxygen-carrying pigment of the blood, the principle protein of the erythrocyte, or red blood cell.

hemolysis: rupture of erythrocytes (red blood cell) with the release of hemoglobin into the plasma.

hematocrit: the volume percentage of red blood cells in whole blood.

intima: the innermost coat of a blood vessel; also called tunica intima.

in vitro: referring to studies performed under artificial conditions in the laboratory on tissues removed from a living organism.

in vivo: referring to studies performed on tissues and organs not removed from the living organism.

ischemia: deficiency of blood in a part, due to functional constriction or actual obstruction of a blood vessel.

lesions: any damage to a tissue.

lumen: the cavity or channel within a tube or tubular organ, as a blood vessel or the intestine.

media: middle, especially the middle coat of a blood vessel, or tunical media.

microwave: a wave typical of electromagnetic radiation between far infrared and radiowaves.

myocardial: pertaining to the muscular tissue of the heart.

myocardial infarction: formation of an infarct (a localized area of ischemic necrosis produced by occlusion of the arterial supply or the

venous drainage of the part) in the heart muscle, due to interruption of the blood supply to the area.

necrosis: death of a cell or group of cells as the result of disease or injury.

occlusion: the act of closure or state of being closed. In the case of coronary occlusion, this term refers to the obstruction blood flow through an artery of the heart.

percutaneous: performed through the skin.

perfusion: the act of pouring through or into; especially the passage of a fluid through the vessels of a specific organ or body part.

recanalization: dilation of a previously occluded blood vessel to restore normal blood flow.

restenosis: recurrent stenosis, especially of a cardiac valve after surgical correction of the primary condition.

stenosis: narrowing or contraction of a body passage or opening.

sterol: a solid alcohol of animal or vegetable origin, having properties like the fats.

transluminal: through the lumen or channel of a blood vessel.

tissue: a group or layer of similarly specialized cells that together perform certain special functions.

tunica: a covering or coat; used in anatomic nomenclature to designate a membranous covering of an organ or a distinct layer of the wall of a hollow structure, as a blood vessel.

vasospasm: a sudden involuntary contraction of a blood vessel.

vein: a vessel through which blood passes from various organs or parts back to the heart, in the systemic circulation carrying blood that has given up most of its oxygen.

REFERENCES

- Abela, G.S., Normann, S., Cohen D.J., et al., 1982, "Effects of Carbon Dioxide, Nd-YAG, and Argon Laser Radiation on Coronary Atheromatous Plaques," *American Journal of Cardiology*, Vol. 50, pp. 1199-1205.
- Atkinson, L.V., Harley, P.J., and Hudson, J.D., 1989, Numerical Methods with Fortran 77, Addison-Wesley Publishing Company, Wokingham, England.
- Barakat, H.Z., and Clark, J.A., 1966, "On the Solution of the Diffusion Equations by Numerical Methods," *ASME Transactions, Journal of Heat Transfer*, November, pp. 421-427.
- Bluestein, M., Harvey, R.J., and Robinson, T.C., 1968, "Heat Transfer Studies of Blood-Cooled Heat Exchangers", Thermal Problems in Biotechnology, ASME, New York, pp. 46-60.
- Burden, Richard L. and Faires, J. Douglas, 1989, Numerical Analysis, 4th Edition, PWS-Kent Publishing Company, Boston.
- Cameron, John R. and Skofronick, James G., 1978, Medical Physics, John Wiley and Sons, Canada.
- Carslaw, H.S. and Jaeger, J.C., 1946, Conduction of Heat in Solids, Clarendon Press, Oxford.
- Chan, A.K., Sigelmann, R.A., Guy, A.W., and Lehmann, J.F., 1973, "Calculation by the Method of Finite Differences of the Temperature Distribution in Layered Tissues," *IEEE Transactions on Biomedical Engineering*, Vol. 20(2), March, pp. 86-90.
- Chao, B.T., 1969, Advanced Heat Transfer, University of Illinois Press, Urbana.
- Christensen, D.A. and Durney, C.H., 1981, "Hyperthermia Production for Cancer Therapy: A Review of Fundamentals and Methods," *Journal of Microwave Power*, Vol. 16(2), pp. 89-105.
- Davi, S.K., 1985, "Continuous Wave and Pulsed Laser Effects on Vascular Tissues and Occlusive Disease In Vitro," *Lasers in Surgery and Medicine*, Vol. 5, pp. 239-250.
- Decker-Dunn, D., Christensen, D.A., Mackie, W., Fox, J., and Vincent, G.M., 1989, "Opto-thermal Mathematical Model and Experimental Studies for Laser Irradiation of Arteries in the Presence of Blood Flow," *Applied Optics*, Vol. 28, pp. 2263-2272.

Diller, Kenneth R., 1985, "Analysis Of Skin Burns," Heat Transfer in Medicine and Biology, (Edited by Shitzer, A. and Eberhart, R.C.) Plenum Press, New York, pp. 85-134.

Duber, C., et al., 1986, "Morphology of the Coronary Arteries After Combined Thrombolysis and Percutaneous Transluminal Angioplasty for Acute Myocardial Infarction," *American Journal of Cardiology*, Vol. 58, pp. 698-703.

Furzikov, Nickolay P., 1987, "Different Lasers for Angioplasty: Thermo-optical Comparison," *IEEE Journal of Quantum Electronics*, Vol. 23(10), October, pp. 1751-1755.

Goldsmith, Marsha F., 1987, "More Light Shed on Structure and Destruction of Plaque as Laser Angioplasty Research Heats Up," *Journal of the American Medical Association*, Vol. 257, January 16, pp. 288.

Incropera, Frank P. and DeWitt, David P., 1985, Fundamentals of Heat and Mass Transfer, Second Edition, John Wiley & Sons, New York.

Isner, J.M., DeJesus, S.R., Clarke, R.H., et al., 1988, "Mechanism of Laser Ablation in an Absorbing Fluid Field," *Lasers in Surgery and Medicine*, Vol. 8, pp. 543-554.

Jain, Rakesh K., 1985, "Analysis Of Heat Transfer and Temperature Distributions In Tissues During Local and Whole-Body Hyperthermia," Heat Transfer in Medicine and Biology, (Edited by Shitzer, A. and Eberhart, R.C.) Plenum Press, New York, pp. 3-45.

Jang, G. David, 1986, Angioplasty, McGraw-Hill Book Company Inc., New York.

Kays, W.M. and Crawford, M.E., 1980, Convective Heat and Mass Transfer, McGraw-Hill Book Company Inc., New York.

Labs, J.D., Merillat, J.C. and Williams, G.M., 1988, "Analysis of Solid Phase Debris from Laser Angioplasty: Potential Risks of Atheroembolism," *Journal of Vascular Surgery*, Vol. 7, pp. 326-335.

Miller, Benjamin F. and Keane, Claire B., 1987, Encyclopedia and Dictionary of Medicine and Nursing, Fourth Edition, W.B. Saunders Company, Philadelphia.

Mnitentag, J., Marques, E.F., Ribeiro, M.P., et al., 1987, "Thermographic Study of Laser on Arteries," *Lasers in Surgery and Medicine*, Vol. 7, pp. 307-329.

Morcos, N.C., Berns, M., Henry, W.L., 1988, "Effect of Laser-Heated Tip Angioplasty on Human Atherosclerotic Coronary Arteries," *Lasers in Surgery and Medicine*, Vol. 8, pp. 22-29.

Rosen, A., Walinsky, P., Smith, D., et al., 1989, "Percutaneous Transluminal Microwave Balloon Angioplasty," *IEEE Transactions on Microwave Theory and Techniques*, Vol. 38(1), January, pp. 90-93.

Selkurt, Ewald E., 1982, Basic Physiology for the Health Sciences, Little, Brown, and Company, Boston.

Shepard, J., Morgan, H.G., Packard, C.J., Brownlie, S.M., 1987, Atherosclerosis Developments, Complications and Treatment, Excerpta Medica, Amsterdam, New York, Oxford.

Shitzer, A. and Chato, J.C., 1979, "Analytical Solutions to the Problem of Transient Heat Transfer in Living Tissue," *ASME Transactions, Journal of Biomechanical Engineering*, Vol. 100, pp. 202-210.

Shitzer, Avraham and Eberhart, Robert C., 1985, Heat Transfer in Medicine and Biology, Volumes I and II, Plenum Press, New York.

Silverman, S.H., Khoury, A.I., Abela, G.S., and Seeger, J.M., 1988, "Effects of Blood Flow on Laser Probe Temperature in Human Arteries," *Lasers in Surgery and Medicine*, Vol. 8, pp. 555-561.

Singleton, D.L., Paraskevopoulos, G., Taylor, R.S., and Higginson, L.S.J., 1987, "Excimer Laser Angioplasty: Tissue Ablation, Arterial Response, and Fiber Optic Delivery," *IEEE Journal of Quantum Electronics*, Vol. 23(10), October, pp. 1772-1781.

Simpfendorfer, C., et al., 1988, "A Six-Year Evolution of Percutaneous Transluminal Coronary Angioplasty," *Cleveland Clinic Journal of Medicine*, Vol. 55, pp. 299-302.

Srinivasan, R., 1986, "Ablation of Polymers and Biological Tissue by Ultraviolet Lasers," *Science*, Vol. 234, pp. 559-565.

Truitt, Robert W., 1960 Fundamentals of Aerodynamic Heating, The Ronald Press Company, New York.

Walsh, J.T. and Deutsch, T.F., 1988, "Pulsed CO₂ Laser Tissue Ablation: Measurement of the Ablation Rate," *Lasers in Surgery and Medicine*, Vol. 8, pp. 264-275.

Welch, A.J., Bradley, A.B., Torres, J.H., et al., 1987, "Laser Probe Ablation of Normal and Atherosclerotic Human Aorta In Vitro: A First Thermographic and Histologic Analysis," *Circulation*, Vol. 76(5), pp. 1353-1363.

Welch, A.J., Valvano, J.W., Pearce, J.A., Hayes, L.J., and Motamedi, M., 1985, "Effect of Laser Radiation on Tissue During Laser Angioplasty," *Lasers in Surgery and Medicine*, Vol. 5, pp. 251-264.

Welch, A.J., 1985, "Laser Irradiation Of Tissue," Heat Transfer in Medicine and Biology, (Edited by Shitzer, A. and Eberhart, R.C.), Plenum Press, New York.

White, R.A., White, G.H., Vlasak, J., Fujitani, R. and Kopchok, E., 1988, "Histopathology of Human Laser Thermal Angioplasty Recanalization," *Lasers in Surgery and Medicine*, Vol. 8, pp. 469-476.

Wilson, E.B., Knauf, M.A., and Iserson, K.V., 1988, "Red Cell Tolerance of Admixture with Heated Saline," *Transfusion*, Vol. 28, pp. 170-172.